Title
Molecular and Systems Analysis of Cell-Cell Communication and Social Behavior in Trypanosoma brucei

Author
DeMarco, Stephanie Francesca

Publication Date
2019

UNIVERSITY OF CALIFORNIA

Los Angeles

Molecular and Systems Analysis of Cell-Cell Communication and Social Behavior in *Trypanosoma brucei*

A dissertation submitted in partial satisfaction of the

requirements for the degree Doctor of Philosophy

in Molecular Biology

by

Stephanie Francesca DeMarco

2019

ABSTRACT OF THE DISSERTATION

Molecular and Systems Analysis of Cell-Cell Communication

and Social Behavior in *Trypanosoma brucei*

by

Stephanie Francesca DeMarco

Doctor of Philosophy in Molecular Biology

University of California, Los Angeles, 2019

Professor Kent L. Hill, Chair

Endemic to sub-Saharan African, African trypanosomes are devastating protozoan pathogens that present a significant medical and economic burden. Transmitted by the bite of an infected tsetse fly, *Trypanosoma brucei* causes Human African Trypanosomiasis (HAT) and a related diseased called Nagana in animals. In both its tsetse fly and mammalian hosts, *T. brucei* closely interacts with host tissue environments. Parasites must traverse a number of tissue barriers and enact specific developmental changes to complete their transmission cycle. How *T. brucei* senses and responds to signals from its extracellular environment, however, is not well-understood. When tsetse fly midgut stage *T. brucei* is cultivated on a surface *in vitro*, they coordinate their movements to engage in a group behavior termed social motility (SoMo), an ability that requires sensing both surfaces and other cells then engaging signal transduction cascades to respond. Thus, investigating the mechanisms that control social motility may

elucidate *T. brucei* signaling systems that are important for their transmission through their hosts *in vivo*. *In vitro* studies have demonstrated the importance of cAMP signaling in the regulation of social motility.

This dissertation describes the use of molecular and systems-level analyses to investigate the regulation of social motility and signaling systems in *T. brucei*. Through labeling of tsetse fly tissues in conjunction with infection of fluorescently labeled *T. brucei*, we show that phosphodiesterase B1 (PDEB1) knockout parasites, which are unable to engage in SoMo, are blocked in a specific step in their fly transmission cycle, demonstrating the requirement for *T. brucei* cAMP signaling *in vivo*. To identify novel regulators of social motility that may or may not act in the cAMP pathway, two different RNA sequencing experiments were performed, leading to the identification of three novel candidate genes as potential social motility regulators. Additionally, we show that when engaged in SoMo, *T. brucei* exhibits positive chemotaxis toward a neighboring *E. coli* colony. Further characterization of *T. brucei* signaling systems will provide greater insight into how these deadly pathogens navigate through their hosts, potentially leading to new treatments and transmission-blocking agents.

The dissertation of Stephanie Francesca DeMarco is approved.

Peter John Bradley

Alison Renee Frand

Elissa A. Hallem

Matteo Pellegrini

Kent L. Hill, Committee Chair

University of California, Los Angeles

2019

Dedication

To my family, most of all my parents for their endless love and support.

To my friends and colleagues for their support, encouragement, and so many coffee runs.

And to Michael for his constant love and encouragement.

Table of Contents

List of Figures

List of Tables

List of Supplementary Materials

Movie 2-1: Compilation of high-speed videos of WT cells

Movie 2-2: Compilation of high-speed videos of PDEB1 KO cells

Movie 2-3: Compilation of high-speed videos of TPN KO cells

Movie 2-4: Proventriculus of a fly co-infected with untagged WT and PDEB1 KO-dsRed at day 14 post infection.

Movie 2-5: Z-stacks of proventriculi from flies infected with WT-dsRed at day 14 post infection.

Movie 2-6: Z-stacks of proventriculi from flies infected with WT-dsRed at day 14 post infection.

Movie 2-7: Z-stacks of midguts infected with WT-dsRed at day 14 post infection.

Movie 2-8: Z-stacks of midguts infected with WT-dsRed at day 14 post infection.

Movie 2-9: Z-stacks of midguts infected with WT-dsRed at day 14 post infection.

Movie 4-1: Time-lapse video of *T. brucei* engaging in SoMo.

Movie 4-2: Time-lapse video of *T. brucei* engaging in positive chemotaxis toward *E. coli*.

Movie 4-3: Time-lapse video of *T. brucei* engaging in SoMo.

Movie 4-4: Time-lapse video of *T. brucei* engaging in positive chemotaxis toward *E. coli*.

Movie 4-5: Live video of *T. brucei* cells at the tip of a projection upon initial impact with an *E. coli* colony.

Movie 4-6: Time-lapse video of a projection impacting an *E. coli* colony.

Acknowledgements

Chapter 2 is adapted from Shaw S*, DeMarco SF*, Rehmann R, Wenzler T, Florini F, Roditi I, Hill KL (2019). Flagellar cAMP signaling controls trypanosome progression through host tissues. *Nature Communications*, **10**(1):803. doi: 10.1038/s41467-019-08696-y. S.S. and S.D. are co-first authors, and K.H. and I.R. are co-corresponding authors. S.S., S.D., I.R., and K.H. designed the experiments and wrote the paper. S.S., S.D., R.R., T.W. and F.F. conducted the experiments. S.S., S.D., T.W., I.R. and K.H. analyzed the data. K.H. conducted the statistical analyses.

Chapter 3 is a compilation of currently unpublished work. For the suspension culture versus surface cultivated RNAseq project, Dr. Michael Oberholzer isolated the RNA and worked with the Pellegrini laboratory to determine the differential gene expression analysis. Rina Kim, Dr. Kent Hill, and myself filtered lists of differentially expressed genes, and picked the 9 candidate genes to test. Construction and analysis of RNAi cell lines was completed by Alexandra Stream, Shahriyar Jahanbakhsh, and myself. For the wild type versus PDEB1 KO RNAseq analysis, I isolated the RNA and worked with the Clinical Microarray Core at UCLA for library construction and sequencing. Differential gene expression analysis was completed in collaboration with Dr. Najib El-Sayed and Keith Hughitt. Filtering and GO-term analysis was done by myself. The CMF-34 RNAi construct was designed by Desiree Baron in Baron DM, Ralston KS, Kabututu ZP, Hill KL (2007). Functional genomics in *Trypanosoma brucei* identifies evolutionarily conserved components of motile flagella. 120(Pt 3):478-91. The Carbonic anhydrase knockout line was constructed by Dr. Edwin Saada, Walter Hardesty, and myself. Analysis of the Carbonic anhydrase knockout line was done by myself.

Chapter 4 is a draft of a manuscript in preparation written by myself and Dr. Kent Hill with edits, feedback, and additional writing from Dr. Edwin Saada and Dr. Miguel Lopez. E.S. and M.L. discovered BacSoMo. S.D. and K.H. designed the experiments and analyzed the data. S.D. conducted the experiments and performed the statistical analysis and mathematical modeling

Appendix 1 is adapted from Saada EA, DeMarco SF, Shimogawa MM, Hill KL (2015). "With a Little Help from My Friends"-Social Motility in *Trypanosoma brucei*. *PLoS Pathogens*, **11**(12):e1005272. doi: 10.1371/journal.ppat.1005272. This was an invited review about social motility for PLoS Pathogens. E.A., S.D., M.S., and K.H. wrote the manuscript.

Biographical Sketch

Education:

University of California, Berkeley. Molecular and Cell Biology, B.A. 2009 - 2013
Emphasis in Genetics, Genomics, and Development

Research Experience:

- Dr. Kent Hill laboratory. University of California, Los Angeles 2013 – present
  - Graduate Student Researcher: Molecular and systems analysis of social motility.
- Dr. Gian Garriga laboratory. University of California, Berkeley 2012 – 2013
  - Undergraduate Researcher. Studied axon fasciculation between neurons in the nematode *Caenorhabditis elegans*.
- Dr. Ahmet Yildiz laboratory. University of California, Berkeley 2011
  - Prepared protein extractions of telomeric proteins and purified them using FPLC.
- Dr. Paul Sternberg laboratory. California Institute of Technology Summer 2010
  - Summer Undergraduate Research Fellowship (SURF). Studied which genes enriched in the BAG neurons in the nematode *Caenorhabditis elegans* are necessary for its repulsive response to carbon dioxide.
- Dr. William Smythe laboratory. Jet Propulsion Laboratory Summer 2009
  - NASA Space Grant Program. Designed an experimental setup to examine the effect of low temperatures and pressure on the charging of soil particles as they are transferred from a pouring device to analyzing instruments.
- Dr. Paul Sternberg laboratory. California Institute of Technology Summer 2008
  - Studied chemotaxis in two species of insect parasitic nematodes and identified differences in chemotactic behaviors between them.

Selected Honors and Awards

- Dissertation Year Fellowship, UCLA Graduate Division 2018 – 2019
- Best Talk Prize, 34th Annual Swiss Trypanosome Meeting, Leysin, Switzerland 2017
- NIH-NRSA Award, Microbial Pathogenesis Training Grant Fellowship 2017 – 2018
- Cell and Molecular Biology Training Grant Associate Member 2017
- MBIDP Travel Award to the Roditi laboratory at the University of Bern 2016
- NIH-NRSA Award, Cell and Molecular Biology Training Grant Fellowship 2015 – 2017
- Best Poster Prize, Southern California Eukaryotic Pathogens Symposium 2015

Publications:

- **DeMarco, S.F.**, Saada, E.A., Lopez, M.A., and Hill, K.L. Identification of positive chemotaxis in the protozoan pathogen *Trypanosoma brucei*. In preparation.
- Shaw, S.*, **DeMarco, S.F.***, Rehmann, R., Florini, F., Wenzler, T., Roditi, I, and Hill, K.L. (2019) Flagellar cAMP signaling controls trypanosome movement through host tissues. *Nature Communications*, 10(1):803. doi: 10.1038/s41467-019-08696-y. ***co-first authors**
  - Invited blog post: **DeMarco, S.F.** (22 February, 2019) Tackling trypanosome biology takes a lot of guts. Behind the Paper, Nature Microbiology Community.

- Saada, E.A., **DeMarco, S.F.**, Shimogawa, M.M., and Hill, K.L. (2015) "With a Little Help from My Friends"—Social Motility in *Trypanosoma brucei*. *PLoS Pathog* 11(12): e1005272. doi:10.1371/journal.ppat.1005272.
- Hallem, E.A., Dillman, A.R., Hong, A.V., Zhang, Y., Yano, J.M., **DeMarco, S.F.**, and Sternberg, P.W. (2011) A sensory code for host seeking in parasitic nematodes. *Current Biology* 21, 377-383.

Mentoring and Teaching Experience:

- **CIRTL Course**: An Introduction to Evidence-Based Undergraduate STEM Teaching
  - Certificate of Completion with Distinction — Summer 2018
- **Entering Mentoring Training Program**, UCLA, — Summer 2017
- **Undergraduate Research Mentor**, Hill laboratory, UCLA, — 2015 – 2017
- **CityLab: www.citylabatucla.org**: Volunteer member — 2016
- **SciComm Hub at UCLA:** Education Specialist — 2016
- **Advancing Women in Science and Engineering (AWiSE) UCLA:** STEM Day Volunteer — 2015 – 2016
- **Teaching Assistant:** Microbiology, Immunology, and Molecular Genetics Department, UCLA — 2014 – 2015
- **Missionario di Cristo**: Volunteer Teaching Assistant, Rome, Italy — Spring 2012
- **La Sapienza University:** Volunteer Conversation Leader, Rome, Italy — Spring 2012

Science Communication Experience:

- **AAAS Mass Media Fellow 2019:** Los Angeles Times — Summer 2019
- **Freelance Science Writer, EpiBeat:** www.epibeat.com: — 2018 – 2019
  - "Cellular Antivirus: How Foreign DNA is Hushed" selected by Science Seeker as one of the best science posts of the week.
- **Signal to Noise Magazine:** www.signaltonoisemag.com — 2016 – present
  - A non-profit online science magazine founded and run by graduate students
    - Editor-in-Chief: February 2017 – present
    - Style and Formatting Editor: November 2016 – February 2017
    - Staff Writer January 2016 – February 2017
- **ComSciCon-SciWri 2019 Organizing Committee** — January 2019 – present
- **ComSciCon 2018:** — June 2018
  Selected to attend this international science communication workshop for graduate students and to present a poster highlighting my work with *Signal to Noise Magazine*.

Selected Conference Presentations

- **2018:** Oral Presentation: **Southern California Eukaryotic Pathogens Symposium**, UC Riverside, CA.
- **2017:** Oral Presentation: **VIIth International Kinetoplastid Molecular Cell Biology Meeting**, Woods Hole, MA.
- **2017:** Oral Presentation: **34th Annual Swiss Trypanosome Meeting**, Leysin, Switzerland. **Awarded Best Talk Prize.**

Chapter 1 – Introduction

Microbial social behavior

The oldest evidence of life – fossils from 3,480 million years ago – depicts a group of microorganisms, not living as individuals as typically thought, but in close, intimate contact with one another [1]. From microbial mats serving as homes for species of bacteria and archaea to the drug-resistant bacterial biofilms colonizing catheters, the world is teeming with social microbes. While often studied as single cells in the laboratory, in their natural environments, microbes primarily live in groups [2, 3].

The advantages of microbial group behavior are numerous including the ability to move more efficiently across surfaces and through barriers, increased drug resistance and opportunities for genetic exchange, greater access to nutrients, and the division of labor amongst members of the group [2, 4-7]. In order to engage and benefit from these social behaviors, microbes have to be able to sense and respond to cues from both their environment and other microbes. This response is often exemplified by changes in individual cell motility and/or physiology, which leads to the manifestation of group behavior. For example, in swarming motility, a type of social behavior enacted by some bacterial species, individual cells can become multi-flagellated, secrete a surfactant, and/or become associated with other bacteria in "rafts," which comprise of many other swarming cells moving together [8]. Even more dramatic of a transition, individual cells of the eukaryotic microbe, *Dictyostelium discoideum*, completely alter their behavior and morphology to form a multicellular fruiting-body structure [9].

While the regulation of social behaviors have been well-described for bacteria and social amoeba, protozoan parasites, which must also be able to sense and respond to cues in their diverse host environments, have not been as well-characterized. This dissertation will describe

the use of both molecular and systems-level analyses to characterize the social behavior of the human and animal parasite, *Trypanosoma brucei*.

African Trypanosomes and the Kinetoplastids

Trypanosoma brucei is a single-celled eukaryotic parasite endemic to sub-Saharan Africa. *T. brucei* causes African Trypanosomiasis, also known as African sleeping sickness, and is transmitted to its mammalian hosts through the bite of an infected tsetse fly. As an individual cell, it is characterized by a single flagellum attached along the length of the cell body with a small section protruding from the end (Figure 1-1). When *T. brucei* beats its flagellum, the beat originates at the tip of the flagellum [10, 11], in contrast to most other flagellated eukaryotic cells [11]. The attachment of the flagellum along the cell body and the origination of the beat at the tip of the flagellum causes trypanosomes to move in a corkscrew-like fashion with the tip of the flagellum leading in the direction of forward movement. In fact, the name "trypanosoma" comes from Greek where "trypano" means auger or corkscrew, and "soma" means body [12], making trypanosomes literal "auger-bodies."

Trypanosoma brucei is a member of the Trypanosomatid order, a sub-group of the Kinetoplastid class made up exclusively of parasitic species [13, 14]. Kinetoplastids are single-celled eukaryotes characterized by a unique subcellular structure called the kinetoplast [15, 16], which is made up of concatenated mini- and maxi-circles of DNA [17]. Of the Trypanosomatid species, those that cause the greatest disease burden include *T. brucei*, *Trypanosoma cruzi* and *Leishmania* species [18]. *T. cruzi* is the causative agent of American Trypanosomiasis, also called Chagas disease. Transmitted by the triatomine bug, *T. cruzi* is endemic to Central and South America, with an increasing host range in North America [19]. Of triatomine bugs found

in the United States, approximately 50% are infected with *T. cruzi,* with some variation among different species of triatomine bugs [20]. Additionally, recent work suggests that climate change could result in expanding the host-range of the triatomine bug in both Mexico and the United States [21]. *Leishmania* parasites, on the other hand, are found world-wide and cause three forms of leishmaniasis: visceral (lethal if untreated), cutaneous, and mucocutaneous [22, 23]. They are transmitted to humans through the bite of infected phlebotomine sandflies and disproportionately affect the poorest populations in the world [23]. 700,000 to 1 million new cases of leishmaniasis occur annually [23], underscoring the need to investigate the biology of these and related trypanosomatid parasites.

Among the trypanosomatids, a subset of species called African trypanosomes are transmitted to mammals through the bite of a tsetse fly (*Glossina* species) [24]. These include the *T. brucei* sub-species: *T. brucei gambiense* and *T. brucei rhodesiense*, which cause human African Trypanosomiasis (HAT), and at least seven species that cause the related disease Nagana or Animal African Trypanosomiasis (AAT): *T. brucei brucei*, *T. congolense*, *T. godfreyi*, *T. simiae*, *T. vivax*, *T. uniforme*, and *T. suis* [25]. The animal-infective species vary in their host preferences with some infecting primarily domesticated pigs and others preferentially infecting cattle. They also differ in their lifecycle within the tsetse fly [25]. Importantly, the human-infective sub-species *T. b. rhodesiense* can be harbored by animal hosts, resulting in a reservoir for human infection [26, 27]. While *T. b. gambiense* is typically spread from human to human via the tsetse fly, animal reservoirs have also been reported [28, 29].

Clinical Manifestation of Sleeping Sickness

African sleeping sickness is characterized by two diseases stages corresponding to whether the parasite is in the bloodstream of the host or if it has crossed the blood brain barrier to enter the central nervous system [30]. In the first stage of the disease, patients experience flu-like symptoms and waves of fever, which are similar to symptoms of many common infections, often delaying diagnosis [31]. As the disease develops, symptoms such as enlargement of the lymph nodes, spleen, and liver appear along with cardiac issues [31]. Additionally, the appearance of a large swelling in the neck due to an enlarged lymph node, called Winterbottom's sign, is an indication of infection by *T. b. gambiense* [31].

It is the second stage of the disease that gives "sleeping sickness" its name. In this stage patients exhibit neurological symptoms including sleepiness during the day and insomnia at night [31]. Recent work has postulated that the altered sleep-cycle exhibited by patients with sleeping sickness is a circadian rhythm disorder caused by infection with *T. brucei* [32]. If left untreated, patients will develop seizures, have disruptions in consciousness, and eventually die [31].

Epidemiology and Global Impact of African sleeping sickness

African sleeping sickness is endemic to sub-Saharan Africa in regions where the tsetse fly vector is found. While the parasite is typically transmitted by the tsetse fly to its mammalian host, congenital transmission has been observed [33, 34]. The two human infective sub-species are geographically separated, with *T. brucei gambiense* occupying the western and central endemic regions and *T. brucei rhodesiense* in the south-eastern areas [30] (Figure 1-2). Depending on the sub-species, human African sleeping sickness can be either acute (*T. b. rhodesiense*) or chronic (*T. b. gambiense*) [30]. In acute infections, patients without treatment

succumb to the disease in a matter of weeks to month [35]; whereas, chronic infections can last for three years on average [36].

Tsetse flies can be found in both semi-urban and rural parts of sub-Saharan Africa, often making their homes in forested, riverine, and savannah regions [37]. They can typically be found in areas with low vegetation which allows for a suitable mating environment and access to hosts [38]. Due to this distribution, humans are bitten as they perform their daily tasks such as farming, collecting water, hunting, or any other activity that brings them within the tsetse fly's habitat [39]. Tsetse flies have also been found in and around buildings in urban environments and have been shown to be attracted to cars [40], presenting an increased risk to humans.

The economic burden imposed on communities by sleeping sickness is substantial. The people primarily affected by sleeping sickness live in rural areas where access to healthcare is already low as is income and food security [41]. People who become infected have to miss work to travel to the doctor, often located far from their home, and they often have to endure long hospital stays for treatment [41]. The United Nations estimated that Africa loses $1.5 billion per year due to sleeping sickness [42]. Recent work investigating the socio-economic effects of sleeping sickness found that families bore the financial brunt of a relative infected with sleeping sickness, often resulting in increased hunger, financial instability, and less education for children [42].

Fortunately, the incidence of human African sleeping sickness has decreased drastically in recent years with only 1446 cases reported in 2017 [43]. In fact, the World Health Organization has declared that sleeping sickness will no longer be classified as a Neglected Tropical Disease by 2020 [43]. However, it is important to note that resurgent epidemics of sleeping sickness have occurred in the past due to lack of adequate control mechanisms [44].

Moreover, Animal African trypanosomiasis still presents an important problem. Infection of animals, cattle in particular, leads to a loss of income for farmers in already poverty-stricken areas. Cattle that are too weak to plow the fields and not healthy enough to serve as a source of milk or meat present a substantial burden [45], especially in developing countries that primarily rely on agriculture. Also, as mentioned earlier, animals can serve as reservoirs for human infective strains of *T. brucei*, leading to the potential for a resurgence of human infections.

History of Sleeping Sickness

African trypanosomes likely influenced the evolution of early humans [46]. Co-existing for centuries, humans have developed resistance to all African trypanosomes species with the exception of the two sub-species *T. b. gambiense* and *T. b. rhodesiense.* A factor found in human serum has been known to kill *T. brucei brucei* since 1912 [47]. Later, this was identified as trypanolytic factor 1 and 2 (TLF1 and TLF2) [48-50]. These factors are made up of the proteins apolipoprotein A1 (APOA1), apolipoprotein L1 (APOL1), and haptoglobin-related protein (HRP) [51]. It is against these factors that *T. b. gambiense* and *T. b. rhodesiense* have developed resistance. In *T. b. rhodesiense*, evolution of a single protein, Serum Resistance Associated (SRA) protein confers complete resistance to the function of human APOL1 [52-54]. The situation is slightly more complex in *T. b. gambiense*, where three factors including the expression of *T. b. gambiense*-specific glycoprotein (TgsGP), modification of its TLF receptor, and changes in its lysosomal physiology allow for resistance [55]. Intriguingly, some African people express variant APOL1 genes (G1 and G2), and serum from these people have been shown to lyse *T. b. rhodesiense in vitro* [56]. Expressing only one of these APOL1 variants, however, is associated with a 7-30 fold higher risk of developing kidney disease compared to

people without the variant [56-58], and recent genetic association work indicates that there is likely a heterozygote advantage to expressing these variants [59]. Baboons, interestingly, are resistant to infection by all species and sub-species of African trypanosomes due to their expression of variant APOL1 genes, which are not associated with the kidney diseases seen in humans [60-62].

The first historical descriptions of mammalian sleeping sickness date back to the ancient Egyptians [63]. A veterinary papyrus from the 2nd millennium BCE describes a bull afflicted with a wasting disease reminiscent of Nagana [64]. The lush environment of the Nile River valley during the Old Kingdom (3000 – 2000 BCE) would have provided a favorable habitat for tsetse flies, and records of Egyptian cattle breeding practices from this time supports the likelihood of the presence of infective tsetse flies [63]. For example, domesticated animals were bred with game animals to produce offspring with resistance to trypanosome infection, as some wild animals exhibit resistance to trypanosomes [65]. When the course of the Nile River was adjusted during the Middle Kingdom (2000 – 1300 BCE), however, the tsetse fly habitat was likely destroyed [63]. The timing of this shift in the course of the Nile correlates with the change in Egyptian breeding practices to raise purebred lines of cattle [63, 66].

In the Middle Ages (1100-1400 CE), Arab traders who traveled to West African kingdoms provide the first descriptions of humans suffering from sleeping sickness [63]. Ibn Khaldun, a famous Arab historian of the time, describes what one of his contemporaries told him about the late king of Mali:

> He told me that Jata had been smitten by the sleeping illness, a disease which frequently afflicts the inhabitants of that climate, especially the chieftains who are habitually affected by sleep. Those afflicted are virtually never awake or alert. The sickness harms

the patient and continues until he perishes. He said that the illness persisted in Jata's humour for a duration of two years after which he died in the year 775 AM (1373/4) [63, 67].

The next descriptions of sleeping sickness appear in the context of the Atlantic slave trade (15^{th}-19^{th} centuries CE) [63], with the first medical report describing the neurological symptoms of human sleeping sickness published in 1734 [68]. The underlying cause of sleeping sickness, however, was still unknown.

About 100 years later in 1841, the first description of trypanosomes was reported by Gabriel Valentin at the University of Bern, who isolated them from fish blood [69, 70]. In the following approximately 60 years, trypanosomes were found in the blood of a myriad of species [69]. Around the same time in 1852, the explorer David Livingston first suggested that Nagana is caused by a bite from the tsetse fly [68]. The first unequivocal connection between tsetse flies, trypanosomes, and Nagana came from work by the microbiologist David Bruce in 1895, who found that tsetse flies transmitted trypanosomes from infected cattle, dogs, and horses, to uninfected ones [71]. Soon after in 1902, the surgeon Robert Forde and his colleague Joseph Dutton linked trypanosomes to the cause of sleeping sickness when they identified trypanosomes in the blood of a Gambian steamboat captain [63, 72, 73]. At the same time, the Italian doctor Aldo Castellani found trypanosomes in the brain of sleeping sickness patients, also indicating the link between trypanosomes and the disease [74]. In 1910, *T. b. rhodesiense* was identified as different from the *T. b. gambiense* sub-species discovered by Ford and Dutton, and it was found to cause the acute form of sleeping sickness [75].

Following the identification of the causative agents of African sleeping sickness, a number of treatments and vector control measures were implemented (see discussion in *Past and*

Current Treatments below). During this time, however, serious outbreaks of sleeping sickness occurred in tsetse endemic areas [63]. The first outbreak took place primarily in Uganda and the Congo from 1896 to 1906 as colonizers settled in the region, upheaving the way of life of the local people and thus bringing massive economic and social change [76]. Increased settlement also brought people into closer contact with tsetse fly habits than they were before. Seeing the devastation wreaked by the outbreak, European countries sent scientists to the colonies to try to understand the disease, find a cure, and implement control and screening procedures [77]. This work eventually reduced the number of cases. In the mid-1960's many African countries had gained independence from their colonizers and had seen hardly any cases of trypanosomiasis for years. With the political instability that comes with regime change and the complacency of the low number sleeping sickness cases, trypanosomiasis control and screening programs were stopped, leading to a devastating resurgence of the disease from 1970's to the late 1990's [63]. Rigorous screening efforts and the development of new drug treatments eventually lowered the incidence of African sleeping sickness to the low levels seen today [43].

Past and Current Treatments

One of the first drugs developed to treat sleeping sickness was the arsenic-based drug, Atoxyl, so named because it was said to be considerably less toxic than arsenic acid [78]. It turned out, however, to actually be quite harmful as 2% of patients treated with it developed blindness [78]. The next drug treatments to be developed were based on synthetic dyes [78]. The chemist Paul Ehrlich developed Trypan Red and Trypan Blue as a chemotherapy for trypanosome infection. While Trypan Red killed a horse-infective species of trypanosomes, it did not kill other mammalian or human-infective ones [78]. Trypan Blue was very effective at killing

all species of trypanosomes tested, but it had the unfortunate side-effect of turning the skin of the patient or animal blue [79]. In an effort to find a colorless compound that would still effectively kill trypanosomes, Bayer developed suramin in 1917, which is still used today to treat the first stage of *T. b. rhodesiense* infection [39, 80]. Soon after in 1919, the drug tryparsamide, a derivative of Atoxyl, was developed [81]. Although it still caused blindness is some patients, it was the first drug effective against the second stage of the disease and was used until the late 1960's [78]. In the late 1930's, the drug pentamidine was found to be a highly effective treatment for the first stage of *T. b. gambiense* infections and is still used today [39, 82]. In the 1940's, another arsenic-based drug, melarsoprol, was developed to treat the second stage of the disease [78]. It improved upon tryparsamide in that it did not cause blindness, but it did cause encephalopathy in 5-10% of patients, of which 1-5% died [83]. Due to melarsoprol's effectiveness but high toxicity, today it is only used to treat second stage *T. b. rhodesiense* or relapsed *T. b. gambiense* infections [39]. In the 1960's nifutimox, which was used to treat American trypanosomiasis was also found to be effective against the second stage of *T. b. gambiense* infections when used in combination with eflornithine, which was developed as an anti-cancer drug in the 1970's [78, 84]. This combination therapy, called NECT, is still in use today [39]. The World Health Organization provides all current treatment methods to endemic countries free of charge [43].

The administration of these drugs for the first and second stage of the disease are quite invasive. Of the first stage drugs, most require either intravenous or intramuscular infusions during a week-long stay in the hospital [39]. Because parasites have crossed into the central nervous system in the second stage of the disease, the drugs that treat this stage require even longer hospital stays with sometimes hours-long intravenous or intramuscular infusions [39]. As

mentioned above, these long hospital stays make treatment an arduous process for people likely having to travel from distant rural areas.

An exciting development in the past year, however, has led to the implementation of a novel drug for sleeping sickness called fexinidazole, which treats both the first and second stages of the disease [43]. This treatment comes in the form of a pill, and the World Health Organization is working to update their guidelines to include it in their treatment plan [43, 85]. Its oral administration will allow for increased access to treatment and significantly decreased complexity in administration. People in rural areas will not be taken away from work or family to get treatment at a hospital, and doctors can easily and sanitarily bring treatment to patients in remote areas or to those who have difficulty travelling. There is always the possibility for the development of drug resistance, so fexinidazole's use and effectiveness should be monitored. It does, however, present a promising new strategy in the treatment of African sleeping sickness.

Life Cycle of Trypanosoma brucei

To initiate mammalian infection, human-infective metacyclic forms of *T. brucei* are injected into human or animal tissue by the bite of an infected tsetse fly [86]. Upon entering the bloodstream, metacyclics differentiate into long-slender bloodstream stage parasites, both changing their overall morphology and expressing a Variant Surface Glycoprotein (VSG) coat on their cell surface [86, 87]. As a mechanism to avoid recognition by the immune system, *T. brucei* uses antigenic variation to switch the identity of the main VSG expressed on its surface [88]. In addition to mounting a bloodstream infection, parasites have also been found in skin and adipose tissue [89, 90], with those in adipose tissue being transcriptionally distinct from those in the bloodstream [91]. Although, it is not yet known how parasites move to these areas or what they

do there, it has been hypothesized that these tissues could serve as sources of reinfection into the bloodstream, or, in the case of skin, serve as a reservoir for tsetse fly transmission [89, 90, 92]. Supporting the hypothesis of the skin as a reservoir, asymptomatic patients and animals have been found to infect tsetse flies, even though it appears that they have no parasites in their bloodstream [92].

Over the course of the infection, long-slender *T. brucei* eventually cross the blood-brain barrier into the central nervous system [86]. In order for *T. brucei* to continue its transmission cycle, it must differentiate into the tsetse fly-transmissible and quiescent stage, short-stumpy cells [86]. *T. brucei* regulates this process through a quorum sensing signaling system, although the identity of the quorum sensing signal, called the Stumpy Induction Factor (SIF), remains unknown [93]. Recent work has identified the *T. brucei* surface protein GPR89, an oligopeptide transporter, as the quorum sensing signaling sensor for stumpy form induction [94]. This work also found that *in vivo*, long-slender *T. brucei* secrete oligopeptidases that act as a paracrine signal to induce the transition from long-slender form to short-stumpy, suggesting that SIF is likely an oligopeptide [94].

When short-stumpy cells are taken up by a tsetse fly during a blood meal, the parasites are flushed from the mouthparts, through the crop, and into the lumen of the midgut [95]. Once short-stumpy cells find themselves in the midgut of the fly, they differentiate into early procyclic cells, which in addition to changing their morphology also replace the VSG surface coat with a mixture of GPEET and EP procyclin proteins on their surface [96]. About one week after parasites have established an infection in the midgut lumen, they traverse the peritrophic matrix to reach the ectoperitrophic space [97]. The peritrophic matrix is a barrier made up of chiton, glycoproteins, and glycosaminoglycans that insulates the midgut lumen from the midgut

epithelial cells [98]. It is constantly produced throughout the life of the fly by the proventriculus, an organ thought to also be involved in immune regulation [99, 100]. There is some debate as to whether parasites penetrate through the peritrophic matrix or if parasites swim around it at the end of the hindgut [101], but regardless of how they manage it, *T. brucei* parasites must reach the other side to continue their transmission cycle.

The timing of the transmission of early procyclics across the peritrophic matrix and into the ectoperitrophic space correlates with the differentiation of early procyclics into late procyclics, which are morphologically identical to early procyclics except that they no longer express GPEET procyclin [96]. In the ectoperitrophic space, parasites elongate slightly as they migrate through the ectoperitrophic space until they reach the proventriculus and establish an infection there [102]. In the proventriculus *T. brucei* cells undergo an asymmetric division into both a long and short epimastigote, which then migrate to the salivary glands via an unknown mechanism [103, 104]. Once in the salivary gland, the short epimastigotes attach to the salivary gland epithelial cells via their flagellum and differentiate into mammalian-infective metacyclic cells [86]. The metacyclics are then injected into the mammalian host when the fly next takes a bloodmeal.

Flagellum as a Signaling Organelle

To move through and navigate these diverse host environments, *T. brucei* uses its single motile flagellum. As a eukaryote, *T. brucei's* flagellum is characterized by a canonical 9+2 axoneme with nine doublet pairs of microtubules surrounding a single central pair [11]. While most of the flagellum structure is conserved with other eukaryotes, the *T. brucei* flagellum does have some parasite-specific features. One of these parasite-specific features is the paraflagellar

rod, which is a cytoskeletal structure that runs along the length of the axoneme [11]. It is thought to provide structural support and has also been postulated to serve as a scaffold for flagellar signaling proteins [105-107].

In addition to its role in motility, flagella are important sensory and signaling organelles [108-110]. Involved in both mechanosensation and chemosensation, flagella (also called cilia), function as antennas for cells. Cilia have been shown to be important mechanosensors of fluid flow in mammalian kidneys [110-113] and in the development of endothelial vasculature [114, 115]. As chemosensors, ciliated photoreceptor cells in our eyes detect light [116], and ciliated olfactory neurons allow for our sense of smell [117]. Cilia are also important for sensing developmental cues, such as those involved in regulating planar cell polarity [118, 119] and Hedgehog signaling [120-122]. Diseases known as ciliopathies occur when flagellar proteins important for sensing or signal transduction are lost or mutated, such as Bardet-Biedl syndrome or Polycystic Kidney Disease [123].

Many protozoan parasites also have flagella, such as Malaria, Trichomonas, Leishmania, and Giardia [124]. Because parasites are exposed to diverse environmental cues during their host transmission cycles, they need a way to sense and transduce signals from their host environments, which may be a role for their flagella. *T. brucei's* flagellum has been postulated to have a role in sensing and signaling [125, 126]. Supporting this, when *T. brucei* is in the tsetse fly, it intimately intercalates its flagellum with the salivary gland epithelial cells to become mammalian-infective [86, 127]. This close interaction between *T. brucei's* flagellum and the host suggests that the flagellum may have a sensory and/or signaling role for the parasite in the tsetse fly.

Signaling Systems in Trypanosoma brucei

The best understood signaling system in *T. brucei* is the quorum sensing pathway that regulates the transition from long-slender to short-stumpy bloodstream form *T. brucei* [93, 94], as discussed above. Other aspects of signaling in *T. brucei* are not as well-characterized, leaving open fundamental questions as to how these parasites sense their environment and transduce those signals. In an effort to identify *T. brucei* signaling proteins, a proteome of the flagellar surface, membrane, and matrix of long-slender bloodstream form parasites was profiled [128]. Many potential signaling proteins were identified, including adenylate cyclases, calcium channels, and receptor kinases [128]. Additionally, proteomic analysis of the flagellar membrane of procyclic cells identified a family of six adenylate cyclase (AC) proteins exclusively expressed in procyclic-stage *T. brucei* [129], indicating a potential important role for flagellar cAMP signaling in fly midgut-stage *T. brucei*.

In *T. brucei* and other kinetoplastids, cAMP signaling is quite different compared to other eukaryotes [130]. Typically G-protein coupled receptors bind extracellular ligands, which in turn regulate the activity of adenylate cyclase proteins to modulate its production of cAMP [131]. In many eukaryotic signaling pathways protein kinase A (PKA) then binds cAMP and enacts downstream signaling cascades [131]. In *T. brucei*, however, PKA is expressed but does not bind cAMP [132, 133]. A screen for cAMP effectors in *T. brucei* identified four proteins called Cycle AMP Response Proteins (CARPs), indicating the presence of a diverse cAMP signaling pathway in *T. brucei* [134]. Additionally, *T. brucei* does not encode typical G-protein coupled receptors [135]. It does, however, encode approximately 75 receptor-type adenylate cyclases [130, 136]. These adenylate cyclases have large extracellular domains, a single transmembrane domain, and an intracellular cyclase domain [130], thus likely combining the functions of mammalian GPCRs

and ACs into one protein. *T. brucei* ACs differ most in their extracellular domain [130], which has structural similarity to periplasmic-binding proteins from bacteria [137], suggesting that they may act as sensors for different extracellular cues. This is supported by the differential expression of *T. brucei* ACs throughout its lifecycle [129, 136, 138-141].

All of the *T. brucei* ACs studied so far localize to the flagellar membrane [129, 138]. They do, however, differ in their flagellar localization with a subset localized along the entire length, while others are found exclusively at the flagellum tip [129]. A subset of *T. brucei's* phosphodiesterase proteins, which convert cAMP into AMP, are also found in the flagellum [106]. *T. brucei* encodes five phosphodiesterase proteins: PDEA, PDEB1, PDEB2, PDEC, and PDED [130]. It has been shown that PDEB1 localizes to the flagellum, and PDEB2 localizes to both the cytoplasm and the flagellum [106]. Loss of PDEB1 and PDEB2 together is lethal in bloodstream-form *T. brucei*, but loss of either one alone is not [106]. In procyclic forms loss of either PDEB1 or PDEB2 together or individually is not lethal [106]. The flagellar localization of both ACs and PDEs in *T. brucei* suggests that they may function in signaling.

T. brucei Social Motility

Evidence for the importance of the cAMP pathway in *T. brucei* comes from studies of *T. brucei* social motility [142, 143]. Similar to social behaviors in other microbes as discussed above, when inoculated on a semi-solid surface, *T. brucei* cells from suspension culture assemble into groups in a cell-density dependent manner and migrate away in projections consisting of hundreds of thousands of parasites from the initial point of inoculation (Figure 1-3) [144, 145]. The ability to engage in this social behavior, called social motility (SoMo) requires *T. brucei* to be able to sense and respond to cues from its external environment, which includes both physical

surfaces and other parasites. Therefore, identifying parasite signaling systems that regulate SoMo could reflect signaling systems important for *T. brucei* transmission through its diverse host environments.

To assess the role of cAMP signaling in SoMo, either PDEB1 expression or expression of the individual six procyclic-enriched ACs were knocked down [142, 143]. Upon loss of PDEB1 expression, either by RNAi or pharmacological inhibition, there was no difference in growth rate or morphology in suspension culture, but SoMo was completely blocked [143]. Parasites did not form any projections. Additional work demonstrated that intracellular cAMP increased in the cell upon loss of PDEB1, and experiments with cAMP analogs revealed that cAMP itself is the active molecule, not metabolic breakdown products [143]. On the other hand, upon loss of AC1, AC1 and AC2 together, or AC6 by RNAi or a catalytic mutant, parasites formed many more projections than wild type *T. brucei* [142]. Knockdown of the other AC proteins (AC3, AC4, or AC5) had no effect on SoMo, suggesting they serve a different function [142]. Altogether, these results indicate that cAMP levels in the cell regulate social motility (Figure 1-4). Because cAMP signaling is important for *T. brucei* behavior *in vitro*, it follows that cAMP signaling may also be important *in vivo*. This question will be addressed in Chapter 2 of this dissertation.

The correlation between the ability to engage in SoMo and to infect a tsetse fly has been demonstrated through the loss of the protein Requires Fifty Three 1 (RFT1), which is involved in N-linked glycosylation [146]. Loss of RFT1 in *T. brucei* results in a delayed SoMo phenotype: projections form later than in wild type [147]. In the fly, this SoMo defect correlated with a defect in tsetse fly midgut infection [147]. The identification of other regulators of social motility is an active area of research, and new work on this topic will be discussed in Chapter 3 of this dissertation.

The discovery of SoMo also demonstrated that *T. brucei* cells moving as a group can reorient their group movements in response to external signals [144]. Adjacent projections of T. brucei maintain an even spacing between one another, suggesting that there may be an inhibitory signal that prevents projections from getting too close to one another. Similarly, when two separate groups of parasites engage in SoMo on the same petri dish, the projections will change their course to avoid intersecting or colliding with projections from the other group (Figure 1-5) [144]. This ability to alter group movement in response to an extracellular cue could be important for *T. brucei* transmission through is hosts, just as group behaviors aid other microbes in surface colonization and infection [2, 5]. The ability of social *T. brucei* to sense cues from the environment and change the direction of group movement in response will be discussed in Chapter 4 of this dissertation.

T. brucei as a Model System

T. brucei and related trypanosomatids represent a devastating public health burden. It is necessary to elucidate the signaling pathways that regulate *T. brucei* behavior in order to identify novel transmission blocking agents and therapeutics. In addition to being a medically and economically important pathogen, *T. brucei* also serves as a model to study the eukaryotic flagellum.

T. brucei is a useful model system in which to address these questions because it is incredibly amenable to molecular biology techniques. Two of the main life-cycle stages can be cultured *in vitro*: long-slender bloodstream form and procyclic-form cells [148], alleviating the need to infect the parasites in animals hosts to continue studying them. However, for *in vivo* analysis, the mouse serves as a well-defined animal model for mammalian infection, and tsetse

flies can be maintained in the laboratory for fly infection studies. Additionally, *T. brucei* are a genetically-tractable system. They undergo efficient homologous recombination, and the existence of multiple drug resistance markers facilitates the generation of genetic knockouts, gene-tagging, and inducible expression [148]. Recent advances have made molecular cloning even faster in trypanosomes through the use of long-primer PCR [149]. Not only can this method be used to tag proteins, but it can also be used to make genetic knockouts. The group behind the development of this technique has used it to attempt to localize every protein in the genome and to make the results publically available on TrypTag.org as a resource for the trypanosome community [150].

T. brucei also has a completely sequenced and annotated genome. This allows for the use of systems-level approaches answer important biological questions about these organisms, as discussed in detail in Chapter 3. Transcriptomics, proteomics, and APEX proximity proteomics have been important tools in the study of these parasites.

This dissertation will describe the use of these tools to understand the signaling systems that underlie social motility in *T. brucei*. Over the course of this dissertation work, new techniques were also developed and implemented to address these questions. Chapter 2 will describe new tsetse fly dissection methods developed my Sebastian Shaw and myself. Additionally, Chapter 4 describes the development of a *T. brucei* chemotaxis assay and the use of time-lapse video and motility analysis to study cells engaging in social motility. The work presented here deepens the *T. brucei* field's knowledge of *T. brucei* signaling and social motility and will serve as the basis for future studies.

Figures:

Figure 1-1: A single procyclic-form *Trypanosoma brucei* cell

A scanning electron micrograph of *T. brucei* is shown. The cell body is pseudo-colored orange, and the flagellum is pseudo-colored red. Image by: Richard Wheeler. It is licensed for reuse under the Creative Commons Attribution-Share Alike 3.0 Unported license.

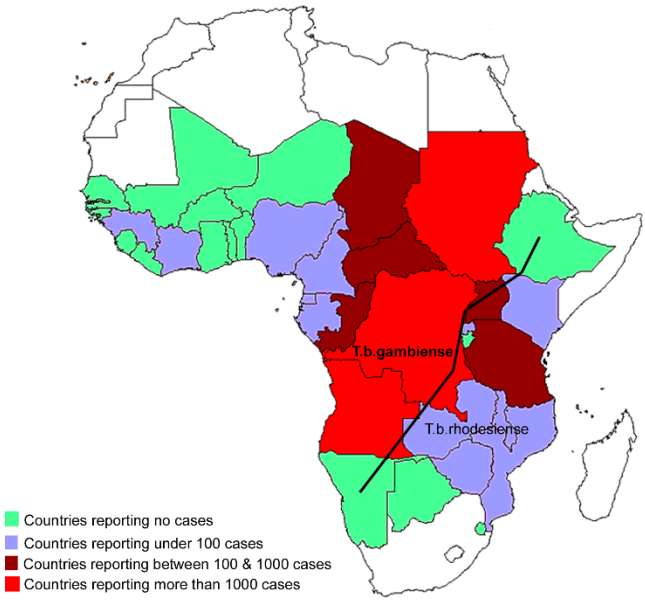

Figure 1-2: The distribution of sleeping sickness in sub-Saharan Africa

T. brucei gambiense is endemic to the western and central regions of sub-Saharan Africa, while *T. brucei rhodesiense* is found in the eastern and southern regions. This image is from Simarro et al (2008). Eliminating Human African Trypanosomiasis: Where Do We Stand and What Comes Next? PLoS Med 5(2): e55. https://doi.org/10.1371/journal.pmed.0050055 [151]. Licensed for reuse under the Creative Commons license.

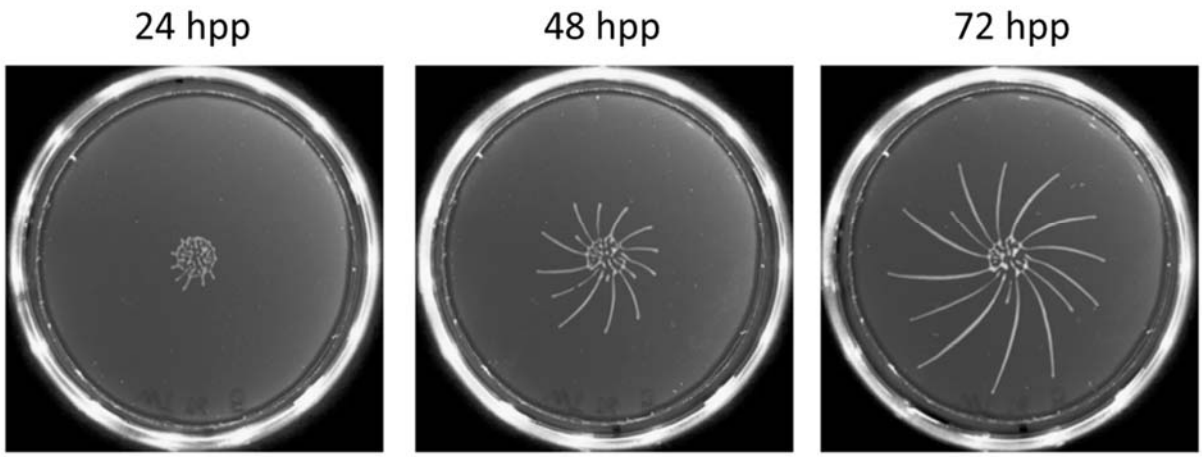

Figure 1-3: Social Motility (SoMo) in *Trypanosoma brucei*

Early-procyclic *T. brucei* cells engage in social motility on semi-solid agarose plates. Image adapted from Imhof et al (2014). Social Motility of African Trypanosomes Is a Property of a Distinct Life-Cycle Stage That Occurs Early in Tsetse Fly Transmission. PLoS Pathog 10(10): e1004493. https://doi.org/10.1371/journal.ppat.1004493 [145]. Image licensed for reuse under the Creative Commons Attribution License.

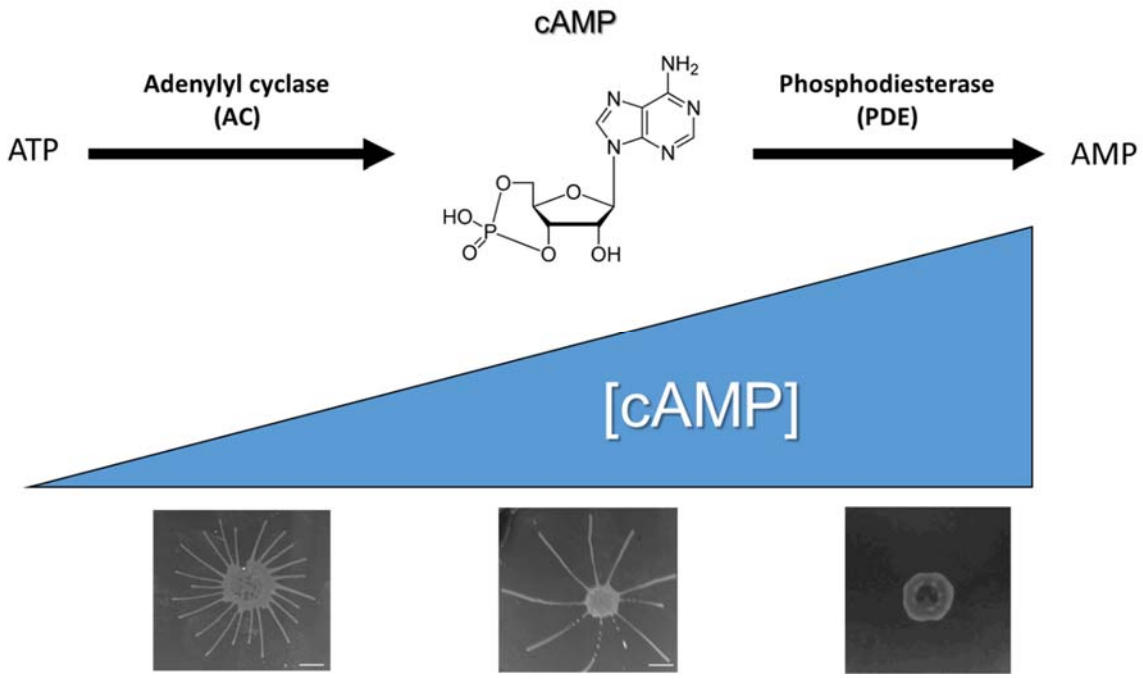

Figure 1-4: *T. brucei* cAMP levels regulate Social Motility

Low levels of cAMP production due to loss of adenylate cyclase expression induces hypersocial behavior (left) compared to wild type (center) [142]. High levels of intracellular cAMP lead to a block in social motility (right) [143].

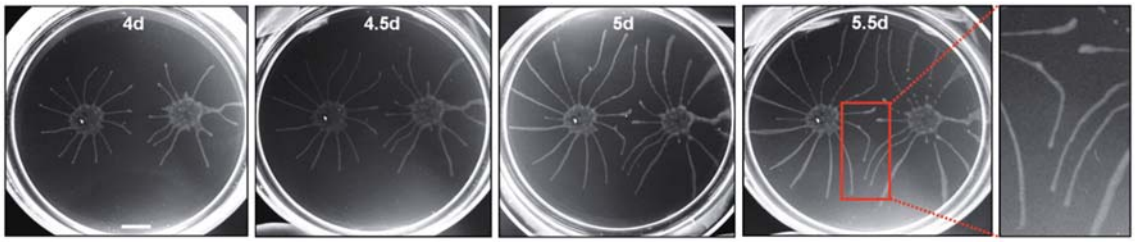

Figure 1-5: *T. brucei* cells engaging in SoMo can sense and move to avoid intersecting with other projections

Projections of *T. brucei* alter their natural path to avoid colliding with other projections of parasites. Images adapted from Oberholzer et al (2010). Social Motility in African Trypanosomes. PLoS Pathog 6(1): e1000739. https://doi.org/10.1371/journal.ppat.1000739 [144]. Images licensed for reuse by the Creative Commons Attribution License.

Bibliography

1. Noffke, N., et al., *Microbially induced sedimentary structures recording an ancient ecosystem in the ca. 3.48 billion-year-old Dresser Formation, Pilbara, Western Australia.* Astrobiology, 2013. **13**(12): p. 1103-24.
2. Shapiro, J.A., *Thinking about bacterial populations as multicellular organisms.* Annu Rev Microbiol, 1998. **52**: p. 81-104.
3. Li, S.I. and M.D. Purugganan, *The cooperative amoeba: Dictyostelium as a model for social evolution.* Trends Genet, 2011. **27**(2): p. 48-54.
4. Bassler, B.L. and R. Losick, *Bacterially speaking.* Cell, 2006. **125**(2): p. 237-46.
5. Harshey, R.M., *Bacterial motility on a surface: many ways to a common goal.* Annu Rev Microbiol, 2003. **57**: p. 249-73.
6. Fraser, G.M. and C. Hughes, *Swarming motility.* Curr Opin Microbiol, 1999. **2**(6): p. 630-5.
7. Butler, M.T., Q. Wang, and R.M. Harshey, *Cell density and mobility protect swarming bacteria against antibiotics.* Proc Natl Acad Sci U S A, 2010. **107**(8): p. 3776-81.
8. Kearns, D.B., *A field guide to bacterial swarming motility.* Nat Rev Microbiol, 2010. **8**(9): p. 634-44.
9. Shaulsky, G. and R.H. Kessin, *The cold war of the social amoebae.* Curr Biol, 2007. **17**(16): p. R684-92.
10. WALKER, P.J., *Organization of function in trypanosome flagella.* Nature, 1961. **189**: p. 1017-8.
11. Langousis, G. and K.L. Hill, *Motility and more: the flagellum of Trypanosoma brucei.* Nat Rev Microbiol, 2014. **12**(7): p. 505-18.

12. Gruby, M., *Recherches et observations sur une nouvelle espèce d'hématozoaire, Trypanosoma sanguinis*. 1843, Comptes Rendus Hebdomadaire Séances l'Académie *Sci.*: Paris. p. 1134-1136.

13. Lukeš, J., et al., *Evolution of parasitism in kinetoplastid flagellates.* Mol Biochem Parasitol, 2014. **195**(2): p. 115-22.

14. Lukeš, J., et al., *Trypanosomatids Are Much More than Just Trypanosomes: Clues from the Expanded Family Tree.* Trends Parasitol, 2018. **34**(6): p. 466-480.

15. Vickerman, K., *Polymorphism and mitochondrial activity in sleeping sickness trypanosomes.* Nature, 1965. **208**(5012): p. 762-6.

16. Lukes, J., H. Hashimi, and A. Zíková, *Unexplained complexity of the mitochondrial genome and transcriptome in kinetoplastid flagellates.* Curr Genet, 2005. **48**(5): p. 277-99.

17. Liu, B., et al., *Fellowship of the rings: the replication of kinetoplast DNA.* Trends Parasitol, 2005. **21**(8): p. 363-9.

18. Stuart, K., et al., *Kinetoplastids: related protozoan pathogens, different diseases.* J Clin Invest, 2008. **118**(4): p. 1301-10.

19. Montgomery, S.P., et al., *What Do We Know About Chagas Disease in the United States?* Am J Trop Med Hyg, 2016. **95**(6): p. 1225-1227.

20. Curtis-Robles, R., et al., *Analysis of over 1500 triatomine vectors from across the US, predominantly Texas, for Trypanosoma cruzi infection and discrete typing units.* Infect Genet Evol, 2018. **58**: p. 171-180.

21. Carmona-Castro, O., D.A. Moo-Llanes, and J.M. Ramsey, *Impact of climate change on vector transmission of Trypanosoma cruzi (Chagas, 1909) in North America.* Med Vet Entomol, 2018. **32**(1): p. 84-101.

22. Akhoundi, M., et al., *A Historical Overview of the Classification, Evolution, and Dispersion of Leishmania Parasites and Sandflies.* PLoS Negl Trop Dis, 2016. **10**(3): p. e0004349.

23. WHO. *Leishmaniasis*. 2019 March 14, 2019 [cited 2019 May 14].

24. Cayla, M., et al., *African trypanosomes.* Parasit Vectors, 2019. **12**(1): p. 190.

25. Rotureau, B. and J. Van Den Abbeele, *Through the dark continent: African trypanosome development in the tsetse fly.* Front Cell Infect Microbiol, 2013. **3**: p. 53.

26. Welburn, S.C., et al., *Identification of human-infective trypanosomes in animal reservoir of sleeping sickness in Uganda by means of serum-resistance-associated (SRA) gene.* Lancet, 2001. **358**(9298): p. 2017-9.

27. Enyaru, J.C., et al., *Detection of T.b. rhodesiense trypanosomes in humans and domestic animals in south east Uganda by amplification of serum resistance-associated gene.* Ann N Y Acad Sci, 2006. **1081**: p. 311-9.

28. Gibson, W., et al., *The identification of Trypanosoma brucei gambiense in Liberian pigs and dogs by isoenzymes and by resistance to human plasma.* Tropenmed Parasitol, 1978. **29**(3): p. 335-45.

29. Funk, S., et al., *Identifying transmission cycles at the human-animal interface: the role of animal reservoirs in maintaining gambiense human african trypanosomiasis.* PLoS Comput Biol, 2013. **9**(1): p. e1002855.

30. Brun, R., et al., *Human African trypanosomiasis.* Lancet, 2010. **375**(9709): p. 148-59.

31. Kennedy, P.G.E. and J. Rodgers, *Clinical and Neuropathogenetic Aspects of Human African Trypanosomiasis.* Front Immunol, 2019. **10**: p. 39.

32. Rijo-Ferreira, F., et al., *Sleeping sickness is a circadian disorder.* Nat Commun, 2018. **9**(1): p. 62.

33. Lindner, A.K. and G. Priotto, *The unknown risk of vertical transmission in sleeping sickness--a literature review.* PLoS Negl Trop Dis, 2010. **4**(12): p. e783.

34. De Kyvon, M.A., et al., *Congenital Trypanosomiasis in Child Born in France to African Mother.* Emerg Infect Dis, 2016. **22**(5): p. 935-7.

35. Odiit, M., F. Kansiime, and J.C. Enyaru, *Duration of symptoms and case fatality of sleeping sickness caused by Trypanosoma brucei rhodesiense in Tororo, Uganda.* East Afr Med J, 1997. **74**(12): p. 792-5.

36. Checchi, F., et al., *Estimates of the duration of the early and late stage of gambiense sleeping sickness.* BMC Infect Dis, 2008. **8**: p. 16.

37. Cecchi, G., et al., *Land cover and tsetse fly distributions in sub-Saharan Africa.* Med Vet Entomol, 2008. **22**(4): p. 364-73.

38. Ngonyoka, A., et al., *Variation of tsetse fly abundance in relation to habitat and host presence in the Maasai Steppe, Tanzania.* J Vector Ecol, 2017. **42**(1): p. 34-43.

39. Büscher, P., et al., *Human African trypanosomiasis.* Lancet, 2017. **390**(10110): p. 2397-2409.

40. Torr, S.J., et al., *Where, when and why do tsetse contact humans? Answers from studies in a national park of Zimbabwe.* PLoS Negl Trop Dis, 2012. **6**(8): p. e1791.

41. Molyneux, D., et al., *Zoonoses and marginalised infectious diseases of poverty: where do we stand?* Parasit Vectors, 2011. **4**: p. 106.

42. Bukachi, S.A., S. Wandibba, and I.K. Nyamongo, *The socio-economic burden of human African trypanosomiasis and the coping strategies of households in the South Western Kenya foci.* PLoS Negl Trop Dis, 2017. **11**(10): p. e0006002.

43. WHO. *Trypanosomiasis, human African (sleeping sickness).* 2019 [cited 2019 May 15]; Available from: https://www.who.int/news-room/fact-sheets/detail/trypanosomiasis-human-african-(sleeping-sickness).

44. Simarro, P.P., et al., *The human African trypanosomiasis control and surveillance programme of the World Health Organization 2000-2009: the way forward.* PLoS Negl Trop Dis, 2011. **5**(2): p. e1007.

45. FAO, *On target against poverty: the Programme against African Trypanosomiasis (PAAT) 1997–2007* . 2008, United Nations Food and Agricultural Organization: Rome.

46. Lambrecht, F.L., *Trypanosomes and Hominid Evolution.* BioScience, 1985. **35**(10): p. 640-646.

47. Laveran, A. and F. Mesnil, *Trypanosomes et Trypanosomiases. In Trypanosomiase Humaine ou Maladie du Sommeil.* 1912, Masson et Cie: Paris, France.

48. Hajduk, S.L., et al., *Lysis of Trypanosoma brucei by a toxic subspecies of human high density lipoprotein.* J Biol Chem, 1989. **264**(9): p. 5210-7.

49. Rifkin, M.R., *Identification of the trypanocidal factor in normal human serum: high density lipoprotein.* Proc Natl Acad Sci U S A, 1978. **75**(7): p. 3450-4.

50. Raper, J., et al., *Characterization of a novel trypanosome lytic factor from human serum.* Infect Immun, 1999. **67**(4): p. 1910-6.

51. Capewell, P., et al., *A co-evolutionary arms race: trypanosomes shaping the human genome, humans shaping the trypanosome genome.* Parasitology, 2015. **142 Suppl 1**: p. S108-19.

52. De Greef, C., et al., *A gene expressed only in serum-resistant variants of Trypanosoma brucei rhodesiense.* Mol Biochem Parasitol, 1989. **36**(2): p. 169-76.

53. De Greef, C., et al., *Only the serum-resistant bloodstream forms of Trypanosoma brucei rhodesiense express the serum resistance associated (SRA) protein.* Ann Soc Belg Med Trop, 1992. **72 Suppl 1**: p. 13-21.

54. Stephens, N.A. and S.L. Hajduk, *Endosomal localization of the serum resistance-associated protein in African trypanosomes confers human infectivity.* Eukaryot Cell, 2011. **10**(8): p. 1023-33.

55. Uzureau, P., et al., *Mechanism of Trypanosoma brucei gambiense resistance to human serum.* Nature, 2013. **501**(7467): p. 430-4.

56. Genovese, G., et al., *Association of trypanolytic ApoL1 variants with kidney disease in African Americans.* Science, 2010. **329**(5993): p. 841-5.

57. Dummer, P.D., et al., *APOL1 Kidney Disease Risk Variants: An Evolving Landscape.* Semin Nephrol, 2015. **35**(3): p. 222-36.

58. Kopp, J.B., et al., *APOL1 genetic variants in focal segmental glomerulosclerosis and HIV-associated nephropathy.* J Am Soc Nephrol, 2011. **22**(11): p. 2129-37.

59. Cooper, A., et al., *renal risk variants have contrasting resistance and susceptibility associations with African trypanosomiasis.* Elife, 2017. **6**.

60. Thomson, R., et al., *Hydrodynamic gene delivery of baboon trypanosome lytic factor eliminates both animal and human-infective African trypanosomes.* Proc Natl Acad Sci U S A, 2009. **106**(46): p. 19509-14.

61. Kageruka, P., et al., *Infectivity of Trypanosoma (Trypanozoon) brucei gambiense for baboons (Papio hamadryas, Papio papio).* Ann Soc Belg Med Trop, 1991. **71**(1): p. 39-46.

62. Raper, J. and D.J. Friedman, *Parasitology: Molecular one-upmanship.* Nature, 2013. **501**(7467): p. 322-3.

63. Steverding, D., *The history of African trypanosomiasis.* Parasit Vectors, 2008. **1**(1): p. 3.

64. Griffith, F.L., *The Petrie Papyri: Hieratic Papyri from Kahun and Gurob (principally of the Middle Kingdom).* 1898: B. Quaritch. 114.

65. Murray, M., et al., *Genetic resistance to African Trypanosomiasis.* J Infect Dis, 1984. **149**(3): p. 311-9.

66. Winkle, S., *Geißeln der Menschheit. Kulturgeschichte der Seuchen*. 3rd ed. 2005, Düsseldorf: Artemis & Winkler.

67. Williams, B.I., *African Sleeping Sickness*. 1988, Wellcome Trust.

68. WHO. *Human African trypanosomiasis. The history of sleeping sickness. Opening up towards Europe.* 2019 [cited 2019 May 15]; Available from: https://www.who.int/trypanosomiasis_african/country/history/en/index4.html.

69. Cox, F.E., *History of sleeping sickness (African trypanosomiasis).* Infect Dis Clin North Am, 2004. **18**(2): p. 231-45.

70. Valentin, G.G., *Ueber ein Entozoon im Blute von Salmo fario.* Arch Anat Physiol Wissensch Med, 1841: p. 435-436.

71. Bruce, D., *Preliminary report on the tsetse fly disease or nagana, in Zululand*. 1895: Durban.

72. Forde, R.M., *Some clinical notes on an European patient in whose blood a trypanosome was observed.* J Trop Med, 1902. **5**: p. 261-263.

73. Dutton, J.E., *Preliminary note upon a trypanosome occurring in the blood of man.* Thompson Yates Lab Rep, 1902. **4**: p. 455-468.

74. Castellani, A., *On the discovery of a species of Trypanosoma in the cerebrospinal fluid of cases of sleeping sickness.* Proceedings of the Royal Society of London, 1903. **71**: p. 501-508.

75. Stephens, J. and H. Fantham, *On the peculiar morphology of a trypanosome from a case of Sleeping Sickness and the possibility of its being a new species (T rhodesiense).* Proceedings of the Royal Society of London Series B-Containing Papers of a Biological Character, 1910. **83**(561): p. 28-33.

76. WHO. *Human African trypanosomiasis. The history of sleeping sickness. The big transcontinental epidemic.* 2019 [cited 2019 May 15]; Available from: https://www.who.int/trypanosomiasis_african/country/history/en/index5.html.

77. WHO. *Human African trypanosomiasis. The history of sleeping sickness. Scientific missions.* 2019 [cited 2019 May 15]; Available from: https://www.who.int/trypanosomiasis_african/country/history/en/index6.html.

78. Steverding, D., *The development of drugs for treatment of sleeping sickness: a historical review.* Parasit Vectors, 2010. **3**(1): p. 15.

79. Travis, A.S., *Paul Ehrlich: a hundred years of chemotherapy 1891-1991*. 1991, Biochemist. p. 9-12.

80. Dressel, J. and R.E. Oesper, *The discovery of Germanin by Oskar Dressel and Richard Kothe.* Journal of Chemical Education, 1961. **38**: p. 620-621.

81. Jacobs, W. and M. Heidelberger, *Aromatic arsenic compounds VN-substituted glycylarsanilic acids.* Journal of the American Chemical Society, 1919. **41**: p. 1809-1821.

82. Lourie, E.M., *Treatment of sleeping sickness in Sierra Leone.* Annals of Tropical Medicine & Parasitology, 1942. **36**: p. 113-131.

83. Kuzoe, F.A., *Current situation of African trypanosomiasis.* Acta Trop, 1993. **54**(3-4): p. 153-62.

84. Meyskens, F.L. and E.W. Gerner, *Development of difluoromethylornithine (DFMO) as a chemoprevention agent.* Clin Cancer Res, 1999. **5**(5): p. 945-51.

85. Deeks, E.D., *Fexinidazole: First Global Approval.* Drugs, 2019. **79**(2): p. 215-220.

86. Vickerman, K., *Developmental cycles and biology of pathogenic trypanosomes.* Br Med Bull, 1985. **41**(2): p. 105-14.

87. Cross, G.A., *Identification, purification and properties of clone-specific glycoprotein antigens constituting the surface coat of Trypanosoma brucei.* Parasitology, 1975. **71**(3): p. 393-417.

88. Mugnier, M.R., G.A. Cross, and F.N. Papavasiliou, *The in vivo dynamics of antigenic variation in Trypanosoma brucei.* Science, 2015. **347**(6229): p. 1470-3.

89. Caljon, G., et al., *The Dermis as a Delivery Site of Trypanosoma brucei for Tsetse Flies.* PLoS Pathog, 2016. **12**(7): p. e1005744.

90. Capewell, P., et al., *The skin is a significant but overlooked anatomical reservoir for vector-borne African trypanosomes.* Elife, 2016. **5**.

91. Trindade, S., et al., *Trypanosoma brucei Parasites Occupy and Functionally Adapt to the Adipose Tissue in Mice.* Cell Host Microbe, 2016. **19**(6): p. 837-48.

92. Capewell, P., et al., *Resolving the apparent transmission paradox of African sleeping sickness.* PLoS Biol, 2019. **17**(1): p. e3000105.

93. Mony, B.M., et al., *Genome-wide dissection of the quorum sensing signalling pathway in Trypanosoma brucei.* Nature, 2014. **505**(7485): p. 681-5.

94. Rojas, F., et al., *Oligopeptide Signaling through TbGPR89 Drives Trypanosome Quorum Sensing.* Cell, 2019. **176**(1-2): p. 306-317.e16.

95. Moloo, S.K. and S.B. Kutuza, *Feeding and crop emptying in Glossina brevipalpis Newstead.* Acta Trop, 1970. **27**(4): p. 356-77.

96. Vassella, E., et al., *A major surface glycoprotein of trypanosoma brucei is expressed transiently during development and can be regulated post-transcriptionally by glycerol or hypoxia.* Genes Dev, 2000. **14**(5): p. 615-26.

97. Gibson, W. and M. Bailey, *The development of Trypanosoma brucei within the tsetse fly midgut observed using green fluorescent trypanosomes.* Kinetoplastid Biol Dis, 2003. **2**(1): p. 1.

98. Lehane, M.J., P.G. Allingham, and P. Weglicki, *Composition of the peritrophic matrix of the tsetse fly, Glossina morsitans morsitans.* Cell Tissue Res, 1996. **283**(3): p. 375-84.

99. Lehane, M.J., *Peritrophic matrix structure and function.* Annu Rev Entomol, 1997. **42**: p. 525-50.

100. Hao, Z., I. Kasumba, and S. Aksoy, *Proventriculus (cardia) plays a crucial role in immunity in tsetse fly (Diptera: Glossinidiae).* Insect Biochem Mol Biol, 2003. **33**(11): p. 1155-64.

101. Rose, C., et al., *An investigation into the protein composition of the teneral Glossina morsitans morsitans peritrophic matrix.* PLoS Negl Trop Dis, 2014. **8**(4): p. e2691.

102. Sharma, R., et al., *The heart of darkness: growth and form of Trypanosoma brucei in the tsetse fly.* Trends Parasitol, 2009. **25**(11): p. 517-24.

103. Van Den Abbeele, J., et al., *Trypanosoma brucei spp. development in the tsetse fly: characterization of the post-mesocyclic stages in the foregut and proboscis.* Parasitology, 1999. **118 (Pt 5)**: p. 469-78.

104. Sharma, R., et al., *Asymmetric cell division as a route to reduction in cell length and change in cell morphology in trypanosomes.* Protist, 2008. **159**(1): p. 137-51.

105. Portman, N. and K. Gull, *The paraflagellar rod of kinetoplastid parasites: from structure to components and function.* Int J Parasitol, 2010. **40**(2): p. 135-48.

106. Oberholzer, M., et al., *The Trypanosoma brucei cAMP phosphodiesterases TbrPDEB1 and TbrPDEB2: flagellar enzymes that are essential for parasite virulence.* FASEB J, 2007. **21**(3): p. 720-31.

107. Portman, N., et al., *Combining RNA interference mutants and comparative proteomics to identify protein components and dependences in a eukaryotic flagellum.* J Biol Chem, 2009. **284**(9): p. 5610-9.

108. Bloodgood, R.A., *Sensory reception is an attribute of both primary cilia and motile cilia.* J Cell Sci, 2010. **123**(Pt 4): p. 505-9.

109. Singla, V. and J.F. Reiter, *The primary cilium as the cell's antenna: signaling at a sensory organelle.* Science, 2006. **313**(5787): p. 629-33.

110. Berbari, N.F., et al., *The primary cilium as a complex signaling center.* Curr Biol, 2009. **19**(13): p. R526-35.

111. Nauli, S.M., et al., *Polycystins 1 and 2 mediate mechanosensation in the primary cilium of kidney cells.* Nat Genet, 2003. **33**(2): p. 129-37.

112. Praetorius, H.A. and K.R. Spring, *Bending the MDCK cell primary cilium increases intracellular calcium.* J Membr Biol, 2001. **184**(1): p. 71-9.

113. Praetorius, H.A. and K.R. Spring, *The renal cell primary cilium functions as a flow sensor.* Curr Opin Nephrol Hypertens, 2003. **12**(5): p. 517-20.

114. Follain, G. and J.G. Goetz, *Synergistic Mechano-Chemical Sensing by Vascular Cilia.* Trends Cell Biol, 2018. **28**(7): p. 507-508.

115. Goetz, J.G., et al., *Endothelial cilia mediate low flow sensing during zebrafish vascular development.* Cell Rep, 2014. **6**(5): p. 799-808.

116. Insinna, C. and J.C. Besharse, *Intraflagellar transport and the sensory outer segment of vertebrate photoreceptors.* Dev Dyn, 2008. **237**(8): p. 1982-92.

117. McEwen, D.P., P.M. Jenkins, and J.R. Martens, *Olfactory cilia: our direct neuronal connection to the external world.* Curr Top Dev Biol, 2008. **85**: p. 333-70.

118. Jones, C. and P. Chen, *Primary cilia in planar cell polarity regulation of the inner ear.* Curr Top Dev Biol, 2008. **85**: p. 197-224.

119. Fischer, E. and M. Pontoglio, *Planar cell polarity and cilia.* Semin Cell Dev Biol, 2009. **20**(8): p. 998-1005.

120. Huangfu, D., et al., *Hedgehog signalling in the mouse requires intraflagellar transport proteins.* Nature, 2003. **426**(6962): p. 83-7.

121. Goetz, S.C. and K.V. Anderson, *The primary cilium: a signalling centre during vertebrate development.* Nat Rev Genet, 2010. **11**(5): p. 331-44.

122. Kim, J., M. Kato, and P.A. Beachy, *Gli2 trafficking links Hedgehog-dependent activation of Smoothened in the primary cilium to transcriptional activation in the nucleus.* Proc Natl Acad Sci U S A, 2009. **106**(51): p. 21666-71.

123. Pan, J., Q. Wang, and W.J. Snell, *Cilium-generated signaling and cilia-related disorders.* Lab Invest, 2005. **85**(4): p. 452-63.

124. Krüger, T. and M. Engstler, *Flagellar motility in eukaryotic human parasites.* Semin Cell Dev Biol, 2015. **46**: p. 113-27.

125. Maric, D., C.L. Epting, and D.M. Engman, *Composition and sensory function of the trypanosome flagellar membrane.* Curr Opin Microbiol, 2010. **13**(4): p. 466-72.

126. Rotureau, B., et al., *The flagellum-mitogen-activated protein kinase connection in Trypanosomatids: a key sensory role in parasite signalling and development?* Cell Microbiol, 2009. **11**(5): p. 710-8.

127. Tetley, L. and K. Vickerman, *Differentiation in Trypanosoma brucei: host-parasite cell junctions and their persistence during acquisition of the variable antigen coat.* J Cell Sci, 1985. **74**: p. 1-19.

128. Oberholzer, M., et al., *Independent analysis of the flagellum surface and matrix proteomes provides insight into flagellum signaling in mammalian-infectious Trypanosoma brucei.* Mol Cell Proteomics, 2011. **10**(10): p. M111.010538.

129. Saada, E.A., et al., *Insect stage-specific receptor adenylate cyclases are localized to distinct subdomains of the Trypanosoma brucei Flagellar membrane.* Eukaryot Cell, 2014. **13**(8): p. 1064-76.

130. Gould, M.K. and H.P. de Koning, *Cyclic-nucleotide signalling in protozoa.* FEMS Microbiol Rev, 2011. **35**(3): p. 515-41.

131. Marinissen, M.J. and J.S. Gutkind, *G-protein-coupled receptors and signaling networks: emerging paradigms.* Trends Pharmacol Sci, 2001. **22**(7): p. 368-76.

132. Shalaby, T., M. Liniger, and T. Seebeck, *The regulatory subunit of a cGMP-regulated protein kinase A of Trypanosoma brucei.* Eur J Biochem, 2001. **268**(23): p. 6197-206.

133. Bachmaier, S., et al., *Nucleoside analogue activators of cyclic AMP-independent protein kinase A of Trypanosoma.* Nat Commun, 2019. **10**(1): p. 1421.

134. Gould, M.K., et al., *Cyclic AMP effectors in African trypanosomes revealed by genome-scale RNA interference library screening for resistance to the phosphodiesterase inhibitor CpdA.* Antimicrob Agents Chemother, 2013. **57**(10): p. 4882-93.

135. Fredriksson, R. and H.B. Schiöth, *The repertoire of G-protein-coupled receptors in fully sequenced genomes.* Mol Pharmacol, 2005. **67**(5): p. 1414-25.

136. Alexandre, S., et al., *Differential expression of a family of putative adenylate/guanylate cyclase genes in Trypanosoma brucei.* Mol Biochem Parasitol, 1990. **43**(2): p. 279-88.

137. Emes, R.D. and Z. Yang, *Duplicated paralogous genes subject to positive selection in the genome of Trypanosoma brucei.* PLoS One, 2008. **3**(5): p. e2295.

138. Paindavoine, P., et al., *A gene from the variant surface glycoprotein expression site encodes one of several transmembrane adenylate cyclases located on the flagellum of Trypanosoma brucei.* Mol Cell Biol, 1992. **12**(3): p. 1218-25.

139. Savage, A.F., et al., *Transcriptome Profiling of Trypanosoma brucei Development in the Tsetse Fly Vector Glossina morsitans.* PLoS One, 2016. **11**(12): p. e0168877.

140. Naguleswaran, A., N. Doiron, and I. Roditi, *RNA-Seq analysis validates the use of culture-derived Trypanosoma brucei and provides new markers for mammalian and insect life-cycle stages.* BMC Genomics, 2018. **19**(1): p. 227.

141. Shimogawa, M.M., et al., *Cell Surface Proteomics Provides Insight into Stage-Specific Remodeling of the Host-Parasite Interface in Trypanosoma brucei.* Mol Cell Proteomics, 2015. **14**(7): p. 1977-88.

142. Lopez, M.A., E.A. Saada, and K.L. Hill, *Insect stage-specific adenylate cyclases regulate social motility in African trypanosomes.* Eukaryot Cell, 2015. **14**(1): p. 104-12.

143. Oberholzer, M., E.A. Saada, and K.L. Hill, *Cyclic AMP Regulates Social Behavior in African Trypanosomes.* MBio, 2015. **6**(3): p. e01954-14.

144. Oberholzer, M., et al., *Social motility in african trypanosomes.* PLoS Pathog, 2010. **6**(1): p. e1000739.

145. Imhof, S., et al., *Social motility of African trypanosomes is a property of a distinct life-cycle stage that occurs early in tsetse fly transmission.* PLoS Pathog, 2014. **10**(10): p. e1004493.

146. Jelk, J., et al., *Glycoprotein biosynthesis in a eukaryote lacking the membrane protein Rft1.* J Biol Chem, 2013. **288**(28): p. 20616-23.

147. Imhof, S., et al., *A Glycosylation Mutant of Trypanosoma brucei Links Social Motility Defects In Vitro to Impaired Colonization of Tsetse Flies In Vivo.* Eukaryot Cell, 2015. **14**(6): p. 588-92.

148. Oberholzer, M., et al., *Approaches for functional analysis of flagellar proteins in African trypanosomes.* Methods Cell Biol, 2009. **93**: p. 21-57.

149. Dean, S., et al., *A toolkit enabling efficient, scalable and reproducible gene tagging in trypanosomatids.* Open Biol, 2015. **5**(1): p. 140197.

150. Dean, S., J.D. Sunter, and R.J. Wheeler, *TrypTag.org: A Trypanosome Genome-wide Protein Localisation Resource.* Trends Parasitol, 2017. **33**(2): p. 80-82.

151. Simarro, P.P., J. Jannin, and P. Cattand, *Eliminating human African trypanosomiasis: where do we stand and what comes next?* PLoS Med, 2008. **5**(2): p. e55.

Chapter 2 – Flagellar cAMP signaling controls trypanosome progression through host tissues

Abstract

The unicellular parasite *Trypanosoma brucei* is transmitted between mammals by tsetse flies. Following the discovery that flagellar phosphodiesterase PDEB1 is required for trypanosomes to move in response to signals *in vitro* (social motility), we investigated its role in tsetse flies. Here we show that PDEB1 knockout parasites exhibit subtle changes in movement, reminiscent of bacterial chemotaxis mutants. Infecting flies with the knockout, followed by live confocal microscopy of fluorescent parasites within dual-labelled insect tissues, shows that PDEB1 is important for traversal of the peritrophic matrix, which separates the midgut lumen from the ectoperitrophic space. Without PDEB1, parasites are trapped in the lumen and cannot progress through the cycle. This demonstrates that the peritrophic matrix is a barrier that must be actively overcome and that the parasite's flagellar cAMP signaling pathway facilitates this. Migration may depend on perception of chemotactic cues, which could stem from co-infecting parasites and/or the insect host.

Introduction

A common feature of parasitic protozoa is the need to sense and adapt to diverse environments in different hosts and tissues within these hosts. At present, however, little is known about mechanisms of signal transduction in these organisms and how these impact transmission and pathogenesis. *Trypanosoma brucei ssp* are medically and economically important parasites that are prevalent in sub-Saharan Africa. Two sub-species, *T. b. gambiense*

and *T. b. rhodesiense* are responsible for human sleeping sickness, while *T. b. brucei* causes the animal disease Nagana. Restriction of the parasites to sub-Saharan Africa is determined by the geographic range of the tsetse fly, which is their definitive host and is crucial for their transmission between mammals.

Like many unicellular parasites, *T. brucei* has a complex life cycle that requires it to undergo several rounds of differentiation, migrate through diverse tissues, and traverse a variety of barriers in both its mammalian and fly hosts [1]. At least two forms exist in the mammal, a proliferative slender form and a quiescent stumpy form that is preadapted for transmission when tsetse flies take a blood meal from an infected animal [2]. Transition between these two developmental forms occurs in response to an extracellular signal [3]. Following ingestion by the fly, the blood meal rapidly passes to the crop, after which it is transferred to the lumen of the posterior midgut (Figure 2-1) [4, 5]. Here, stumpy forms differentiate into early procyclic forms and replace the mammalian-specific variant surface glycoprotein coat with a mixture of GPEET and EP procyclins [6, 7]. To progress further through their life cycle, the parasites must gain access to the ectoperitrophic space. This entails crossing the peritrophic matrix (PM), a trilaminar sheath of chitin, (glyco)proteins, and glycosaminoglycans [8]. At present, the site and mechanism of crossing are unclear [9]. Establishment of midgut infection correlates with parasite differentiation to late procyclic forms, which are EP-positive, but GPEET-negative [7]. As the infection proceeds, parasites fill the ectoperitrophic space and move toward the anterior midgut [10-12]. Two other morphological forms have been described in this compartment, long procyclic forms [12] and mesocyclic forms [1, 10].

In the next phase of the life cycle, parasites must cross the PM a second time. This occurs at the proventriculus (or cardia), the junction between the mid- and foregut and site of PM

secretion [8]. Although colonization of the proventriculus was described more than a century ago [4], relatively little attention has been paid to the role of this organ in the trypanosome life cycle [10-15]. From the proventriculus, the parasites move via the foregut to the salivary glands. A variety of post-mesocyclic forms have been described, including long epimastigotes that undergo an asymmetric division [10, 11] and deliver short epimastigotes to the salivary glands. Short epimastigotes colonize the salivary gland epithelia, completing the cycle with differentiation to metacyclic forms that can be transmitted to a new mammalian host [1].

Throughout its developmental cycle, *T. brucei* must be able to sense its environment and transduce signals that effect its differentiation to the next developmental stage and/or movement to the next compartment. In many organisms, cyclic nucleotides are important second messengers that direct cellular responses to external signals. Well-studied examples include chemotaxis of invertebrate sperm [16], as well as fruiting body formation in *Dictyostelium discoideum*, where cAMP acts as both signal and second messenger [17]. In bacteria, intracellular cyclic nucleotides regulate the transition between biofilm formation and swarming motility in response to quorum-sensing signals [18], thereby impacting both differentiation and movement. In general, cyclic nucleotide levels in these systems are controlled by reciprocal activities of nucleotide cyclases that generate the signal and phosphodiesterases (PDEs) that remove the signal [18].

The *T. brucei* genome encodes cAMP signaling components, although these differ in several respects from those in mammalian cells [19]. For example, the *T. brucei* protein kinase A does not appear to be directly responsive to cAMP [19]. *T. brucei* also lacks conventional G protein-coupled receptors (GPCRs), which typically mediate extracellular ligand-dependent activation of adenylate cyclase (AC) [20]. This deficit seems to be accommodated by a family of

~75 receptor-type ACs [21, 22] that are structurally very different than their mammalian counterparts and not affected by pharmacological treatments that activate mammalian ACs. The catalytic domain of trypanosome ACs is connected by a single transmembrane domain to a variable extracellular domain. This architecture offers the potential to regulate cAMP production by external ligands binding directly to the cyclase, rather than to an upstream GPCR. All ACs investigated so far are localized to the flagellum, where they have been implicated in parasite signaling and motility in culture [23-25]. AC isoforms are differentially expressed throughout the *T. brucei* life cycle [21, 23, 24, 26-28], suggesting they may each respond to distinct cues encountered only in specific host tissues. Consistent with a role for cAMP in differentiation, increased AC activity was observed to coincide with stumpy to procyclic differentiation *in vitro* [29, 30]. In bloodstream form *T. brucei*, the bloodstream stage-specific AC, ESAG4, has been demonstrated to influence infection in the mammalian host [31]. In this case, however, cAMP was proposed to act on host cell function rather than as a second messenger within the parasite.

The *T. brucei* genome encodes five PDEs: PDEA, PDEB1, PDEB2, PDEC, and PDED. PDEA is neither essential for bloodstream or procyclic forms, nor is it required for fly midgut infection [32]. RNAi knockdown of PDEB1 and PDEB2 together is lethal in bloodstream form trypanosomes, but knockdown of either protein alone does not affect viability [33] and their role in trypanosome biology, beyond being essential, is unclear. Knockdown of PDEB1 and PDEB2, singly or in combination, does not have detrimental effects on growth or motility of procyclic forms in liquid culture [33].

Evidence for a role of cAMP beyond parasite viability has come from studies of collective cell motility [25, 34]. When early procyclic forms are cultured on a semi-solid surface, they exhibit a type of coordinated group movement termed social motility (SoMo) in which the

parasites assemble into groups that sense signals from other cells and alter their movement in response [35, 36]. Genetic or pharmacological inhibition of PDEB1 blocks SoMo, while reduced expression or ablation of catalytic activity of specific ACs results in hypersocial behavior [25, 34]. These findings indicate that flux through the cAMP pathway regulates how the parasites respond to signals from their environment. Direct measurement of intracellular cAMP levels in live trypanosomes supports this idea, and experiments with cAMP analogues demonstrate that cAMP itself is the active molecule, rather than metabolic breakdown products [34]. Together, these studies demonstrate that *T. brucei* harbors a functional cAMP signal transduction pathway and that signals from this pathway can alter parasite behavior. To date, however, it is not known whether this pathway is required for infection or transmission.

Here, we infect tsetse flies with a *T. brucei* PDEB1 deletion mutant and use dual labeling of parasites and fly tissues to interrogate the role of flagellar cAMP signaling in parasite movement through the fly. We show that PDEB1 is required for traversal of the peritrophic matrix, a chitinous structure that separates the fly midgut lumen from the midgut epithelium. Without PDEB1, most parasites remain trapped in the midgut lumen and the transmission cycle is aborted. Our results reveal a tissue-specific requirement for cAMP signaling and show that the flagellar cAMP signaling pathway of *T. brucei* is crucial for successful progression through tissues in the tsetse fly host.

Results

Generation of a T. brucei PDEB1-null mutant

Previous work showed that phosphodiesterase PDEB1 mRNA was reduced 90% by RNAi in procyclic forms with only minimal effects on growth [34]. Given the residual PDEB1

mRNA, together with the uncertainty of whether knockdown occurs equally efficiently in different fly tissues, we reasoned that these lines would not be suitable for fly infection studies. Therefore, as a prelude to examining the role of PDEB1 during transmission by the tsetse fly, a null mutant of PDEB1 was generated in early procyclic forms. PCR data (Figure 2-2) and northern blot analysis confirmed that the PDEB1 gene was deleted from the knockout (KO), that mRNA was not detectable, and that the level of PDEB2 mRNA was unchanged compared with the parental line (Figure 2-3a). Knocking out PDEB1 had no impact on the population doubling time (KO, 9.1 ± 0.36 h) compared with the wild-type parent (WT, 9.0 ± 0.21 h; Figure 2-3b). WT and KO cells were also tagged with cytoplasmic dsRed for later experiments. Expression of dsRed had a slight effect on growth, but population doubling times were not substantially different between WT-dsRed (9.5 ± 0.07 h) and KO-dsRed (9.9 ± 0.21 h; Figure 2-3b). Since the environment in the fly is presumed to be glucose-poor, we also tested growth in a medium with or without glucose. Both WT and KO grew equally well irrespective of whether glucose was present or not (Supplementary Figures 2h, i).

Because parasite propulsive motility impacts fly infection [37], we performed motility tracing in suspension culture. We also generated a trypanin knockout (TPN KO) in the same background as PDEB1 KO to serve as a control for a known motility mutant. WT, KO, and TPN KO cells were then assessed for propulsive motility. PDEB1 KO cells do not exhibit a loss of motility; rather, they had a greater mean-squared displacement (MSD) than WT. TPN KO cells have a severe motility defect, as expected (Figure 2-3c). Because MSD incorporates processivity, differences in MSD can be due to the speed of a cell and/or how straight it moves. Therefore, we examined curvilinear (VCL) and straight-line velocity (VSL) for each population of WT, KO, and TPN KO cells. The VCL and VSL distribution of cell trajectories indicate that WT and

PDEB1 KO cells move similarly, while TPN KO clearly shows reduced VSL (Figure 3-5). The mean linearity, a ratio of VSL/VCL [38], of PDEB1 KO is similar though slightly larger than WT, while that of TPN KO cells is substantially reduced (Figure 3-5). These results indicate that the greater MSD in PDEB1 KO cells may reflect less turning compared with WT. Note that reduced turning is also observed in bacterial chemotaxis regulatory mutants [39]. High-speed video analysis of WT, KO, and TPN KO cells shows that WT and KO cells exhibit the normal three-dimensional tip-to-base flagellar waveform, while TPN KO cells do not (Figure 2-3d and Movies 2-1–2-3).

When analyzed for SoMo (Figure 2-3e), the PDEB1 KO showed the same SoMo-negative phenotype as the RNAi line. Since SoMo is restricted to early procyclic forms [40] one possibility was that removal of PDEB1 caused cells to differentiate to late procyclic forms. To test this, expression of the early procyclic form marker GPEET was assessed by community lifts (Figure 2-3e) and flow cytometry (Figure 2-4b, d). These analyses showed that 99% of the KO cells were GPEET-positive, indicating they are indeed early procyclic forms.

PDEB1 knockout has a defect in establishing a fly infection

To address the role of cAMP signaling in *T. brucei* during infection of its insect vector, teneral (newly hatched) tsetse flies were infected with WT or KO parasites. Flies were dissected at 3, 7, and 14 days post infection, and midguts were scored for the prevalence and intensity of infection. Fly midguts were assessed at day 3 to determine whether parasites are able to survive in the midgut lumen. Between days 3 and 7, trypanosomes cross the PM and enter the ectoperitrophic space [12, 41]. Finally, by day 14 parasites should have established a chronic midgut infection and reached the proventriculus [10, 12, 41]. In comparison with WT-infected

flies, flies infected with the KO showed a decreased prevalence and intensity of infection on days 7 and 14 (Figure 2-6a). On day 14, the endpoint of the experiment, there was a statistically significant difference in midgut infection rates ($p = 0.0144$, Fisher's exact test, two-sided). At day 14, proventriculi from flies were also examined and a major difference was observed between WT- and KO-infected flies ($p < 0.0001$, Fisher's exact test, two-sided; Figure 2-6b). In the WT group, 13 flies with a heavily infected midgut were scored for proventriculus infection; all had a heavily infected proventriculus. However, of 10 flies with a heavy midgut infection in the KO group, only one fly showed a proventriculus infection, and the intensity was weak. Therefore, even if a heavy midgut infection was established, the PDEB1-KO mutant was rarely able to progress to proventriculus infection.

PDEB1 addback rescues defects in SoMo and infection

To confirm that the SoMo and fly infection defects of KO cells were due to the absence of PDEB1, the KO was transfected with a copy of PDEB1 that integrates upstream of a procyclin locus. Northern blot analysis indicated that two independent addback clones, AB1 and AB2, expressed PDEB1 at levels 4.3-fold and 4.2-fold higher than WT (Figure 2-7a). We noted that the two clones had slightly longer population doubling times (AB1, 10 h; AB2, 10.4 h) than WT or KO parasites (Figure 2-7b), which might be due to the overexpression of PDEB1. Motility analysis of AB1 and AB2 showed that both clones have MSD and VSL/VCL ratios close to that of WT (Figure 2-7c and Figure 3-5).

The two addback clones were assessed for SoMo. In both cases, the addbacks formed radial projections, although they were fewer in number than WT (Figure 2-7d; Figure 2-8). Monitoring expression of GPEET by flow cytometry confirmed that the vast majority of addback

cells (99%; Supplementary Figures 2f and g) were still early procyclic forms. Note that the differences observed in SoMo between WT and addbacks are not simply due to overexpression of PDEB1, because the same construct did not influence SoMo when transfected into WT cells (Figure 2-8).

Flies infected with either WT, KO, AB1, or AB2 cells were assessed for midgut infection at days 3, 7, and 14, and for proventriculus infection at day 14. In this case, differences in midgut infection rates and intensities (Figure 2-9a) were less pronounced than observed in the initial fly infection experiment and were not statistically significant (Fisher's exact test, two-sided; Figure 2-9a). For each fly with a heavy midgut infection on day 14, the proventriculus was also examined. Most of the flies infected with WT also had a heavily colonized proventriculus, while the KO mutant showed a complete failure to infect the proventriculus ($p = 0.0001$, Fisher's exact test, two-sided). Both AB1 and AB2 infected the proventriculus at rates comparable with WT (Figure 2-9b). Therefore, the defect in colonization of the proventriculus can be attributed specifically to loss of PDEB1.

One possible explanation for the inability of KO cells to reach the proventriculus is that they do not differentiate from early to late procyclic forms in the fly midgut. To assess this, we examined expression of the early procyclic marker GPEET, which is expressed for the first 4–7 days post infection and is then switched off [7]. GPEET expression was monitored by IFA over the course of fly infection (Figure 2-9c, d). The WT, KO, AB1, and AB2 were all $\geq 95\%$ GPEET-positive at day 3, indicating that they were early procyclic forms, as expected. For all lines, GPEET was downregulated with similar kinetics. There was some variability at day 7, but this did not correlate with the presence or absence of PDEB1. Thus, the failure to populate the proventriculus is unlikely to be due to a defect in differentiation to the late procyclic form.

The PDEB1 knockout is not complemented by wild-type cells

Prior work with fluorescently labeled cells showed trans-complementation of the SoMo defect in the PDEB1 RNAi line by WT cells, because a mixed population was able to form radial projections with RNAi and WT cells migrating together in SoMo assays [34]. To determine whether WT cells could rescue the SoMo defect of KO cells, we used the WT-dsRed or KO-dsRed cells described above, mixed with unlabeled WT cells. Prior to performing these experiments, we mixed WT-dsRed or KO-dsRed with untagged WT cells and monitored their growth in suspension culture over a period of 14 days. Pure cultures of WT-dsRed and KO-dsRed were included as controls to assess spontaneous loss of the fluorescent protein. dsRed expression was very stable, with ≥ 94% of the population remaining fluorescent over 14 days (Figure 2-10a). As predicted from the slightly longer population doubling times of tagged cells (Figure 2-3b), these were progressively overgrown by untagged cells in mixed cultures. After 14 days, cultures initiated at a ratio of 2:1 (tagged:untagged) had 23% (WT-dsRed) and 20% (KO-dsRed) fluorescent cells, respectively (Figure 2-10a). This 2:1 ratio was used for all subsequent mixing experiments.

KO-dsRed or WT-dsRed were co-cultured on plates with untagged WT cells. Both mixtures engaged in SoMo and formed projections (Figure 2-10b). When imaged by fluorescence microscopy, WT-dsRed cells were evenly distributed throughout the projections (Figure 2-10b, upper panel). However, in contrast to the PDEB1 RNAi line, a steep gradient of KO-dsRed cells was observed. Although KO-dsRed cells did move into the projections and a few could be seen at the tip, there was a sharp fall-off as the projection extended away from the center (Figure 2-10b, lower panel). These results imply that cells that completely lack PDEB1

have an impaired response to external signals, in contrast to the RNAi line that still expresses PDEB1 at 10% of the level of WT cells [34].

It is not well understood how trypanosomes move from the midgut to the proventriculus. Given that interactions with surfaces *in vitro* [35] and with tsetse tissues *in vivo* [12] promote trypanosome collective behavior, the parasites could migrate individually or cooperatively. Alternatively, some leader cells might pave the way for other cells to follow as seen for example, during lateral line development in zebrafish [42]. We therefore asked if WT or PDEB1 KO cells impact each other's ability to infect the tsetse fly proventriculus. To assess this, coinfection experiments were performed in which flies were infected either with WT-dsRed alone, KO-dsRed alone or mixtures of WT-dsRed + untagged WT (WT + WT-dsRed), or KO-dsRed + untagged WT (WT + KO-dsRed).

On day 14, midgut infection rates with WT-dsRed alone (45%) and KO-dsRed alone (25%) (Figure 2-10c) were consistent with our earlier observations using untagged parasites (Figs. 3 and 5). Likewise, in flies with midgut infections, proventriculus infection rates were similar to those obtained with untagged cells, and there was a clear difference between WT-dsRed (83%) and KO-dsRed (18%). The intensity of proventricular infection was also reduced in the KO relative to WT, as observed for untagged cells. Therefore, dsRed cells are reliable reporters of proventriculus infection. The primary objective of these experiments was to determine whether WT cells could facilitate proventriculus infection by the KO. We therefore examined proventriculi of flies infected with KO-dsRed parasites alone versus flies coinfected with WT + KO-dsRed. Since we have never observed a proventricular infection in the absence of a midgut infection, we limited our analysis to flies that were midgut-positive (Figure 2-10d and Figure 2-11). Coinfection did not influence the proventricular infection rate by KO-dsRed cells,

as the KO-dsRed infection rate in mixed infections (18%) was the same as that observed in flies infected with KO-dsRed alone (Figure 2-10d). Importantly, nine of these seventeen proventriculi were also assessed for total parasites, and all nine showed heavy infection by untagged WT parasites (Movie 2-4). As a control to determine whether dsRed cells might simply be outcompeted by untagged cells in the fly, we assessed the prevalence of WT-dsRed parasites in proventriculi of flies coinfected with WT-dsRed + untagged WT. The prevalence of WT-dsRed in the proventriculus for mixed infections was 85%, nearly identical to that for WT-dsRed cells alone (83%), indicating that competition was not an issue (Figure 2-10d).

When individual proventriculi were examined, heavy infection by WT-dsRed cells was clearly evident, and parasites were distributed throughout (Figure 2-12a), although the thickness of the sample makes this difficult to see in a single focal plane. Z-stacks are shown in Movies 2-5 and 2-6. On the other hand, KO-dsRed cells, if detected at all, were present in extremely low numbers, corroborating earlier experiments with untagged parasites and directly illustrating that reduced prevalence of proventriculus infection is accompanied by reduced intensity of infection. The coinfection experiments with KO-dsRed and WT parasites enabled us to analyze the behavior of the two genotypes within single flies. These experiments demonstrated that, despite having only one or two KO parasites, proventriculi were heavily infected with WT parasites (Movie 2-4). These results prove first, that the poor infection rate with the KO is not because the fly is refractory to proventricular infection per se, and second, that WT and KO parasites act independently of each other. Individual KO-dsRed parasites are motile within fly tissue (Movie 2-4), supporting earlier *in vitro* experiments that showed PDEB1 is not required for motility of individual cells, despite being necessary for collective motility of the group. Taken together,

these data are consistent with the idea that PDEB1 KO is unable to respond to external signals; these signals might emanate from the fly and/or other parasites.

PDEB1 is needed for transition to the ectoperitrophic space

The finding that the PDEB1 KO mutant had a pronounced defect in establishing a proventricular infection, even in flies with heavy midgut infections, indicated that either the transition from the midgut lumen to the ectoperitrophic space or from the ectoperitrophic space to the proventriculus (Figure 2-1) is dependent upon cAMP signaling. In standard dissections, the midgut is considered as a single unit and there is no information on whether parasites are in the lumen or ectoperitrophic space. To distinguish between these compartments, infected flies were fed fluorescently labeled wheat germ agglutinin (FITC-WGA) 24 h before dissection. FITC-WGA binds the PM, delineating the border between the midgut lumen and ectoperitrophic space (Figure 2-1b); when combined with infection by fluorescent parasites, this allows us to investigate their topological distribution within the midgut. At 14–15 days post infection, fly midguts and proventriculi were carefully removed, so that both tissues remained connected and unbroken, and embedded in low melting agarose. Tissue samples were also labeled with Hoechst to visualize nuclei of tsetse fly epithelial cells and examined by fluorescence microscopy. In WT-dsRed-infected flies, parasites could clearly be seen throughout the midgut, including in the ectoperitrophic space (Figure 2-12b; Movies 2-7, 2-8, and 2-9). These results confirm that infection of the ectoperitrophic space is well-established by day 14. In contrast, in KO-dsRed-infected flies, parasites were rarely detected in the ectoperitrophic space, even when the midgut was heavily infected (Figure 2-12b). Of 24 infected flies, 13 had no parasites in the ectoperitrophic space, and in the other 11 flies they were few in number. From these results, we

conclude that PDEB1-dependent cAMP signaling is required for parasites to successfully transition from the midgut lumen to the ectoperitrophic space (see step 1 of Figure 2-1a).

Discussion

T. brucei transmission through the tsetse requires parasite movement through diverse tissues and is accompanied by an ordered series of parasite developmental changes in specific tissues. It is therefore hypothesized that the parasite employs specific signal transduction pathways to sense and respond to different extracellular environments encountered in these tissues. Our results provide the first formal evidence in support of this hypothesis and, additionally, link the requirement for cAMP signaling in SoMo to a specific step in the parasite life cycle.

The primary defect of PDEB1 KO was its inability to make the transition from the midgut lumen to the ectoperitrophic space. To our knowledge, this is the first mutant demonstrated to be defective at this step of the transmission cycle. It has been reported previously that the transition from the midgut to the proventriculus is not a bottleneck for WT trypanosomes [13, 14]. Our results are consistent with this, as > 80% of WT-infected flies with a midgut infection also had a proventriculus infection. Our findings indicate, however, that the PM presents a formidable barrier that must be actively overcome, because loss of PDEB1 prevents parasites from establishing infection in the ectoperitrophic space. The infection defect was not due to a block in parasite differentiation or motility, because the KO showed normal kinetics of differentiation from early to late procyclic forms within the fly and was fully capable of processive motility in liquid culture. Rather, our results indicate the defect results from disruption of cAMP signaling necessary for progression from the midgut lumen to the

ectoperitrophic space. At present, our data do not distinguish between a defect in physical crossing of the PM, versus a defect in survival once the ectoperitrophic space is reached. We favor a defect in crossing, first because the few parasites that do get across are alive and motile (Movie 2-4); second, because the inability to move between compartments correlates with altered movement *in vitro*; and third, because there is a precedent for cyclic nucleotides controlling cell movement in a broad range of organisms [16-18].

It is premature to say whether the coordinated movement exhibited by trypanosomes during SoMo takes the same form as in the insect vector. Recent work has demonstrated trypanosomes exhibit coordinated flagellar beating within tsetse tissues, but the shorter timescale indicates a different mechanism than used for SoMo [12] and it is unknown whether these two types of collective behavior are connected. Nonetheless, our findings demonstrate that SoMo *in vitro* depends on activities that are also required *in vivo*. These entail movement and the ability to respond to signals that might alter the form or direction of motility, i.e., chemotaxis. The reduced turning frequency of PDEB1 KO compared with WT is similar to what is seen with bacterial chemotaxis mutants [39]. This would support that the primary defect lies in responding to signals that control motility. This response could be individual or collective.

Simultaneous visualization of host tissues and individual trypanosomes allowed us to analyze parasite distribution in the lumen and ectoperitrophic space. In addition to defining the step at which the PDEB1 mutant was blocked, this has delivered new insights into how infections develop. When teneral flies are challenged with trypanosomes, approximately half of them manage to eradicate the infection after 6 days [41]. It has been tacitly assumed that trypanosomes had to colonize the ectoperitrophic space in order to establish a chronic infection, and it was unknown whether trypanosomes remained in the lumen for the duration of the

infection [43]. By using a fluorescent lectin to label the PM in combination with fluorescent parasites, we showed that the PDEB1 KO could proliferate and persist in the lumen without colonizing the ectoperitrophic space. Furthermore, numerous WT trypanosomes were present in the lumen as well as in the ectoperitrophic space 14 days post infection. At this time point, they were all late procyclic forms. These findings challenge the paradigm that trypanosomes must gain access to the ectoperitrophic space to maintain a midgut infection, and underline the importance of discriminating between the different sub-compartments in the midgut. It is worth noting that a peritrophic matrix is a common feature among blood-feeding insects, including mosquitos that transmit malaria. Therefore, our findings have relevance for understanding transmission biology of other vector-borne diseases.

Several earlier studies have employed deletion mutants to study trypanosome–tsetse interactions, but these have been restricted to the midgut (as a whole) and the salivary glands [32, 44-46], without examining the intervening tissues. In the light of our finding that the transition from the midgut lumen to the ectoperitrophic space requires specific parasite factors, it will be worth re-examining some of those mutants. For example, trypanosomes lacking PDEA were still able to infect the midgut [32], but it is not known whether they are able to exit the lumen. Another mutant, Δproc, which lacks all procyclin genes [46, 47], showed a mild defect in establishing midgut infections, but was 10 times worse than WT at colonizing the salivary glands [46]. This result seemed paradoxical, given that procyclins are not expressed by salivary gland trypanosomes. EP procyclin is expressed by parasites in the ectoperitrophic space and proventriculus, however, so it is possible that the null mutant has difficulty leaving the lumen or gaining access to the proventriculus.

Our findings suggest that there might be a limited window of opportunity when early procyclic forms are able to egress from the midgut lumen to the ectoperitrophic space. Once the parasites differentiate to late procyclic forms, they can survive in the lumen, but they may not be able to move on and complete the cycle. Successful crossing of the PM could be very rapid, as there are no publications that show trypanosomes in the process of entering the ectoperitrophic space. There are two reports showing electron micrographs of trypanosomes between the layers of the PM [15, 48], sometimes in cyst-like structures. In the latter case, these were seen 40 days post infection, and it is open to debate whether they are intermediates in the process of crossing the PM or dead ends. Continued technological advances in imaging, together with the appropriate choice of time point after infection, may allow these events to be analyzed and to determine whether the parasites make this transition individually or as a group.

Our results provide the first example of tissue-specific requirements for the cAMP signal transduction pathway in the trypanosome life cycle. cAMP is produced by receptor-type ACs that are at the surface membrane. Different AC isoforms are expressed in different life-cycle stages [24, 27] and by trypanosomes in different tsetse tissues [26]. Thus, while signaling molecules remain to be identified, receptor ACs are well-suited to transduce tissue-specific responses. Trypanosome cAMP signaling is thought to act through downstream effectors, termed cAMP response proteins (CARPs) [49]. At least two CARPs, together with PDEB1 and all ACs examined so far, are restricted to the flagellum [23, 24, 49, 50]. Our findings therefore support the paradigm of the flagellum (also known as the cilium) as a signaling platform for directing cellular adaptation to changing extracellular conditions [51] and extend this paradigm to a group of devastating pathogens.

A mechanistic explanation for the infection defect of PDEB1 mutants is provided by considering PDEB1 function in cAMP signaling (Figure 2-13). Flagellar PDEB1 is postulated to provide a barrier to diffusion of cAMP that restricts signal transduction to the site of cAMP generation [33, 34]. Pharmacological inhibition of PDE increases intracellular cAMP [33, 34]. One could therefore imagine that loss of PDEB1 floods the flagellar compartment with cAMP, disrupting highly localized and insulated signals originating from specific ACs that are distributed to specific regions of the flagellum [24]. This would prevent the parasite from properly interpreting signals received in the midgut lumen that enable it to cross the PM and continue the transmission cycle. *T. brucei* encodes two different PDEB isoforms [22]. Prior work has shown that PDEB2 compensates for PDEB1 in maintaining parasite viability in bloodstream forms [33], suggesting some overlap in function for these two proteins. However, our results show that PDEB2 is unable to compensate in the context of tsetse fly infection, thereby demonstrating isoform-specific functions.

The transition of the parasite from one tissue to the next has been described evocatively as a series of gates under the control of the fly [13]. Based on our results, it would seem that while the fly might be the gatekeeper, the parasite employs cAMP signaling to engage keys that unlock these gates. This might also apply in the mammalian host, where the parasite can breach the blood–brain barrier or take up residence in the adipose tissue or skin [52-55]. Given that host and parasite PDEs can be differentially inhibited [56, 57], our findings might have wider implications for development of therapeutics.

Materials and Methods

Trypanosomes

T. brucei brucei Lister 427 and derivatives thereof were used in this study. Procyclic forms were cultured in SDM79 [58] or SDM80 [59] plus/minus glucose (5.55 mM) containing 10% heat-inactivated fetal bovine serum (FBS) at 27 °C and 2.5% CO_2. Procyclic forms of the Bernese stock of Lister 427 can be maintained as early procyclic forms in the absence of glycerol [40, 60]. Parasites were maintained at a density between 10^6 and 10^7 cells ml^{-1}. Population doubling times were determined over a period of at least 5 days in which the cell density was determined daily.

Plasmids and generation of knockout and addback clones

The PDEB1 KO was generated by two rounds of homologous recombination using genes conferring resistance to blasticidin and puromycin, respectively. The resistance genes, flanked by 452 bp upstream and 635 bp downstream of the PDEB1 coding region, were cloned between the Xho I and Bam HI restriction sites in the pTub plasmid backbone [61, 62], thus removing the tubulin sequences. The following primers were used to amplify the PDEB1 flanking sequences:

Upstream FWD: atatGCGGCCGCTGCATTATGTTACTTGGGGGCA
Upstream REV: atatCTCGAGGACGTAGTGTCCAACTGTGC
Downstream FWD: atatGGATCCAGTCAGTTGACCGGTGGTAG
Downstream REV: atatTCTAGACCGCCACAACTCCCTCTTAC

Plasmids were digested with NotI-HF and XbaI to release the insert prior to transformation. The knockout was verified by PCR using primers:

P1 (PDEB1_ORF_fwd): AGTACTCATTGTGCACAGTT

P2 (PDEB1_ORF_rev): TCATGTATATCTGTAGGCAT

P3 (PDEB1_KO_fwd): TCATACGGCTATTTGCCCAGT

P4 (PDEB1_KO_rev): AATGTCACACAACCGCAGTG

A PDEB1 addback plasmid was generated by inserting the coding region between the EcoRI and BglII sites in pGAPRONE-mcs [63]. The coding region was amplified with the following primers:

Forward: atatGAATTCATGTTCATGAACAAGCCCTTTG

Reverse: atatAGATCTTCAACGAGTACTGCTGTTGTTG

The construct was linearized with SpeI, enabling integration upstream of a procyclin locus [44]. Transfection was performed as described previously [60]. Stable transformants were selected using 10 μg ml^{-1} blasticidin, 1 μg ml^{-1} puromycin or 15 μg ml^{-1} G418.

Construction of pTB011_Cas9_T7RNAP_blast: the plasmid pTB011 [64] was digested with Nco I to excise the puromycin N-acetyl-transferase (pac) gene and 350 bp of the upstream alpha-tubulin flanking region. In a second step, the alpha-tubulin flanking region and the open-reading frame (ORF) of T7RNA polymerase were amplified separately by PCR. The vector backbone, the tubulin fragment and the ORF of T7RNA polymerase were cloned together by Gibson assembly. The plasmid was digested with Pac I to release the insert prior to

transformation. Transfection was performed as described previously [60]. Stable transformants were selected using 10 μg ml^{-1} blasticidin.

Primers used to generate individual fragments for the Gibson assembly:

Cas_P1 GibAs: acgtcgcatgctcccggccgccatggccgcgggattttaa

Cas_P2: gcgatgttaatcgtgttcatgaattcgtttgaactatttt

Cas_P3: aaaatagttcaaacgaattcatgaacacgattaacatcgc

Cas_P4 GibAs: caactaaatgggcaccatggttacgcgaacgcgaagtccg

Trypanin knockout: PCR amplification of targeting fragments and sgRNA templates were performed as described previously [64]. To delete trypanin, targeting cassettes were amplified from pPOTv7-hygromycin and pPOTv7-G418 [64]. The knockout was verified by PCR using primers: Tryp-5Flk_Fw: GCTGAGATAGTTTAAGAGGGAGAG and Tryp-ORF_Rv: GACATATGCTACTCAAAGTTGCTCCGTG.

Primers used for PCR amplification of targeting fragments:

Trypan-crKO_Fwd: TACTTTTCAGACTGCATCGTGGCGTACCCCgtataatgcagacctgctgc

Trypan-crKO_Rev: CTGCAACAAAGCCGTAACTTGGAACAACCAccggaaccactaccagaacc

Primers used for PCR amplification of sgRNA templates:

Trypan-crKO_5gR:

gaaattaatacgactcactataggCAAAAACGAGAAGAGCCTACgttttagagctagaaatagc

Trypan-crKO_3gR:

gaaattaatacgactcactataggAGGTGTTGTGGTTCACACGTgttttagagctagaaatagc

RNA isolation and northern blot analysis

Total RNA isolation and northern blot analysis were performed according to standard procedures [65]. Ten micrograms of total RNA were loaded per lane. Radioactively labeled probes were generated using a Megaprime DNA-labeling system (Amersham Biosciences, Buckinghamshire, UK) according to the manufacturer's instructions. Blots were hybridized and washed under stringent conditions. 18S rRNA, detected with a 5′-labeled antisense oligonucleotide, was used as a loading control [66]. Signals were normalized in Fiji (Version 1.0) [67].

Flow cytometry

Flow cytometry (NovoCyte, ACEA Biosciences, Inc., San Diego, USA) was used to monitor the proportion of GPEET-positive or dsRed-positive cells. GPEET was detected with rabbit polyclonal anti-GPEET as described [40].

Social motility assay

SoMo assays were performed as described [36], but without the addition of glycerol. In complementation experiments, either WT-dsRed or KO-dsRed were mixed with WT cells at a ratio of 2:1. Two hundred thousand cells were used as the inoculum. Imaging of fluorescent cells was performed using a Leica DM 5500 B microscope at x20 magnification. Community lifts for the detection of GPEET and EP procyclins were performed as described [36].

Community lifts

Community lifts for the detection of GPEET and EP procyclins were performed as described [36] using K1 rabbit anti-GPEET at a dilution of 1:1000 and TBRP1/247 mouse anti-EP (Cat. no. CLP001A, Cedarlane Laboratories, Burlington, Canada) at a dilution of 1:2500 as primary antibodies. The secondary antibodies goat anti-mouse IRDye 800CW (LI-COR Biosciences, Bad Homburg, Germany) and goat anti-rabbit IRDye 680LT (LI-COR Biosciences) were used at dilutions of 1:10,000.

Fly infection and staining of the peritrophic matrix

Glossina moristans pupae were obtained from the Department of Entomology, Slovak Academy of Science, Bratislava, Slovakia. Teneral flies were infected by membrane feeding with 2.5×10^6 parasites ml^{-1} and maintained as described [60]. For complementation experiments, dsRed-tagged and untagged cells were mixed at a ratio of 2:1. The intensities of midgut infections were graded as described [60]. The infective feed was performed with washed horse red blood cells resuspended in SDM79; all subsequent feeds consisted of whole defibrinated blood (TCS Biologicals, Buckingham, UK).

Staining of the peritrophic matrix: At days 10–13 post infection, flies were collected and fed 40 $\mu g\ ml^{-1}$ fluorescein wheat germ agglutinin (WGA-FITC; Adipogen, Liestal, Switzerland) diluted in SDM79 supplemented with 5% defibrinated horse blood and 10% FBS. Twenty-four hours later, intact fly midguts, still connected to the proventriculus, were removed, placed on a coverslip, submerged in 20 $\mu g\ ml^{-1}$ Hoechst dye in PBS for 1 min, and embedded in 1% low

melting agarose. Images and videos were captured using a TillPhotonics/FEI iMIC digital spinning disc microscope.

Motility traces

Motility assays were performed in motility chambers [68] using a Zeiss Axiovert 200 M inverted microscope at x10 magnification. WT, PDEB1 KO, or TPN KO cells in suspension culture were imaged at 30 frames per second using Adobe Premiere Elements 9. A total of 34 videos each for WT, PDEB1 KO, and TPN KO were analyzed from three biological replicates. In a separate experiment, 34 additional videos each for WT, PDEB1 KO, Addback 1, and Addback 2 were analyzed from two biological replicates. Mean-squared displacement of individual cells was determined using a trypanosome-specific cell tracking algorithm developed in MATLAB [69] based on a single-particle-tracking algorithm [70]. We used a maximum time interval of 10 s and only considered cells that were in focus for a minimum of 300 out of 900 frames.

High-speed cell imaging

Cells were imaged in motility chambers as described above with the modification of placing cells between two coverslips separated by double-stick tape instead of a microscope slide and a coverslip separated by double-stick tape. Videos were taken on an Olympus IX83 microscope using phase contrast with a x10 objective lens and x2 magnification. Videos were taken on a Hamamatsu Orca Flash 4.0 camera at 496 frames per second. Videos were captured as image stacks in MetaMorph Advanced. Image stacks were converted to AVI videos using Fiji-ImageJ Version 1.0 [67]. Still images in Figure 2-3d are taken from the original image stacks.

Four to five videos each were taken of WT, PDEB1 KO, and TPN KO cells and these videos were concatenated in a single Movie for each cell line using Adobe Premier Elements 14 (WT = Movie 2-1; PDEB1-KO = Movie 2-2; TPN-KO = Movie 2-3).

Acknowledgements

Michelle Shimogawa, Simon Imhof, and Gaby Schumann are thanked for their insightful comments on the paper. Markus Engstler and Sara Schuster are thanked for helpful discussions and providing protocols for PM staining. Nicholas Doiron is thanked for assistance in dissecting flies. Aydogan Ozcan, Hatice Koydemir, and Muhammed Veli are thanked for their assistance with high-speed imaging and Sebastian Knüsel and students of the Bachelor Practical 2018 for help with generating the trypanin knockout. K.H.: NIH grant AI052348. I.R.: Swiss National Science Foundation grant 31003A_166427 and HHMI grant 55007650. S.D.: Ruth L. Kirschstein National Research Service Award GM007185 and Ruth L. Kirschstein National Research Service Award AI007323.

Author Contributions

S.S., S.D., I.R., and K.H. designed the experiments and wrote the paper. S.S., S.D., R.R., T.W. and F.F. conducted the experiments. S.S., S.D., T.W., I.R. and K.H. analyzed the data. K.H. conducted the statistical analyses.

Figures

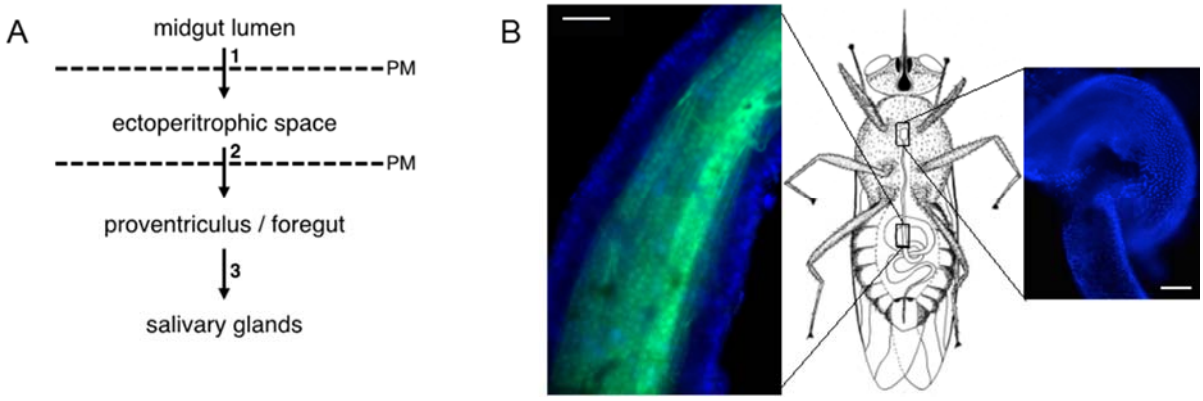

Figure 2-1: Course of migration by trypanosomes and anatomical context in the tsetse fly. A) Schematic depiction of the path taken by trypanosomes during cyclic transmission, with numbers 1–3 marking major tissue transitions. PM: peritrophic matrix. B) Schematic of a tsetse fly (central panel), with boxed regions indicating the location of the midgut (left panel) and proventriculus (right panel). Left panel, an isolated tsetse fly midgut in which the nuclei of epithelial cells are stained with Hoechst dye (blue) and the PM is stained with fluorescein-tagged wheat germ agglutinin (green). Right panel, an isolated tsetse fly proventriculus stained with Hoechst dye (blue) to visualize nuclei. Scale bar: 100 microns

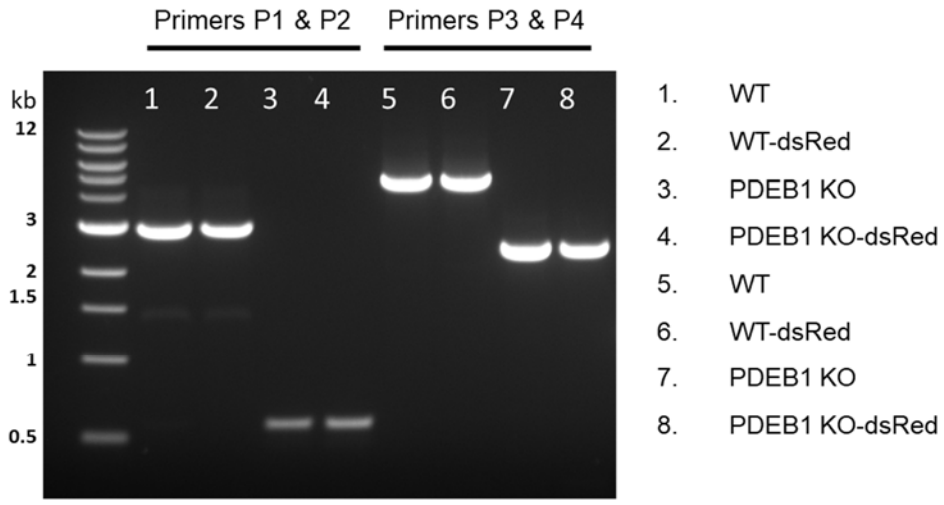

Primer 1: PDEB1 ORF fwd
Primer 2: PDEB1 ORF rev

Primer 3: upstream of 5' homologous region in plasmid
Primer 4: downstream of 3' homologous region in plasmid

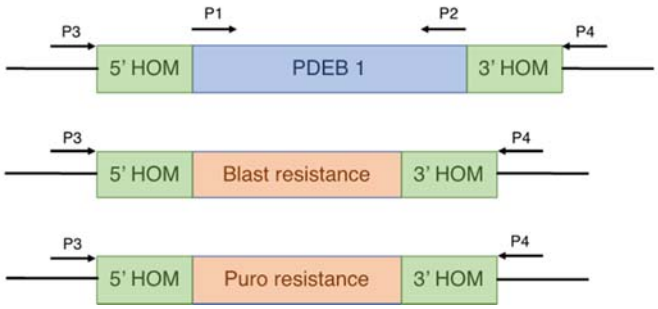

Figure 2-2: PCR confirmation of PDEB1 knockout

Genomic DNA was isolated from individual clones and amplified with the primers shown above.

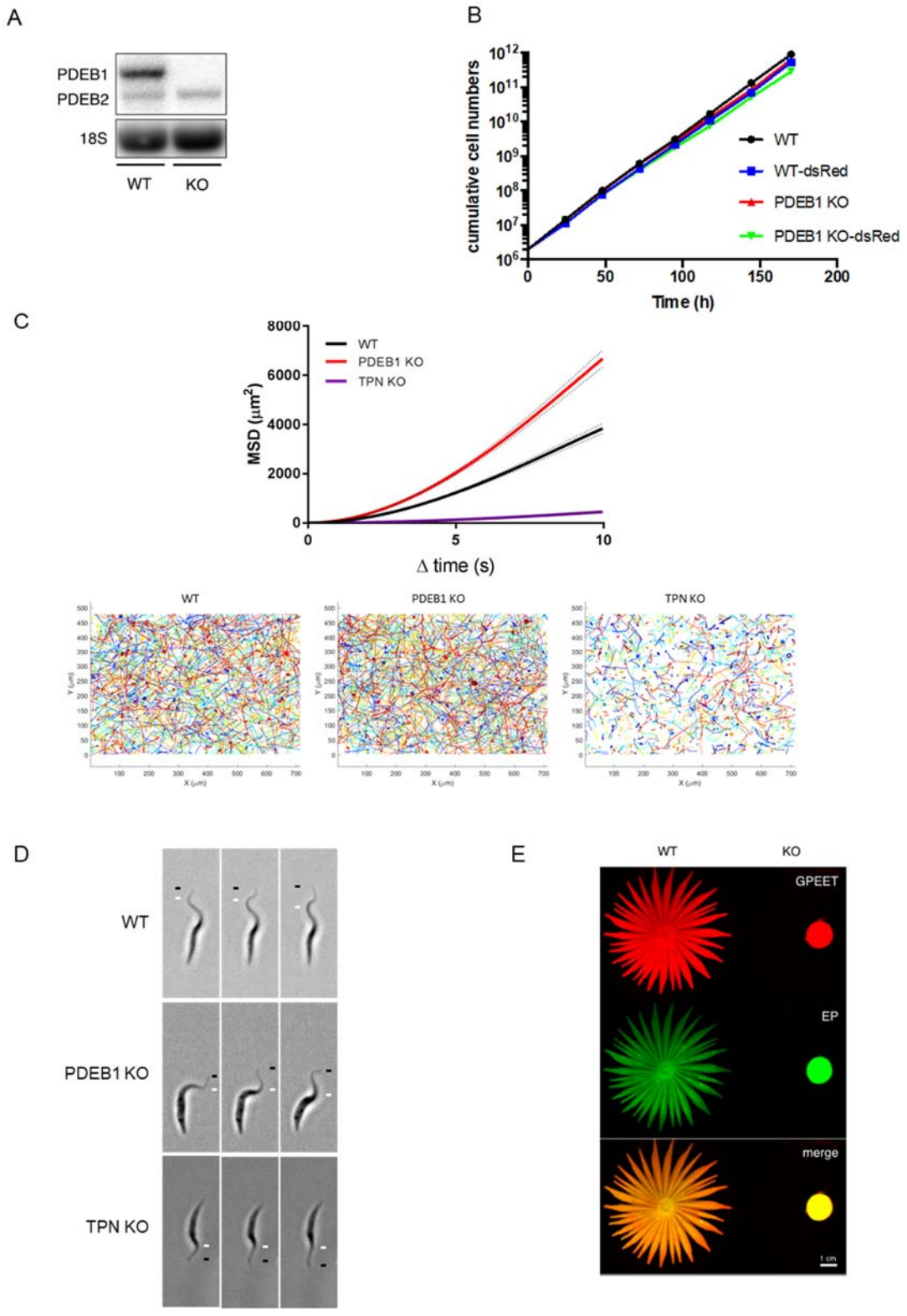

Figure 2-3: Effect of PDEB1 knockout on SoMo, growth and motility.

A) Northern blot analysis of RNA prepared from wild-type parental cells (WT) or PDEB1 knockout cells (KO). Blots were hybridized with a probe corresponding to the coding region of PDEB1. PDEB2 is 93% identical to PDEB1 and the probe cross-hybridizes weakly under the conditions used. 18S rRNA serves as a loading control [66]. B) Comparison of population doubling times of WT, KO, WT-dsRed, and KO-dsRed cell lines in suspension culture over the course of 7 days. Cell densities were adjusted daily to 3×10^6 cells ml^{-1} in order to ensure logarithmic growth. C) Mean-squared displacement (MSD) is measured for WT, PDEB1 KO, and trypanin knockout (TPN KO) cells. Results are from three biological replicates and a total of n = 1449 cell traces for WT, n = 1339 cell traces for KO, and n = 1208 cell traces for TPN KO from a total of 34 videos for each. Dotted lines represent standard error of the mean (SEM). Cell traces from the 34 videos are superimposed over each other for WT, PDEB1 KO, and TPN KO, respectively. D) Still images from high-speed videos of WT, PDEB1 KO, and TPN KO cells taken at 496 frames per second under x20 magnification. Each series of images shows one cell per genotype at six millisecond intervals. The black line indicates the flagellum tip, and the white line indicates the peak of the flagellar wave. See supplemental information for Movies 2-1–2-3. E) Social motility assays were performed with WT and KO cells. Community lifts [36] were performed and incubated with anti-EP (green) and anti-GPEET (red) antibodies

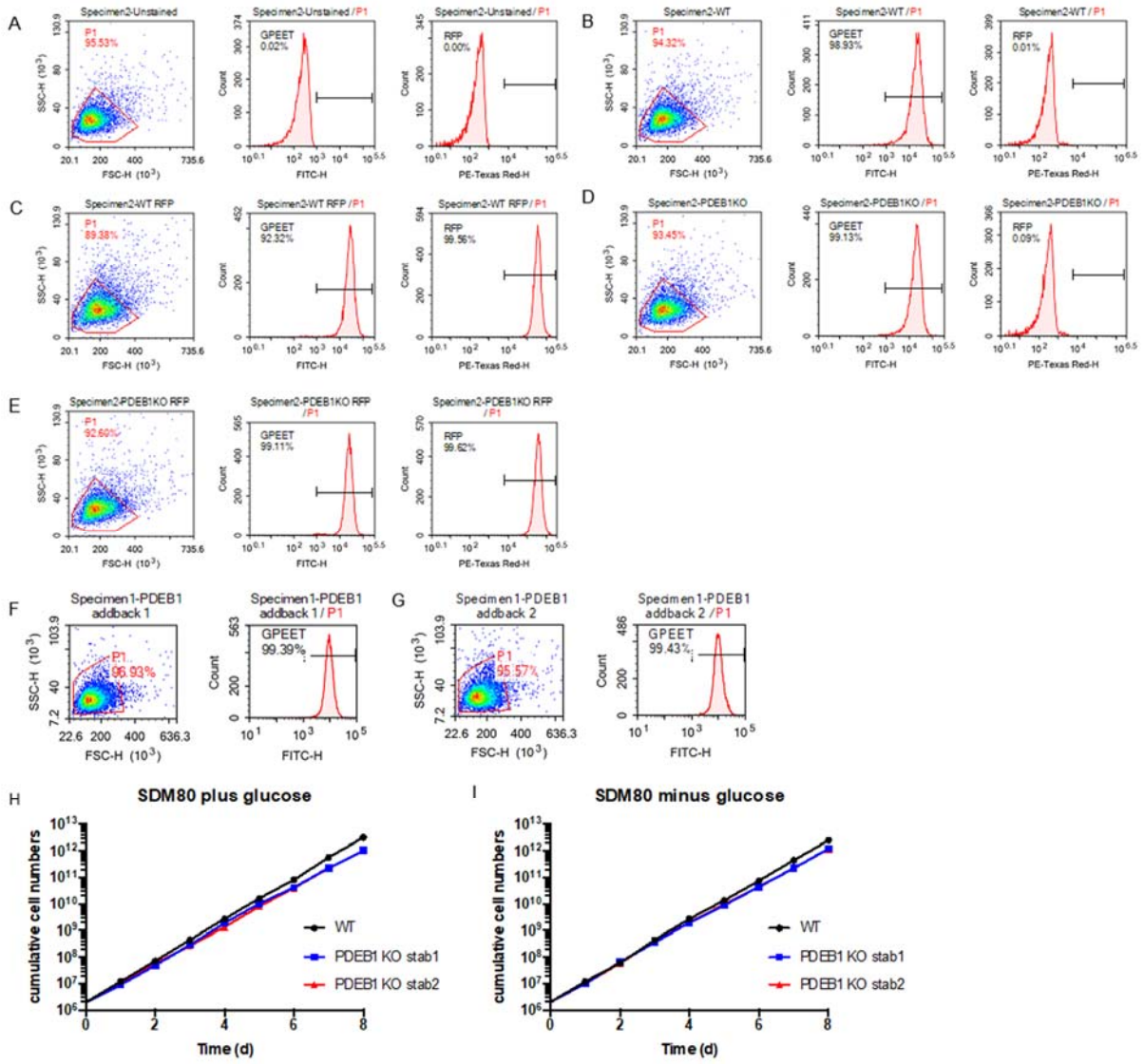

Figure 2-4: Analysis of expression of GPEET and dsRed by flow cytometry of all clones used in this study and growth of wild type and PDEB1 knockout in low glucose medium.

Left panels: gated population (indicated in red) used for analysis. Middle panels: GPEET surface staining. Right panels: dsRed expression. A) untagged WT (no antibody control). B) untagged WT. C) WT-dsRed. D) untagged PDEB1 KO. E) PDEB1 KO-dsRed. F) Addback 1. G) Addback 2. Comparison of population doubling times of wild-type cells and two stabilates of PDEB1 KO either with glucose (H) or without glucose (I).

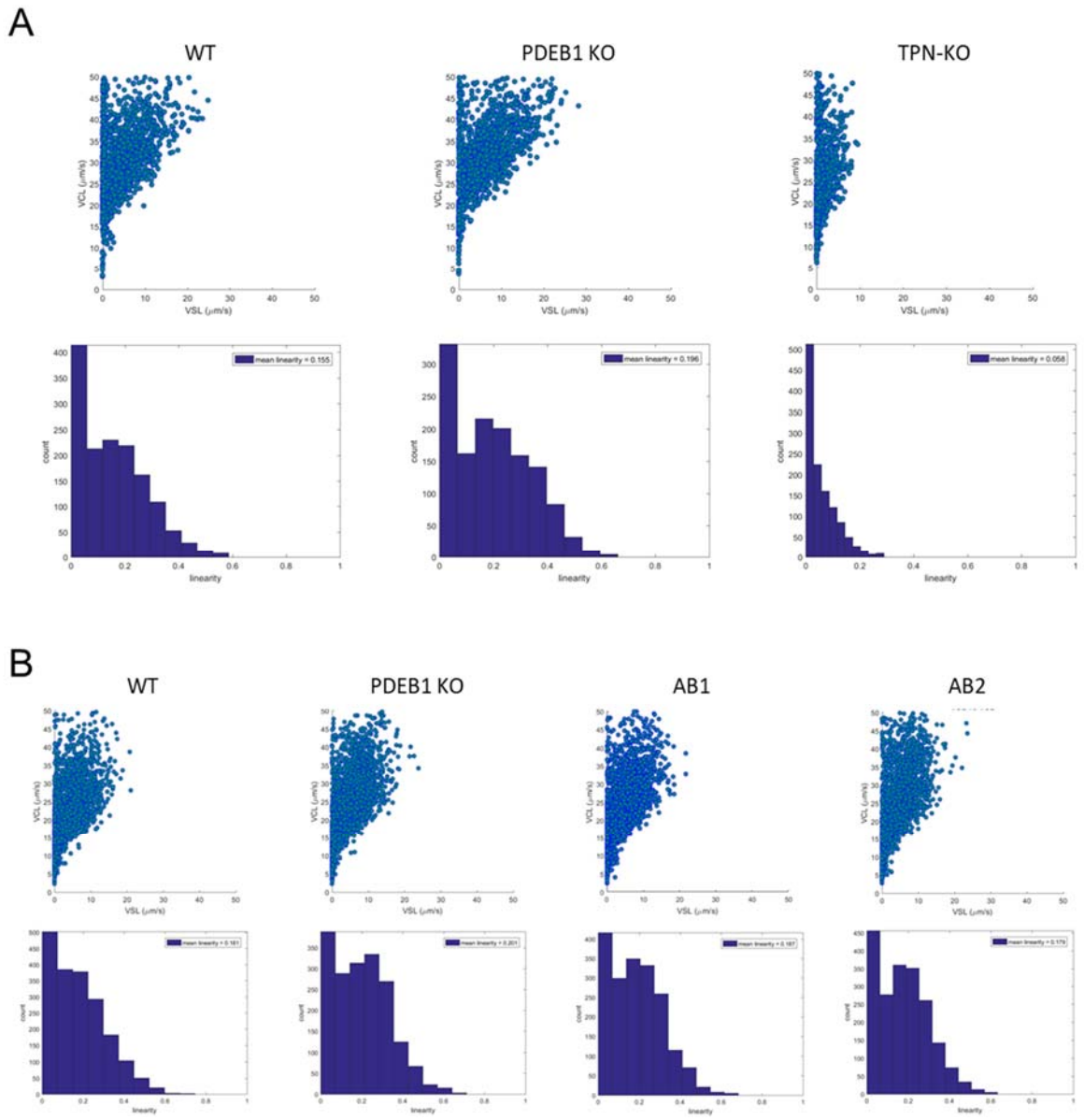

Figure 2-5: PDEB1 KO cells move more linearly than WT which contributes to their increased MSD

(A) Upper row: The curvilinear velocity (VCL) and the straight-line velocity (VSL) for each individual cell are plotted for WT (n=1449), PDEB1 KO (n=1339), and TPN KO (n=1208) respectively. Each blue dot corresponds to one cell. Lower row: Linearity plots for WT, PDEB1

KO, and TPN KO show how linear the motion of the cells in each population (WT, PDEB1 KO, or TPN KO) are. Mean linearity is the ratio of VSL/VCL for the cells in the population.
(B) Upper row: VCL and VSL are plotted for WT (n=1919), PDEB1 KO (n=1824), AB1 (n=1876), and AB2 (n=1973). Lower row: Linearity plots for WT, PDEB1 KO, AB1, and AB2.

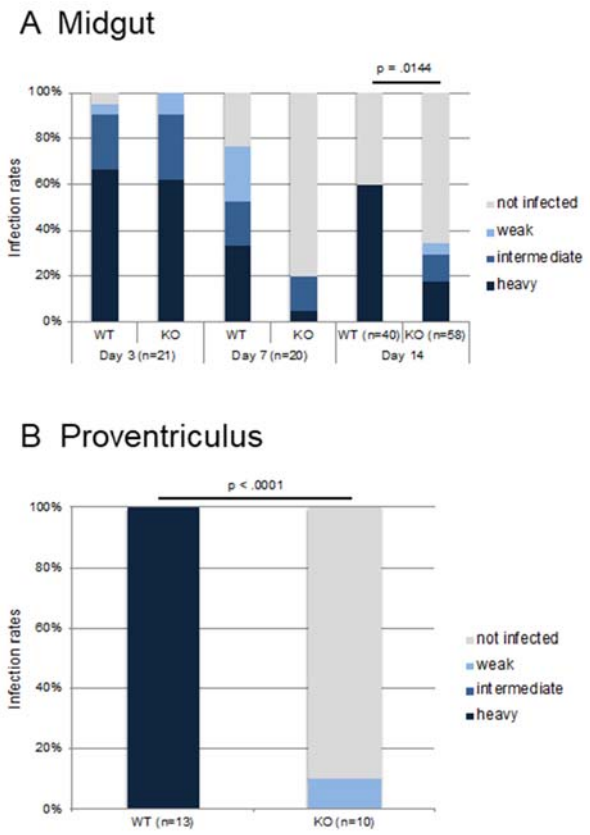

Figure 2-6: PDEB1 is required for colonization of the proventriculus.

A) Prevalence and intensity of midgut infections. Teneral flies were infected at day 0 and dissected to remove the midgut 3, 7, and 14 days post infection. Infections were scored as heavy, intermediate, weak, or uninfected as described [60]. P-value is shown for Fisher's exact test, two-sided. B) Prevalence and intensity of proventriculus infections. For flies with a heavy midgut infection on day 14, the proventriculus was separated from the midgut and intensity of infections was scored using the same criteria as for the midguts. P-value is shown for Fisher's exact test, two-sided

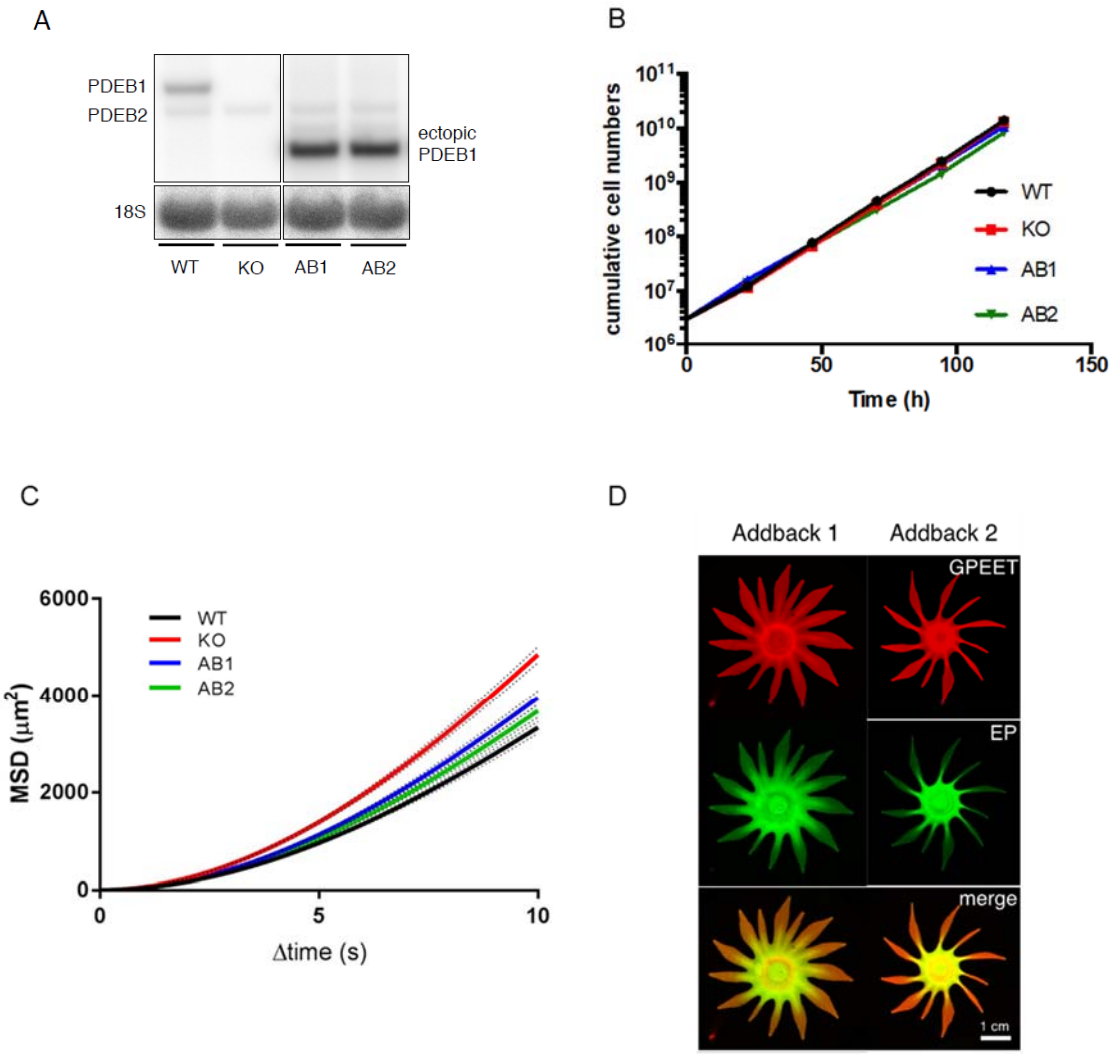

Figure 2-7: Ectopic expression of PDEB1 in the PDEB1 KO restores SoMo.

A) Northern blot analysis of RNA from WT, PDEB1 KO and two addback clones, AB1 and AB2, expressing an ectopic copy of PDEB1 that is integrated upstream of a procyclin locus and transcribed from the procyclin promoter [44]. The addback version has a truncated 3′-untranslated region derived from the EP1 procyclin gene, hence the smaller size of the transcript compared with the endogenous copy. The probe used is described in Figure 2-3. 18S rRNA serves as a loading control [66]. The expression of the ectopic copy relative to the endogenous copy is 4.3-fold for AB1 and 4.2-fold for AB2. B) Growth of WT, PDEB1 KO, AB1, and AB2

parasites was monitored over the course of 5 days in suspension culture as described in Figure 2-3b. C) MSD is measured for WT, PDEB1 KO, AB1, and AB2 cells from two biological replicates. Results are from n = 1919 tracks for WT, n = 1824 tracks for PDEB1 KO, n = 1876 tracks for AB1, and n = 1973 tracks for AB2 from a total of 34 videos for each. Dotted lines represent standard error of the mean (SEM). D) Community lifts demonstrate addbacks AB1 (left) and AB2 (right) are SoMo-positive and express both GPEET (red) and EP (green)

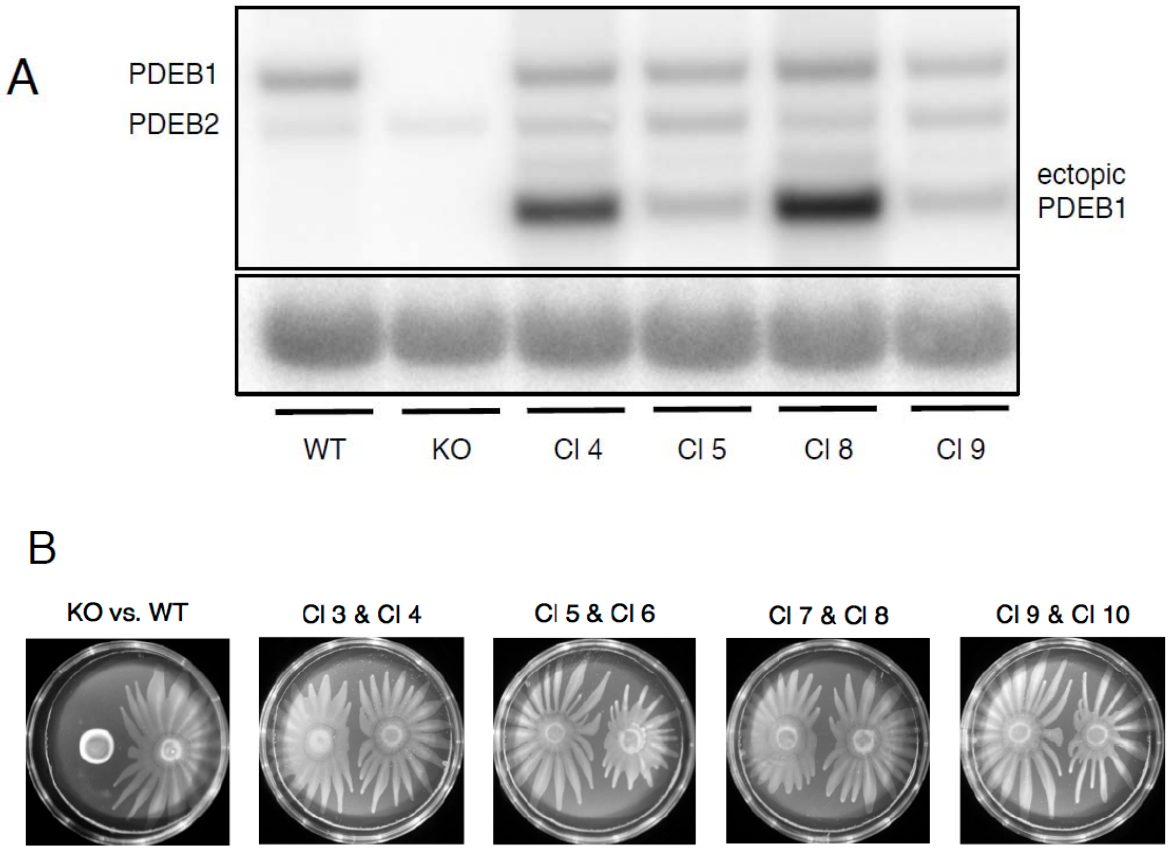

Figure 2-8: Overexpression of PDEB1 in WT cells has no adverse effects on social motility

A) Northern blot analysis with a probe specific for the PDEB1 open reading frame (upper panel) and a loading control (18S rRNA, lower panel). WT: wild-type parent, KO: knockout. Cl4, Cl5, Cl8, and Cl9 are derivatives of WT stably transformed with the same plasmid that was used to generate AB1 and AB2 (see Figure 4). Note that this northern blot and the one shown in Figure 4A were part of the same gel and contain the same controls. B) Representative pictures of social motility assays of KO, WT, and 8 overexpressors (Cl3-Cl10).

A Midgut

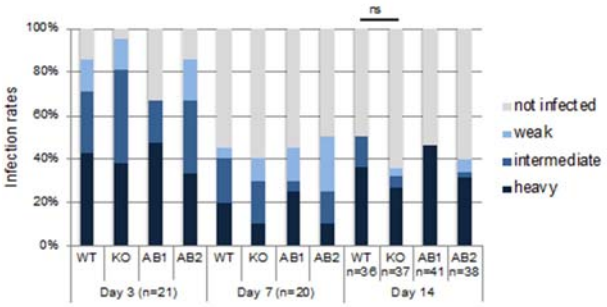

B Proventriculus

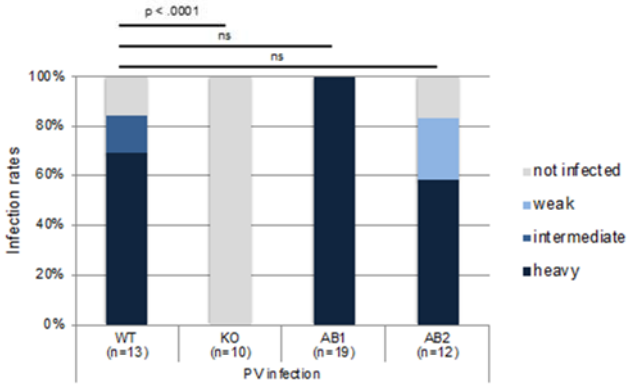

C

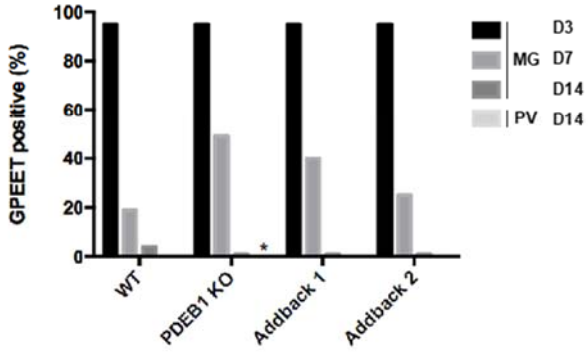

D

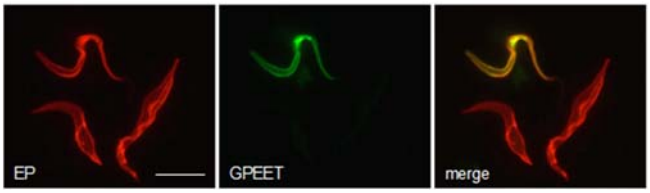

Figure 2-9: Addback of PDEB1 restores invasion of the proventriculus.

A) Teneral flies were infected and the prevalence and intensity of infection were determined as described in Figure 2-6a. Day 14 infection rate was not significantly different between WT and KO (ns, Fisher's exact test, two-sided). B) Prevalence and intensity of proventriculus infections in flies with a heavy midgut infection on day 14. Tissue samples were processed as described in Figure 2-6b. P-value is shown for Fisher's exact test, two-sided, ns: not statistically significant. C) Kinetics of GPEET repression *in vivo*. Parasites from the midgut (days 3, 7, and 14 post infection) and the proventriculus (day 14 only) were stained with anti-GPEET and anti-EP antibodies. One hundred cells were counted per sample. The percentage of GPEET-positive trypanosomes is shown. All parasites were EP-positive. *: no cells were detected in the proventriculus of the KO. D) Representative immunofluorescence image of WT parasites taken from the midgut at day 7 post infection and probed with the indicated antibodies. Scale bar: 10 microns

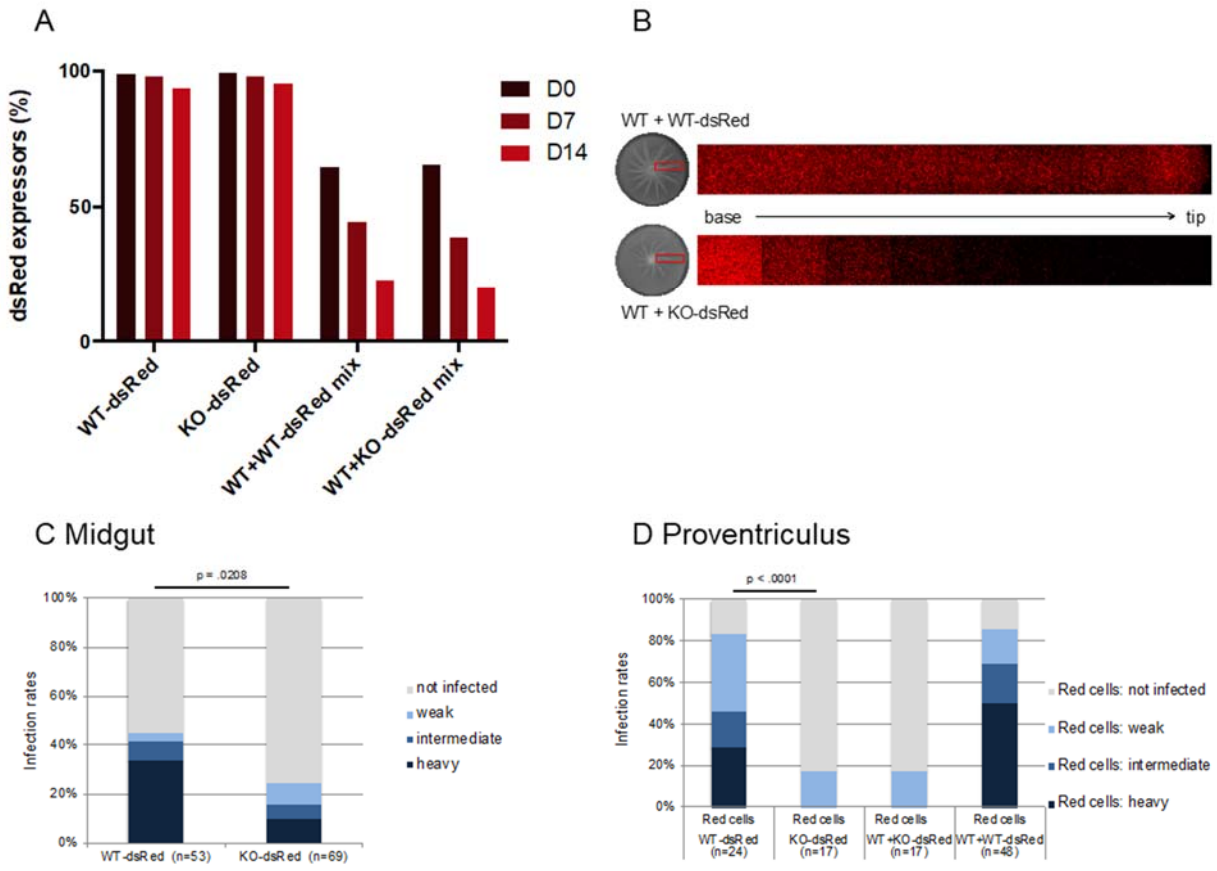

Figure 2-10: WT does not complement PDEB1 KO *in vitro* or *in vivo*.

A) Proportion of dsRed-positive cells in suspension culture. Fluorescence was monitored by flow cytometry (Figure 2-4). Tagged:untagged cells were mixed at a ratio of 2:1. B) WT-dsRed or KO-dsRed was mixed with untagged WT at a ratio of 2:1 and tested for SoMo. Top panel: WT + WT-dsRed co-culture. WT-dsRed parasites are evenly distributed throughout the projections. Lower panel: KO + WT-dsRed co-culture. KO-dsRed cells form a gradient with a high proportion of KO-dsRed cells at the base of the projection and progressively fewer cells extending to the tip. C) Prevalence and intensities of midgut infections at day 14 post infection. P-value is shown for Fisher's exact test, two-sided. D) Proventriculus infection rates at day 14 post infection. In the mixed infections, only dsRed cells were scored. P-value is shown for Fisher's exact test, two-sided

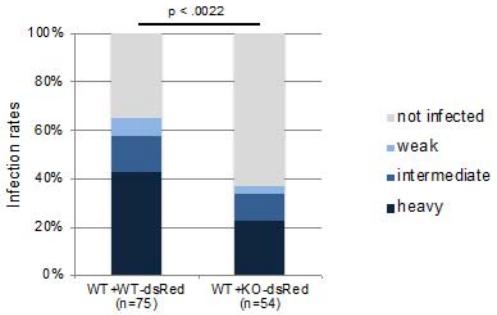

Figure 2-11: Total midgut infection rates for mixed infections with untagged WT and dsRed-tagged WT or KO

See Results, section 5. Fisher's exact test, two-sided was applied.

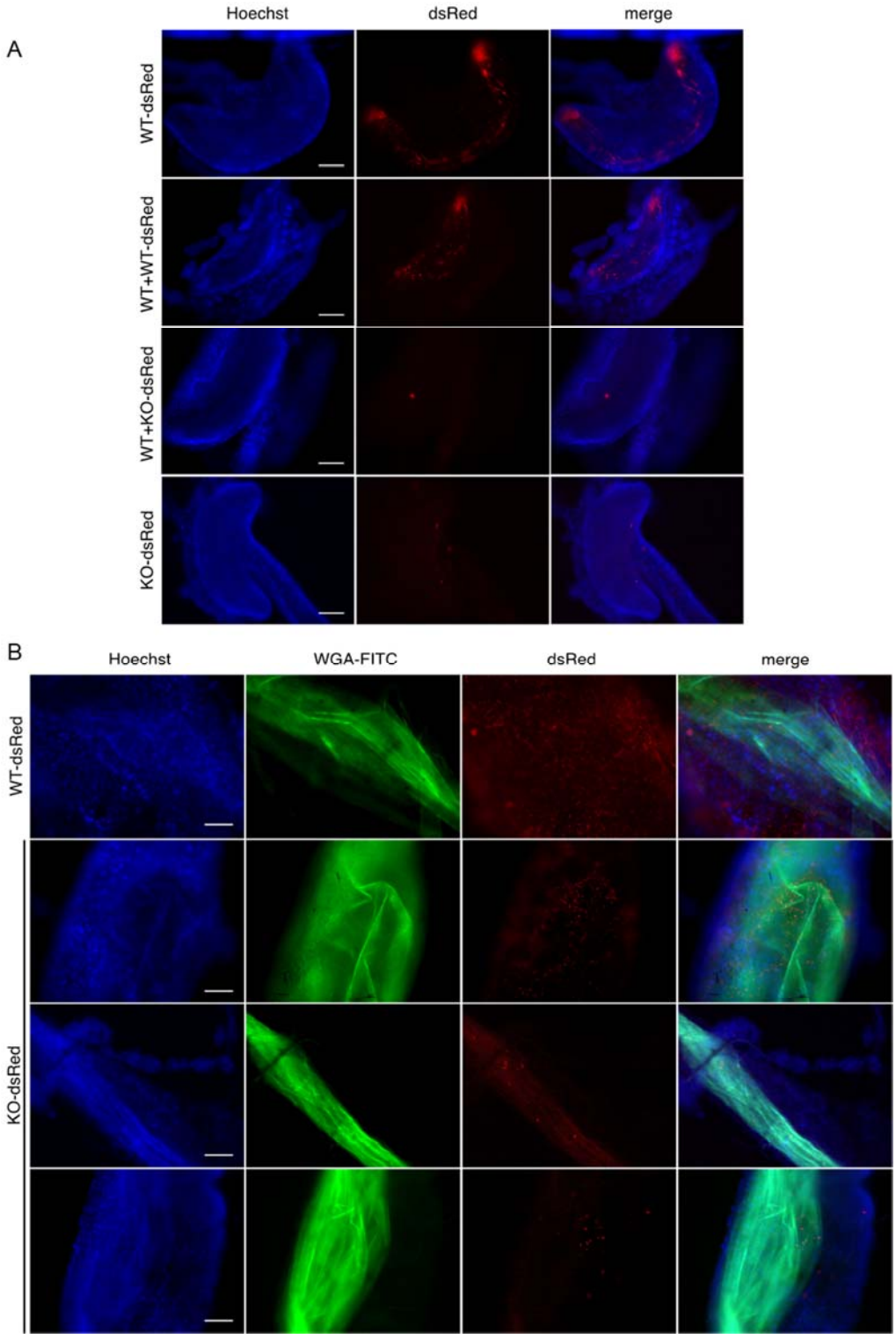

Figure 2-12: Impaired cAMP signaling impacts the prevalence and topology of infection.

A) Proventriculi at day 14 post infection. Nuclei of host cells are stained with Hoechst dye. In mixed infections (middle panels), only the dsRed-tagged cells are visible. Movie 2-4 shows merged DIC and red fluorescent channels for a mixed infection with WT + KO-dsRed. B) Midguts of flies infected with dsRed-tagged trypanosomes and fed with FITC-WGA 24 h prior to dissection at day 14. Nuclei of host cells are stained with Hoechst dye. Images in A and B were captured using a TillPhotonics/FEI iMIC digital spinning disc microscope. Scale bars: 100 microns

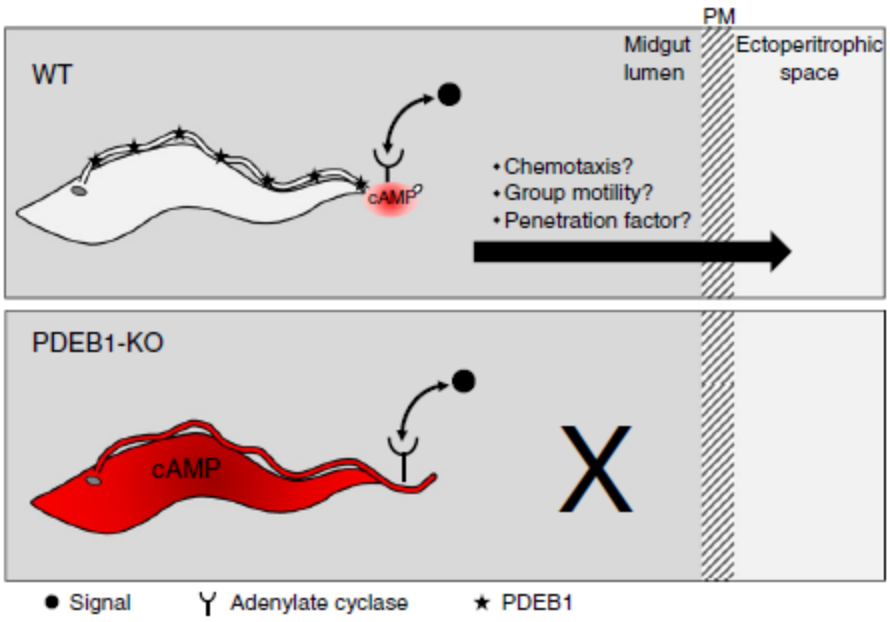

Figure 2-13: Model for infection defect of PDEB1 knockout parasites.

In wild-type *T. brucei* (WT), signals in the midgut lumen (black circle) modulate cAMP production (red) by receptor-adenylate cyclases located in specific regions of the flagellum. PDEB1 is distributed along the flagellum (black stars) and restricts cAMP to site of production by the AC, where local changes in cAMP concentration control chemotaxis, group motility or other factors that facilitate traversal of the peritrophic matrix (PM). In the absence of PDEB1 (PDEB1-KO), cAMP levels rise and diffuse through the flagellum and cell, so the parasite is no longer able to generate localized cAMP fluctuations and is thus unable to respond to signals that direct traversal of the PM.

Supplemental Material Legends:

Movie 2-1 – Movie 2-3: Compilations of high-speed videos of WT, PDEB1 KO, and TPN KO cells. Videos were recorded at 496 frames per second (fps) and played back at 30 fps. Movie 2-1 includes four representative videos of WT cells, Movie 2-2 shows five representative videos of PDEB1 KO, and Movie 2-3 has five representative videos of TPN KO.

Movie 2-4: Proventriculus of a fly co-infected with untagged WT and PDEB1 KO-dsRed at day 14 post infection. Scale bar: 100 microns.

Movie 2-5 and 2-6: Z-stacks of proventriculi from flies infected with WT-dsRed at day 14 post infection. Scale bar: 100 microns.

Movie 2-7 – 2-9: Z-stacks of midguts infected with WT-dsRed at day 14 post infection. The peritrophic matrix is stained with FITC-WGA and the nuclei of midgut endothelial cells are stained with Hoechst dye. Scale bar: 100 microns. Movie 7: Arrow indicates parasites in the ectoperitrophic space (EPS). Movie 8: 1st arrow indicates parasites in the midgut, and 2nd arrow points to parasites in the EPS. Movie 9: 1st arrow shows parasites in the EPS, and the 2nd and 3rd arrows point to parasites in the midgut.

Bibliography

1. Vickerman, K., *Developmental cycles and biology of pathogenic trypanosomes.* Br Med Bull, 1985. **41**(2): p. 105-14.
2. Matthews, K.R., *Controlling and coordinating development in vector-transmitted parasites.* Science, 2011. **331**(6021): p. 1149-53.
3. Rojas, F., et al., *Oligopeptide Signaling through TbGPR89 Drives Trypanosome Quorum Sensing.* Cell, 2019. **176**(1-2): p. 306-317.e16.
4. Robertson, M.R., Muriel and M. Robertson, *Notes on the life-history of Trypanosoma gambienese, with a brief reference to the cycles of Trypanosoma nanum and Trypanosoma pecorum in Glossina palpalis*. 1913, Philosophical Transactions of the Royal Society B. p. 161-184.
5. Moloo, S.K. and S.B. Kutuza, *Feeding and crop emptying in Glossina brevipalpis Newstead.* Acta Trop, 1970. **27**(4): p. 356-77.
6. Turner, C.M., J.D. Barry, and K. Vickerman, *Loss of variable antigen during transformation of Trypanosoma brucei rhodesiense from bloodstream to procyclic forms in the tsetse fly.* Parasitol Res, 1988. **74**(6): p. 507-11.
7. Vassella, E., et al., *A major surface glycoprotein of trypanosoma brucei is expressed transiently during development and can be regulated post-transcriptionally by glycerol or hypoxia.* Genes Dev, 2000. **14**(5): p. 615-26.
8. Lehane, M.J., P.G. Allingham, and P. Weglicki, *Composition of the peritrophic matrix of the tsetse fly, Glossina morsitans morsitans.* Cell Tissue Res, 1996. **283**(3): p. 375-84.
9. Rose, C., et al., *An investigation into the protein composition of the teneral Glossina morsitans morsitans peritrophic matrix.* PLoS Negl Trop Dis, 2014. **8**(4): p. e2691.

10. Van Den Abbeele, J., et al., *Trypanosoma brucei spp. development in the tsetse fly: characterization of the post-mesocyclic stages in the foregut and proboscis.* Parasitology, 1999. **118 (Pt 5)**: p. 469-78.

11. Sharma, R., et al., *Asymmetric cell division as a route to reduction in cell length and change in cell morphology in trypanosomes.* Protist, 2008. **159**(1): p. 137-51.

12. Schuster, S., et al., *Developmental adaptations of trypanosome motility to the tsetse fly host environments unravel a multifaceted in vivo microswimmer system.* Elife, 2017. **6**.

13. Peacock, L., et al., *Dynamics of infection and competition between two strains of Trypanosoma brucei brucei in the tsetse fly observed using fluorescent markers.* Kinetoplastid Biol Dis, 2007. **6**: p. 4.

14. Peacock, L., et al., *The influence of sex and fly species on the development of trypanosomes in tsetse flies.* PLoS Negl Trop Dis, 2012. **6**(2): p. e1515.

15. Vigneron, A., et al., *A fine-tuned vector-parasite dialogue in tsetse's cardia determines peritrophic matrix integrity and trypanosome transmission success.* PLoS Pathog, 2018. **14**(4): p. e1006972.

16. Kaupp, U.B., N.D. Kashikar, and I. Weyand, *Mechanisms of sperm chemotaxis.* Annu Rev Physiol, 2008. **70**: p. 93-117.

17. Firtel, R.A. and R. Meili, *Dictyostelium: a model for regulated cell movement during morphogenesis.* Curr Opin Genet Dev, 2000. **10**(4): p. 421-7.

18. Boyd, C.D. and G.A. O'Toole, *Second messenger regulation of biofilm formation: breakthroughs in understanding c-di-GMP effector systems.* Annu Rev Cell Dev Biol, 2012. **28**: p. 439-62.

19. Shalaby, T., M. Liniger, and T. Seebeck, *The regulatory subunit of a cGMP-regulated protein kinase A of Trypanosoma brucei.* Eur J Biochem, 2001. **268**(23): p. 6197-206.

20. Strader, C.D., et al., *Structure and function of G protein-coupled receptors.* Annu Rev Biochem, 1994. **63**: p. 101-32.

21. Alexandre, S., et al., *Differential expression of a family of putative adenylate/guanylate cyclase genes in Trypanosoma brucei.* Mol Biochem Parasitol, 1990. **43**(2): p. 279-88.

22. Gould, M.K. and H.P. de Koning, *Cyclic-nucleotide signalling in protozoa.* FEMS Microbiol Rev, 2011. **35**(3): p. 515-41.

23. Paindavoine, P., et al., *A gene from the variant surface glycoprotein expression site encodes one of several transmembrane adenylate cyclases located on the flagellum of Trypanosoma brucei.* Mol Cell Biol, 1992. **12**(3): p. 1218-25.

24. Saada, E.A., et al., *Insect stage-specific receptor adenylate cyclases are localized to distinct subdomains of the Trypanosoma brucei Flagellar membrane.* Eukaryot Cell, 2014. **13**(8): p. 1064-76.

25. Lopez, M.A., E.A. Saada, and K.L. Hill, *Insect stage-specific adenylate cyclases regulate social motility in African trypanosomes.* Eukaryot Cell, 2015. **14**(1): p. 104-12.

26. Savage, A.F., et al., *Transcriptome Profiling of Trypanosoma brucei Development in the Tsetse Fly Vector Glossina morsitans.* PLoS One, 2016. **11**(12): p. e0168877.

27. Naguleswaran, A., N. Doiron, and I. Roditi, *RNA-Seq analysis validates the use of culture-derived Trypanosoma brucei and provides new markers for mammalian and insect life-cycle stages.* BMC Genomics, 2018. **19**(1): p. 227.

28. Shimogawa, M.M., et al., *Cell Surface Proteomics Provides Insight into Stage-Specific Remodeling of the Host-Parasite Interface in Trypanosoma brucei.* Mol Cell Proteomics, 2015. **14**(7): p. 1977-88.

29. Rolin, S., et al., *Transient adenylate cyclase activation accompanies differentiation of Trypanosoma brucei from bloodstream to procyclic forms.* Mol Biochem Parasitol, 1993. **61**(1): p. 115-25.

30. Rolin, S., et al., *Simultaneous but independent activation of adenylate cyclase and glycosylphosphatidylinositol-phospholipase C under stress conditions in Trypanosoma brucei.* J Biol Chem, 1996. **271**(18): p. 10844-52.

31. Salmon, D., et al., *Adenylate cyclases of Trypanosoma brucei inhibit the innate immune response of the host.* Science, 2012. **337**(6093): p. 463-6.

32. Gong, K.W., et al., *cAMP-specific phosphodiesterase TbPDE1 is not essential in Trypanosoma brucei in culture or during midgut infection of tsetse flies.* Mol Biochem Parasitol, 2001. **116**(2): p. 229-32.

33. Oberholzer, M., et al., *The Trypanosoma brucei cAMP phosphodiesterases TbrPDEB1 and TbrPDEB2: flagellar enzymes that are essential for parasite virulence.* FASEB J, 2007. **21**(3): p. 720-31.

34. Oberholzer, M., E.A. Saada, and K.L. Hill, *Cyclic AMP Regulates Social Behavior in African Trypanosomes.* MBio, 2015. **6**(3): p. e01954-14.

35. Oberholzer, M., et al., *Social motility in african trypanosomes.* PLoS Pathog, 2010. **6**(1): p. e1000739.

36. Imhof, S., et al., *Social motility of African trypanosomes is a property of a distinct life-cycle stage that occurs early in tsetse fly transmission.* PLoS Pathog, 2014. **10**(10): p. e1004493.

37. Rotureau, B., et al., *Forward motility is essential for trypanosome infection in the tsetse fly.* Cell Microbiol, 2014. **16**(3): p. 425-33.

38. Mortimer, S.T. and D. Mortimer, *Kinematics of human spermatozoa incubated under capacitating conditions.* J Androl, 1990. **11**(3): p. 195-203.

39. Parkinson, J.S. and S.E. Houts, *Isolation and behavior of Escherichia coli deletion mutants lacking chemotaxis functions.* J Bacteriol, 1982. **151**(1): p. 106-13.

40. Imhof, S., et al., *A Glycosylation Mutant of Trypanosoma brucei Links Social Motility Defects In Vitro to Impaired Colonization of Tsetse Flies In Vivo.* Eukaryot Cell, 2015. **14**(6): p. 588-92.

41. Gibson, W. and M. Bailey, *The development of Trypanosoma brucei within the tsetse fly midgut observed using green fluorescent trypanosomes.* Kinetoplastid Biol Dis, 2003. **2**(1): p. 1.

42. Haas, P. and D. Gilmour, *Chemokine signaling mediates self-organizing tissue migration in the zebrafish lateral line.* Dev Cell, 2006. **10**(5): p. 673-80.

43. Sharma, R., et al., *The heart of darkness: growth and form of Trypanosoma brucei in the tsetse fly.* Trends Parasitol, 2009. **25**(11): p. 517-24.

44. Fragoso, C.M., et al., *PSSA-2, a membrane-spanning phosphoprotein of Trypanosoma brucei, is required for efficient maturation of infection.* PLoS One, 2009. **4**(9): p. e7074.

45. Morand, S., et al., *MAP kinase kinase 1 (MKK1) is essential for transmission of Trypanosoma brucei by Glossina morsitans.* Mol Biochem Parasitol, 2012. **186**(1): p. 73-6.

46. Vassella, E., et al., *Major surface glycoproteins of insect forms of Trypanosoma brucei are not essential for cyclical transmission by tsetse.* PLoS One, 2009. **4**(2): p. e4493.

47. Vassella, E., et al., *Procyclin null mutants of Trypanosoma brucei express free glycosylphosphatidylinositols on their surface.* Mol Biol Cell, 2003. **14**(4): p. 1308-18.

48. Ellis, D.S. and D.A. Evans, *Passage of Trypanosoma brucei rhodesiense through the peritrophic membrane of Glossina morsitans morsitans.* Nature, 1977. **267**(5614): p. 834-5.

49. Gould, M.K., et al., *Cyclic AMP effectors in African trypanosomes revealed by genome-scale RNA interference library screening for resistance to the phosphodiesterase inhibitor CpdA.* Antimicrob Agents Chemother, 2013. **57**(10): p. 4882-93.

50. Oberholzer, M., et al., *Trypanosomes and mammalian sperm: one of a kind?* Trends Parasitol, 2007. **23**(2): p. 71-7.

51. Berbari, N.F., et al., *The primary cilium as a complex signaling center.* Curr Biol, 2009. **19**(13): p. R526-35.

52. Castellani, A., *SOME OBSERVATIONS ON THE MORPHOLOGY OF THE TRYPANOSOMA FOUND IN SLEEPING SICKNESS.* Br Med J, 1903. **1**(2216): p. 1431-2.

53. Capewell, P., et al., *The skin is a significant but overlooked anatomical reservoir for vector-borne African trypanosomes.* Elife, 2016. **5**.

54. Trindade, S., et al., *Trypanosoma brucei Parasites Occupy and Functionally Adapt to the Adipose Tissue in Mice.* Cell Host Microbe, 2016. **19**(6): p. 837-48.

55. Caljon, G., et al., *The Dermis as a Delivery Site of Trypanosoma brucei for Tsetse Flies.* PLoS Pathog, 2016. **12**(7): p. e1005744.

56. Blaazer, A.R., et al., *Targeting a Subpocket in Trypanosoma brucei Phosphodiesterase B1 (TbrPDEB1) Enables the Structure-Based Discovery of Selective Inhibitors with Trypanocidal Activity.* J Med Chem, 2018. **61**(9): p. 3870-3888.

57. Veerman, J., et al., *Synthesis and evaluation of analogs of the phenylpyridazinone NPD-001 as potent trypanosomal TbrPDEB1 phosphodiesterase inhibitors and in vitro trypanocidals.* Bioorg Med Chem, 2016. **24**(7): p. 1573-81.

58. Brun, R. and Schönenberger, *Cultivation and in vitro cloning or procyclic culture forms of Trypanosoma brucei in a semi-defined medium. Short communication.* Acta Trop, 1979. **36**(3): p. 289-92.

59. Lamour, N., et al., *Proline metabolism in procyclic Trypanosoma brucei is down-regulated in the presence of glucose.* J Biol Chem, 2005. **280**(12): p. 11902-10.

60. Ruepp, S., et al., *Survival of Trypanosoma brucei in the tsetse fly is enhanced by the expression of specific forms of procyclin.* J Cell Biol, 1997. **137**(6): p. 1369-79.

61. Bullard, W., et al., *Identification of the glucosyltransferase that converts hydroxymethyluracil to base J in the trypanosomatid genome.* J Biol Chem, 2014. **289**(29): p. 20273-82.

62. Langousis, G., et al., *Loss of the BBSome perturbs endocytic trafficking and disrupts virulence of Trypanosoma brucei.* Proc Natl Acad Sci U S A, 2016. **113**(3): p. 632-7.

63. Furger, A., et al., *Stable expression of biologically active recombinant bovine interleukin-4 in Trypanosoma brucei.* FEBS Lett, 2001. **508**(1): p. 90-4.

64. Beneke, T., et al., *A CRISPR Cas9 high-throughput genome editing toolkit for kinetoplastids.* R Soc Open Sci, 2017. **4**(5): p. 170095.

65. Roditi, I., M. Carrington, and M. Turner, *Expression of a polypeptide containing a dipeptide repeat is confined to the insect stage of Trypanosoma brucei.* Nature, 1987. **325**(6101): p. 272-4.

66. Flück, C., et al., *Cycloheximide-mediated accumulation of transcripts from a procyclin expression site depends on the intergenic region.* Mol Biochem Parasitol, 2003. **127**(1): p. 93-7.

67. Schindelin, J., et al., *Fiji: an open-source platform for biological-image analysis.* Nat Methods, 2012. **9**(7): p. 676-82.

68. Baron, D.M., et al., *Functional genomics in Trypanosoma brucei identifies evolutionarily conserved components of motile flagella.* J Cell Sci, 2007. **120**(Pt 3): p. 478-91.

69. Shimogawa, M.M., et al., *Parasite motility is critical for virulence of African trypanosomes.* Sci Rep, 2018. **8**(1): p. 9122.

70. Jaqaman, K., et al., *Robust single-particle tracking in live-cell time-lapse sequences.* Nat Methods, 2008. **5**(8): p. 695-702.

Chapter 3 – Transcriptomic analyses reveal candidate regulators of *T. brucei* social motility

Abstract

During transmission through the tsetse fly, *Trypanosoma brucei* lives and grows in intimate contact with fly tissue surfaces. In bacteria, surface growth profoundly influences bacterial physiology, pathogenesis and behavior, including promoting social behaviors such as biofilm formation and social motility. Likewise, when cultivated on surfaces *in vitro*, fly midgut-stage *T. brucei* parasites assemble into multicellular groups that can sense and respond collectively to extracellular signals, a behavior termed social motility (SoMo). While surface-associated group behaviors have been well-studied in bacteria, the genes and signaling systems that underlie social behaviors in protozoan pathogens are mostly unknown. SoMo relies on cAMP regulatory systems in the *T. brucei* flagellum, specifically members of the adenylate cyclase (AC) family and cAMP-specific phosphodiesterase B1 (PDEB1). When a subset of AC proteins are knocked down, *T. brucei* exhibits a "hypersocial" phenotype, yet when PDEB1 is lost, *T. brucei* can no longer engage in SoMo. Moreover, *in vivo* fly infection studies reveal that PDEB1 knockout *T. brucei* cannot proceed through their infection cycle, thus demonstrating the predictive power of SoMo to study parasite signaling systems (Chapter 2). To further define gene expression programs that control social motility, we have utilized transcriptomics to compare gene expression profiles of trypanosomes engaging in SoMo on a surface versus planktonic cells in suspension culture, as well as wild type (WT) parasites compared to PDEB1 knockout cells. Our results reveal large-scale changes in gene expression connected with the transition from a planktonic lifestyle to a surface-associated parasite community. As parasites advance outward from the initial site of surface colonization, expression of hundreds of genes is further altered,

indicating substantial developmental changes in parasite physiology. RNAi or gene knockouts against differentially regulated genes in both RNAseq experiments was used to assess their requirement for SoMo and identified new candidate SoMo genes. This work offers insight into genes directing parasite social behavior and parasite cell-cell signaling.

Introduction

Often thought of as individuals, in nature, microbes are typically found living in groups [1-3]. In such cases, group-specific behaviors, such as swarming motility or biofilm formation, are often observed and can be triggered by interaction with a surface [4]. Living as groups on surfaces provides microbes with many advantages over living as individuals, including more efficient surface penetration and migration, enhanced drug-resistance, and increased pathogenesis [4, 5]. Microbial group behaviors have been well-studied in bacteria and social amoeba [1, 6]. Although less well-characterized, the protozoan parasite *Trypanosoma brucei* also engages in group behavior, termed social motility (SoMo) upon interaction with a surface [7].

T. brucei is the causative agent of African sleeping sickness in humans and a related disease called Nagana in animals. The parasite is transmitted to its mammalian hosts through the bite of an infected tsetse fly. In both of its hosts, *T. brucei* must undergo a series of precise migrations and differentiations in specific tissues in order to complete its transmission cycle [8, 9]. Prior work has shown that *T. brucei* up- and down-regulates specific genes as it makes these migrations through its hosts [10-12]. The parasites must sense and transduce signals from the environment to properly time and control these movements and developmental changes, but *T. brucei* signaling systems, however, have been vastly understudied.

Studies of *T. brucei* social motility (SoMo) provide opportunities to interrogate how the parasites sense and respond to cues from their extracellular environment [7, 13]. By exploiting this fact, prior SoMo studies have identified a number of different components of *T. brucei* signaling systems [14-16]. The proteins adenylate cyclase 1 (AC1) and cAMP-specific phosphodiesterase B1 (PDEB1), components of flagellar cAMP signaling, have been shown to be required for social motility [14, 15]. Moreover, recent *in vivo* work has demonstrated that this cAMP signaling pathway is also required for *T. brucei* to move to specific tissue compartments within the tsetse fly [17]. A similar correlation between the *in vitro* requirement for the Requires Fifty Three (RFT1) gene in SoMo and for fly infection has been identified [16]. Thus, SoMo provides a convenient and controllable *in vitro* assay to identify signaling systems that may be important for *T. brucei* transmission *in vivo*.

Given the correlation between social motility *in vitro* and fly infection *in vivo* [16, 17], we sought to identify genes involved in social motility through transcriptome analysis. Two different transcriptome studies were performed. First, parasites engaging in SoMo were compared to cells grown in suspension culture to identify genes whose expression is altered when parasites encounter surfaces. Second, the transcriptome of wild-type (WT) *T. brucei* either on SoMo plates or in suspension culture were compared to that of the social motility mutant, phosphodiesterase B1 knockout cells (PDEB1 KO), in suspension or on SoMo plates.

We report that a vast array of gene expression changes occur when *T. brucei* transitions from suspension culture to cultivation on a surface, indicating substantial changes in cell physiology. Many changes were also observed between cells that can engage in SoMo (WT) versus those that cannot (PDEB1 KO), likely underscoring a major role for cAMP signaling in *T. brucei* biology. Candidate genes identified from both analyses were assayed for SoMo, and a

subset of those are suggested to be novel regulators of social motility. Additional work is needed to further examine role of these genes in *T. brucei* signaling, but they are promising candidates.

Materials and Methods

Cell culture and social motility

T. brucei brucei 29-13 procyclic forms [18] were used for all experiments in this study, with the exception of the 927, 427, and YTAT procyclic forms which were used in the surface versus suspension culture transcriptome. Cells in suspension culture were maintained using Cunningham's semi-defined medium (SM) [19] at 28°C with 5% CO_2. Social motility assays in the surface versus suspension culture transcriptome were performed as described [7]. For the WT versus PDEB1 KO transcriptome and all other SoMo analyses described in this work, SoMo was performed as described in [7] with the differences that the initial density of cells inoculated was 2e7 cells/ml and SoMo plates were shifted to 0% CO_2 24 hours post-plating. These conditions were standard for all experiments except where otherwise noted in the text.

Surface versus Suspension Culture Transcriptomics

T. brucei strains 927, 427, and YTAT were cultivated both in suspension culture and on SoMo plates. Total RNA was isolated using the Qiagen RNeasy kit from two independent replicates of cells grown in each condition and treated with DNase. cDNA libraries were prepared in collaboration with the Merchant laboratory at the University of California Los Angeles. The cDNA libraries were sequenced using 50 base pair single-end reads at a sequence depth of greater than 45 million reads per sample. Reads were mapped to the *T. brucei* reference

genome, and differential gene expression was determined in collaboration with the group of Matteo Pellegrini at UCLA.

WT versus PDEB1 KO Transcriptomics

Both WT and PDEB1 KO *T. brucei* were cultured in suspension culture and on SoMo plates. Total RNA was isolated using the Qiagen RNeasy kit from three biological replicates per condition and treated with DNase. Note that projections from WT plates were isolated in separate samples as the center formation of WT cells on plates. Libraries were prepared by the Clinical Microarray Core at UCLA, and RNA was subjected to 50 base pair single-end reads with the Illumina HiSeq 3000 sequencer. Collaborators in the El Sayed laboratory at the University of Maryland mapped the data to version 29 of the *T. brucei* reference genome, and the program Limma was used to determine differential gene expression.

Generation cell lines

RNAi target regions for the genes listed in Table 3-1 were identified using the Trypanofan RNAit algorithm [20]. These were amplified from 29-13 genomic DNA using the following primers:

Translation elongation factor – 1β (Tb927.10.5840):

FWD: ATATTCTAGATAAAGGAAATCAACGGTCGC

REV: ATATAAGCTTTGTGGTCACCCCACAGTAGA

Histone H3 (Tb927.1.2510):

FWD: ATATTCTAGAAGGCCTCAAAGGGTTCTGAT

REV: ATATAAGCTTTTGTCTCAACCCTGACCCTC

S-adenosylhomocysteine hydrolase (Tb927.11.9590):

FWD: ATATTCTAGACTCGTGCAACATCTTCTCCA

REV: ATATAAGCTTTATCCACAGACACATGCGGT

Universal minicircle sequence binding protein (Tb927.10.6060):

FWD: ATATTCTAGATTGAAACGTCTCCAACCCTC

REV: ATATAAGCTTCTTTTCCATCCCTCCTCTCC

RNA-binding protein (Tb927.8.4450):

FWD: ATATTCTAGAGGAGTGACGACTTTGGTGGT

REV: ATATAAGCTTGCGGCTATGGGATTCTTGTA

RNA-binding protein (Tb927.8.3670):

FWD: ATATTCTAGAACGAGGACGGTTACATGGAG

REV: ATATAAGCTTCACCTCAGTCAAGGAGCACA

Nucleoside diphosphate kinase (Tb927.11.16130):

FWD: ATATTCTAGAGCCAAGCAGCACTACATTGA

REV: ATATAAGCTTTTGAAAATCATCCGCTTTCC

Cyclophilin type peptidyl-propyl cis-trans isomerase (Tb927.11.880):

FWD: AGTCGATCTAGAATGTGAGCATTGCAGGTCAG

REV: AGTCGAAAGCTTTAGTCGGTGTTCGTCTGTGC

Zinc Finger protein (Tb927.10.12330):

FWD: ATATTCTAGAACCCGCCTCAACAGTATCAC

REV: ATATAAGCTTCACATCATGTTTTCCATCGG

Each resulting RNAi fragment was ligated into the p2T7-177 RNAi plasmid [21], which was linearized with Not1 restriction digest and transfected into 29-13 *T. brucei* cells as described

previously [19]. Clonal lines were selected with 10 μg/ml blasticidin in the culture medium. For the CARP4 RNAi cell line, 29-13 cells were transfected with the plasmid containing the amplified RNAi region that had previously been established for CMF34 RNAi [22], and 2.5 μg/ml phleomycin was used for selection. To induce knockdown in all RNAi cell lines, 1 μg/ml tetracycline was added to the culture medium once every 24 hours, i.e. when cell were diluted, for three days to ensure gene knockdown.

For knockout cells lines, PDEB1 KO was generated as described in the Materials and Methods section of Chapter 4 of this Dissertation. This PDEB1 knockout construct is the same as that which was independently generated [17], but it was transfected into the 29-13 background as opposed to the 427 background for this work and that of Chapter 4. Carbonic anhydrase knockout cells were generated through two rounds of homologous recombination using blasticidin and phleomycin resistance genes. The knockout plasmids contained 536 bp upstream and 284 bp downstream of the coding sequence, which were cloned into the pTub plasmid backbone [23]. The primers used to amplify the upstream and downstream regions of homology were:

Upstream FWD: ATATGGTACCGCGGCCGCCCTTCAAGCACGAGAACCAGCGTAGTAG

Upstream REV: ATATCTCGAGAACTCTGGCGGAAGAGTTGCGTACCTAATG

Downstream FWD: ATATGGATCCATTGTTCCTCTGTGCGTTTG

Downstream REV: ATATTCTAGATGGGACGTTAAATACAATGT

The primers used to verify the CA knockout were:

FWD: TGGGGTAGGTTACAGTGGCA

REV: AGTGGGCATTCCCAAGGTTC

The N-terminal YFP-tagged Cyclophilin A cell line was generated using long primer PCR tagging [24]. Regions of homology were generated by PCR amplification from the plasmids pPOTv2 and pPOTv6 [24] using the following primers:

FWD:

TCGTCAAGGCAATGGAAGCTGTCGGCTCGCAAGGGGGAAGCACAAGCAAGCCCGTC

AAGATTGACTCGTGCGGCCAACTAGGTTCTGGTAGTGGTTCC

REV:

TATCAGTACGGGGAGGGGAGGGAAGCAGTGGGATCGGAGCGTAATTTCATGTTGCA

TGTGCACGCCTCTACGTGCTCTTCCCAATTTGAGAGACCTGTGC.

Transfection was done as described above, and clonal cell lines were selected with the blasticidin resistance marker. Cells were then imaged under GFP fluorescence microscopy at 100x magnification using a Zeiss Axioscope II compound microscope. Fluorescent images were taken with an exposure time of 2 seconds.

Growth and Motility Analysis

Growth was monitored in suspension culture over the course of 4 to 10 days depending on the cell line under study. In some cases growth was monitored twice per day, but in most cases, growth was monitored once per day, approximately every 24 hours. At each time point, each cell culture was counted in triplicate and then averaged. Cells were maintained in mid-log growth during the duration of the analysis and maintained between 5e5 cells/ml to approximately 1e7 cells/ml. Cumulative growth was then calculated and plotted over time. In most cases at least two independent clonal lines of each RNAi cell line were assessed for growth, but in the case of RNA-binding protein (Tb927.3.3670) only one clone was assessed. Motility assays were

performed in pre-warmed motility chambers as described [25]. Motility of all cell lines was analyzed as described in [26], except for the Zinc finger protein and Cyclophilin A motility traces, which were analyzed as described in [27].

Quantitative real-time PCR analysis

Level of expression in knockdown and knockout cell lines was assessed by RT-qPCR. Knockdown cells were induced with 1 mg/ml tetracycline for three days before RNA was isolated. RNA was isolated using a Qiagen RNeasy kit. RNA was treated with DNase, and cDNA was prepared. Quantitative real-time PCR was performed as described previously [28]. Primers were designed using NCBI Primer-BLAST [29] and are listed here:

Translation elongation factor – 1β (Tb927.10.5840):

FWD: GTCGTTTGGAATGTGGCGAG

REV: TTTACGGTTGAGGAGGCTGC

Histone H3 (Tb927.1.2510):

FWD: ACCACAACTCTCAAACCAAGCA

REV: ACCCTTTGAGGCCTTCTTGC

S-adenosylhomocysteine hydrolase (Tb927.11.9590):

FWD: GTTTTCGTAACCGCACGCTG

REV: GCGTATCGGTAACACCCTCC

Universal minicircle sequence binding protein (Tb927.10.6060):

FWD: CTTTCGCCATAAAGCGGTGC

REV: CACTACGACCACCACCCAC

RNA-binding protein (Tb927.8.4450):

FWD: ATGCAAACGTGTCAATGCGT

REV: AGGAGAAACTCCCTACGGCT

RNA-binding protein (Tb927.8.3670):

FWD: CGCCGTATTCATAAGCGCAC

REV: TCGTTCCCTTCCTTAGTCGC

Nucleoside diphosphate kinase (Tb927.11.16130):

FWD: GGGAACGCTGGGGATTTCTTA

REV: TTTTCGGGAGATGTCGGGTT

Cyclophilin type peptidyl-propyl cis-trans isomerase (Tb927.11.880):

FWD: ATGGACGTCGTCAAGGCAAT

REV: TAGTCGGTGTTCGTCTGTGC

Zinc Finger protein (Tb927.10.12330):

FWD: GCTGCCGAATCCCCCTAATG

REV: ATGCAAGAGGACGGTCGAGA

CARP 4 (Tb927.3.1060):

FWD: CACACGTTACTGTTGCCACG

REV: TTCCCGATTGAAGCCACCTC

Carbonic anhydrase-like protein (Tb927.11.8260):

FWD: AATGGGCAAGGTGTATGGGG

REV: GCCTTTTACCCCCTCCTCAC

Gene expression was assessed in duplicate and normalized to non-induced cells and two stage-independent control genes, TERT and PFR2 [30], and to non-induced cells.

Western Blot and Secretion analysis

Immunoblotting was done as described previously [28]. Anti-GFP antibody (Molecular Probes rabbit A6455) was used at 1:5,000. β-tubulin was used as a loading control, and the monoclonal antibody E7 [31] was used at 1:10,000.

For Cyclophilin A secretion experiments, *T. brucei* cells were grown to log-phase in 15 ml suspension cultures. Supernatant from the liquid culture was collected by centrifugation at 2800 rpm for 5 minutes and was filter sterilized. To concentrate the supernatant, 12 ml of filtered supernatant was added to Amicon Ultra centrifugal filter units and spun for 20 minutes at 5,000x g. Concentrated supernatant was recovered and boiled in Laemmli Sample Buffer with β-mercaptoethanol, after which it analyzed by Western Blot. Ponceau staining was used as a loading control.

Results

Transcriptomic analysis of surface versus suspension cultured T. brucei identified candidate regulators of social motility

Living as single cells in suspension presents many different challenges compared to life on a surface. To identify *T. brucei* gene expression programs that are important for this difference in lifestyle, RNA from parasites grown in liquid suspension culture (suspension) and from parasites engaging in social motility on a semi-solid surface (plates) was isolated and RNA sequencing was performed (Figure 3-1A). About 2000 genes were differentially expressed between the two conditions ($p < .01$) for two independent biological replicates (Figure 3-1B). Additionally, two different WT strains (2913 and 927) were used to account for strain variation.

The differentially expressed genes between the suspension and plates comparison were filtered in two different ways (Figure 3-1B). First, genes that were differentially expressed in either of the two WT strains and were highly expressed with an RPKM value greater than 50 were assessed. Of these genes, those that were either 2-fold up or down-regulated were identified, and from the 2-fold up-regulated group, 4 candidate genes were chosen for subsequent RNAi analysis. Secondly, differentially expressed genes found in both WT strains which had an RPKM value of 500 or greater were identified. These genes were then separated into either up- or down-regulated categories, and from the up-regulated on plates group, 5 candidate genes were chosen for downstream RNAi analysis. The nine chosen candidate genes are listed in Table 3-1.

Analysis of candidate genes identified in surface versus suspension cultured transcriptomes

Independent tetracycline-inducible RNAi knockdown cell lines for the 9 candidate genes were generated and assessed for growth and efficacy of knockdown (Figure 3-2, Figure 3-3, and Table 3-1). Six of the candidate genes proved to be essential, as exhibited by their reduced growth in suspension culture, and thus, they were not studied further (Figure 3-2, Table 3-1). RT-qPCR analysis for the RNAi line for RNA binding protein (Tb927.8.4450) was currently in progress at the time of this writing, so it is not included. However, growth analysis indicated that knockdown of this gene was lethal, so Tb927.8.4450 was not studied further. Additionally, while the candidate gene, Nucleoside diphosphate kinase was non-essential and sufficiently knocked down, knockdown cell lines exhibited delayed growth in suspension culture. Therefore, this gene was placed on hold and not studied further at this point.

Growth analysis of two genes, Zinc finger protein (Tb927.10.12330) and Cyclophilin A (Tb927.11.880) indicated that they are non-essential (Figure 3-3A & B). Expression of each gene

in their respective RNAi cell lines was significantly reduced in the presence of tetracycline compared to non-induced control cells (Figure 3-3C &D). Because growth of the knockdown cells was normal and because motility in suspension culture is a requirement for SoMo [7], we next asked if reduced expression of the genes affected motility of individual cells in suspension culture. Both Zinc finger protein and Cyclophilin A knockdown lines had similar but slightly increased mean-squared displacements compared to their non-induced controls, but these increases were not statistically significant (Figure 3-3E & F). The total distance each cell traveled in 30 seconds was measured, and while Zinc finger protein knockdown cells moved a smaller distance than their non-induced control ($p \leq 0.01$, unpaired two-tailed t-test) (Figure 3-3G), Cyclophilin A knockdown cells moved a greater distance than their non-induced control ($p \leq 0.05$, unpaired two-tailed t-test) (Figure 3-3H). While the knockdown cells moved either smaller or greater distances compared to their non-induced controls, they still moved similarly to the non-induced controls (Figure 3-3E & F, Table 3-1), so analysis of these knockdown cell lines continued.

To ask if Zinc finger protein or Cyclophilin A were important for social motility, knockdown cell lines were inoculated on SoMo plates in either the absence (-Tet) or presence (+Tet) of tetracycline. Loss of expression of either Zinc finger protein or Cyclophilin A resulted in a delay in SoMo (Figure 3-4A & B). Knocked-down cells formed projections about 48 hours after non-induced cells did. These results suggest that both Zinc finger protein and Cyclophilin A are regulators of social motility.

Cyclophilin A is expressed intracellularly and may be secreted

Work in mammalian cells and other trypanosome species has found that Cyclophilin A is secreted and plays a role in chemotaxis [32, 33]. Therefore, we asked if Cyclophilin A is also secreted in *T. brucei*. To do this, one copy of the Cyclophilin A gene was N-terminally in situ-tagged with YFP. Western blot analysis revealed that the tagged copy of Cyclophilin A was expressed (Figure 3-5A), and immunofluorescence assays indicated that Cyclophilin A localized to both the cytoplasm and the flagellum of *T. brucei* (Figure 3-5B). To ask if Cyclophilin A was being secreted by *T. brucei*, supernatants from YFP-Cyclophilin A suspension cultures were concentrated and analyzed by Western blot (Figure 3-5C). A protein the size of YFP-Cyclophilin A was detected in the supernatant, but a band of the same size was also detected in the WT untagged control (2913) (Figure 3-5C). Additional work is needed to determine if Cyclophilin A is indeed secreted by *T. brucei*.

Transcriptomic analysis of WT versus a cAMP signaling mutant identifies candidate regulators of social motility

Due to the importance of flagellar cAMP signaling for transmission through the fly and the *in vitro* regulation of SoMo [14, 17], a second approach, comparing WT versus PDEB1 knockout (PDEB1 KO) cells, was used to identify novel signaling genes important for SoMo. According to our model (Figure 3-6A), we expect that to engage in SoMo, a decrease in cAMP occurs when cells from suspension culture are inoculated on a surface. This decrease in cAMP likely influences downstream effectors, which in turn alter the expression of genes that are important for SoMo. In the case of cells without PDEB1, cAMP floods the cell [14], thus likely preventing the fine-tuning of downstream effectors and disrupting proper gene expression of SoMo regulators.

To assess these changes, RNA was isolated from both WT and PDEB1 KO cells grown in suspension culture and SoMo plates (Figure 3-6B). For WT cells on SoMo plates, cells from the projections and the center were harvested separately. This was done for two reasons. Firstly, cells that have moved into the projections are likely expressing genes that control that behavior, while those that remain in the center are likely expressing specific genes as well. Secondly, PDEB1 KO cells are restricted to the center, so by comparing the gene expression of cells stuck in the center to those that remain in the center, any genes that change expression simply as a consequence of remaining in the center can be assessed.

RNA sequencing revealed that hundreds to thousands of genes change expression in the five different conditions assessed (Figure 3-6C). This suggests that cells actively engaging in SoMo have enacted large-scale modulations of cell physiology compared to those that cannot. Gene Ontology analysis highlighted intriguing insights into categories of genes that are up- or down-regulated in specific comparisons. Particularly interesting, in the comparison between WT cells from the center on plates and PDEB1 KO on plates, processes involved in directional and forward locomotion were up-regulated in PDEB1 KO cells on plates compared to WT cells in the center, suggesting an importance in the ability to change how the cell is moving. Additionally, further supporting the role of cAMP in the regulation of SoMo, in the WT projections on plates versus WT center on plates comparison, cyclic nucleotide biosynthesis and adenylate cyclase activity are down-regulated in the projections compared to the center, reflecting what has been demonstrated previously [14, 15, 34], that decreased cAMP levels promote SoMo.

Identification of candidate genes from WT versus PDEB1 KO transcriptome analysis

Two particularly interesting genes, cAMP response protein 4 (CARP4) and Carbonic anhydrase-like protein (CA), were identified in this transcriptome analysis (Table 3-3). CARP4 was significantly down-regulated on PDEB1 KO plates compared to WT plates – center. CARP4 was recently identified in a screen for downstream effectors of cAMP in *T. brucei* [35], making it a logical candidate to probe for its role in SoMo. Additionally, prior work also identified CARP4 as a protein highly conserved in motile flagella and called it "conserved component of motile flagella" (CMF34) [22]. Knockdown of CMF34 in an earlier study found that loss of its expression had no effect on growth or motility of individual cells [22]. Therefore, we asked if loss of CARP4 expression affected social motility. We found that while expression of CARP4 was knocked down to 25.9% expression, this loss in expression had no effect on SoMo (Figure 3-7A & B).

Carbonic Anhydrase-like protein (CA) also presented an interesting candidate because prior preliminary work in the Hill laboratory has shown that low levels of carbon dioxide (CO_2) cause *T. brucei* engaging in SoMo to form projections sooner and in greater number than they would at higher levels (Hill laboratory, unpublished). Carbonic anhydrase proteins catalyze both the forward and reverse reactions of the conversion of CO_2 and water into bicarbonate and a proton. CA was down-regulated on plates in both PDEB1 KO suspension vs PDEB1 KO plates and WT suspension vs both WT plates – projections and WT plates – center, indicating that it might be important for *T. brucei* behavior on a surface. A CA knockout (CA KO) was generated, and RT-qPCR and PCR confirmed the knockout (Figure 3-8A & B). If 1e5 WT or CA KO cells were inoculated on a SoMo plate, no difference in SoMo was observed (Figure 3-8C). The SoMo assay was done at both high levels of CO_2 (3.0%) and at ambient levels (0%) to ask if there was a difference because of the relationship between carbonic anhydrase and CO_2. No difference in

SoMo was observed between WT or CA KO cells in high or low CO_2 conditions. Because SoMo is cell density-dependent [13], we asked if a difference could be observed with a lower initial number of cells inoculated. In fact, when the initial cell inoculum of both WT and CA KO was reduced to 0.25e5 cells, CA KO was unable to engage in SoMo in a CO_2-dependant manner (Figure 3-8D). While projections were completely blocked on SoMo plates with CA KO at 3.0% CO_2, at 0% CO_2 SoMo of CA KO was identical to that of WT (Figure 3-8D). The morphology of both WT and CA KO groups are also different in 3.0% versus 0% CO_2 conditions, with a larger center group forming in 3.0% CO_2 conditions compared 0% CO_2. These results indicate that CA is an important regulator of SoMo in an initial cell density and CO_2 dependent manner, highlighting it as an important candidate for future study.

Discussion

Transcriptomic analysis of *T. brucei* grown in suspension or on a surface and *T. brucei* social motility mutants compared to WT has revealed many changes in gene expression. From both of these RNAseq approaches, candidate genes were identified, and a subset of these are important for the regulation of social motility. These data sets are rich with gene candidates and comparisons, and future work is needed to explore these data sets further to identify and test other candidate genes.

For the two genes identified in the suspension versus surface cultivated transcriptome that had normal growth and motility in suspension but delayed SoMo, Zinc finger protein (Tb927.10.12330) and Cyclophilin A (Tb927.11.880), additional work is needed to further confirm their requirement for SoMo. For example, it is possible that the delayed SoMo phenotype exhibited by both could be a consequence of slower growth on a surface. Prior work

has shown that *T. brucei* much reach a specific cell density before projections form [13]. Thus, experiments counting the number of cells on Zinc finger knockdown SoMo plates are needed. Additionally, SoMo has been reported to be a developmentally regulated behavior characteristic of the early-procyclic lifecycle stage [13]. Thus, it is possible that the delayed phenotype could be a result of a subset of cells having differentiated from early-procyclics to late-procyclics, which do not engage in SoMo. Immunofluorescence assays and Western blot analysis with antibodies against early-procyclic markers for both knockdown cell lines from SoMo plates will be needed to address this possibility.

Considering the candidate genes individually, Zinc finger protein (Tb927.10.12330) is part of a family of zinc finger proteins that bind RNA [36]. In trypanosomes most gene expression regulation occurs at the post-transcriptional level with RNA binding proteins serving as key regulators of gene expression [37, 38]. In fact, an mRNA tethering screen for post-transcriptional regulators in *T. brucei* found that our candidate Zinc finger protein (Tb927.10.12330) serves as an activator of gene expression [38]. Localization work has found that it localizes to the cytoplasm [39], where post-transcriptional modification takes place. Based on these data and its influence on SoMo, it is possible that this Zinc finger protein regulates the expression of gene(s) involved in SoMo. RNA-immunoprecipitation experiments with this Zinc finger protein will be needed to identify its target genes.

Cyclophilin A is a member of the cyclophilin family, proteins that serve as chaperones for the isomerization of peptide bonds from *trans* to *cis* at proline residues [32]. In addition to being expressed intracellularly, Cyclophilin A has been shown to be secreted in a number of different cell types, including in the related kinetoplastid parasites *Trypanosoma cruzi* and *Trypanosoma congolense* [40, 41]. In *T. cruzi*, Cyclophilin A secreted by epimastigote-stage

parasites, the lifecycle stage found in the midgut of the reduviid bug, promotes parasite survival by inactivating the host's cationic antimicrobial peptides (CAMPs) [41]. This secreted Cyclophilin A also acts on the *T. cruzi* parasites themselves to drive calcineurin phosphatase signaling, which leads to ATP production and increased infectivity [41]. Thus, it is possible that secreted Cyclophilin A may also be important for *T. brucei* to establish an infection in the midgut of its insect host. Additionally, in mammalian systems, Cyclophilin A has also been shown to serve as a chemoattractant for eosinophils and neutrophils [42]. The cell-cell coordination of social motility likely relies on the ability to respond to chemotactic cues. It is possible that *T. brucei* cells respond to secreted Cyclophilin A from other cells to engage in social behavior. Although we cannot yet say if *T. brucei* secretes Cyclophilin A, we plan to refine and troubleshoot our secretion experiment. Because we saw a band of the same size in supernatants from cultures with YFP-Cyclophilin A and untagged WT cells, it is likely that either the primary or secondary antibody used in this experiment reacts with something in the culture medium or a naturally secreted *T. brucei* factor. To address this possibility, we have tagged CYPA with nanoluciferase, and we will assay for luciferase activity released into the culture medium. It is also possible that the N-terminal tag blocks secretion, so a C-terminal tag will also be assessed.

Preliminary work has shown that CO_2 levels influence SoMo (Hill laboratory unpublished). Thus, due to its putative role in catalyzing the conversion of CO_2 into bicarbonate, Carbonic anhydrase-like protein (Tb927.11.8260) may be a regulator of social motility. Carbonic anhydrase-like protein (Tb927.11.8260) is the only carbonic anhydrase encoded in the *T. brucei* genome [43], suggesting it is a significant player in CO_2 regulation in these parasites. In addition to its mRNA being down-regulated on plates in both suspension versus plates conditions for both

WT and PDEB1 KO, CA was also identified in the *T. brucei* flagellar matrix proteome [44], lending support to its role in *T. brucei* signaling. Bicarbonate has been shown to activate soluble adenylyl cyclases (AC's) in mammalian systems and bacteria [45], and work in pathogenic fungi has shown that CO_2/bicarbonate stimulation of AC's mediates virulence [46, 47]. In fact, CO_2/bicarbonate has been shown to regulate cyclic nucleotide signaling in many diverse species and cell types [48-52]. These findings support the hypothesis that CA may regulate the *T. brucei* adenylyl cyclases that regulate SoMo, perhaps having wider implications on *T. brucei* cAMP signaling regulation. In other kinetoplastid parasites, carbonic anhydrase proteins have been proposed as potential drug targets [53], providing additional motivation to understand how CA affects *T. brucei* biology more fully.

We found that CA is required for SoMo at high levels of CO_2 when there is a low population of cells present (Figure 3-8). The timing of projection formation in SoMo is cell-density dependent [13], suggesting a quorum sensing signaling process is involved. It is possible that higher density of cells may produce a quorum sensing cue, perhaps through acidification of the medium, to a critical amount to allow for the formation of projections. Lower numbers of cells may not be able to produce enough of the necessary cue under high CO_2 conditions. Changes to the acidity of the medium due to difference CO_2 concentrations and the number of cells may serve as a signal for *T. brucei* to form projections. It has been shown that tsetse fly tissues have differential pH environments, with increasingly basic conditions along its infection route from the midgut to the parasite's next infection site, the proventriculus [54]. Thus, it is possible that *T. brucei* uses pH changes as a signal to direct its behavior. Future experiments investigating the possible interaction between CO_2/bicarbonate, carbonic anhydrase, and pH with

T. brucei AC's involved in SoMo and PDEB1 will likely prove informative for understanding regulatory systems that influence social motility and parasite response to environmental changes.

In addition to exploring these two RNAseq datasets more thoroughly to identify other candidate regulators of SoMo, it would also be valuable to compare these transcriptomes with other published *T. brucei* gene expression datasets, particularly flagellar proteomes. The flagellum is a conserved sensory and signaling organelle, so it is possible that flagellar proteins with altered gene expression in either of our two transcriptome datasets are candidate regulators of social motility. We also plan to profile the proteome and phospho-proteome of cells in these comparisons to identify novel candidates and to refine our list of candidate genes from our transcriptome data. We expect the proteomes and phospho-proteomes to be informative because proteins involved in intracellular signaling cascades are often regulated by phosphorylation events. We have now begun these proteomic analysis with collaborators in the Wohlschlegel laboratory at UCLA and will use these data to identify additional candidates for regulators of SoMo.

Overall, these two independent transcriptomic analyses have demonstrated the extensive changes *T. brucei* cells undergo when they encounter a surface and engage in social motility. The candidate genes identified from these screens require further analysis to better understand their function, including assessment of their role on *T. brucei* function *in vivo*. Future work will also include efforts to determine how or if the identified candidates interact genetically utilizing double knockouts in epistasis experiments to gain a deeper understanding of the signaling systems in these deadly pathogens. Elucidating these signaling systems will not only lead to new insights into the biology of *T. brucei* and protozoan parasites, but it may also lead to the development of new transmission-blocking targets and therapeutic strategies.

Figures and Tables

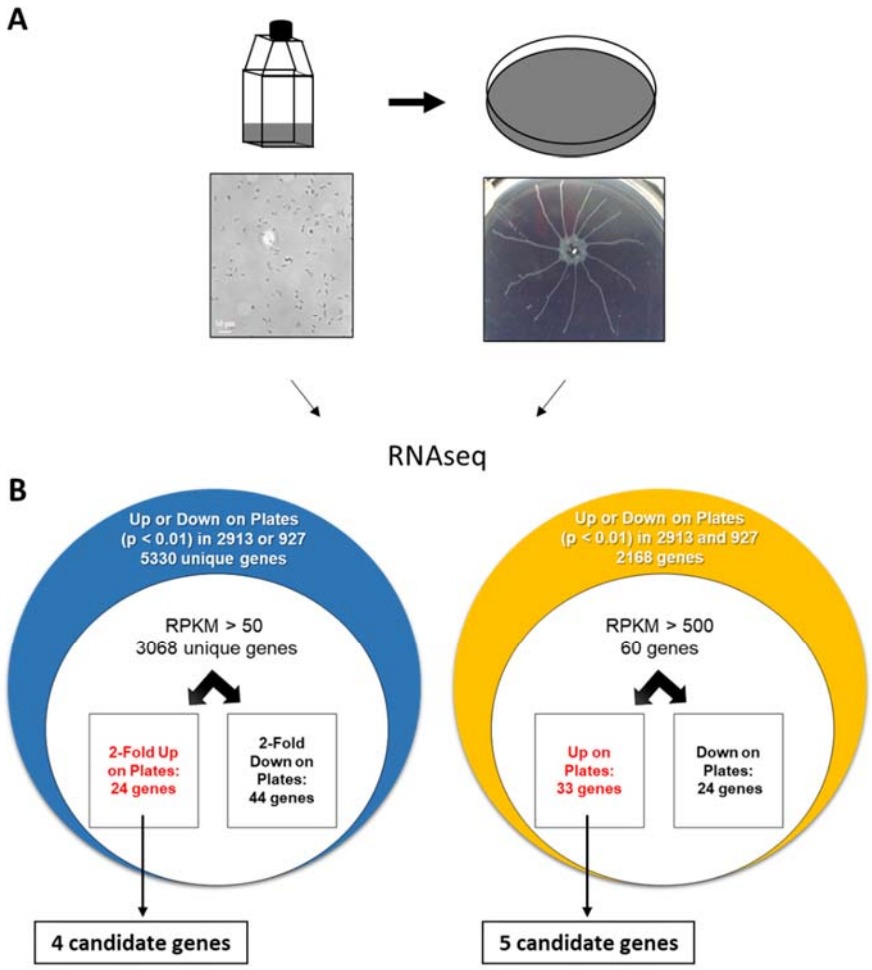

Figure 3-1: RNAseq of *T. brucei* cultured in suspension versus on a surface reveals many significant changes in gene expression.

A) Schematic of transcriptome analysis. Briefly, the transcriptome of *T. brucei* cultured in suspension culture was compared to that of *T. brucei* cultivated on a surface.

B) Differentially expressed transcripts ($p < 0.01$) were identified and filtered by those with reads per kilobase mapped (RPKM) values either greater than 50 or greater than 500. Of these genes, those that were either up or down-regulated were identified, and from both filtering steps, 9

candidate genes were selected for downstream analysis. Full list of candidates is shown in Table 3-1.

Gene ID #	Gene Name	Gene expression in knockdown cell line	Growth in suspension culture	Motility in suspension culture	Social Motility
Tb927.10.5840	Translation elongation factor – 1β	16.4% ± 11.5% (n=2)	Lethal	-	-
Tb927.1.2510	Histone H3	29.14% (n=1)	Lethal	-	-
Tb927.11.9590	S-adenosylhomocysteine hydrolase	18.0% ± 14.0% (n=2)	Lethal	-	-
Tb927.10.6060	Universal minicircle sequence binding protein	22.1% (n=1)	Lethal	-	-
Tb927.8.4450	RNA-binding protein	In progress	Lethal	-	-
Tb927.3.3670	RNA-binding protein	47.5% ± 25.8% (n =3)	Lethal	-	-
Tb927.11.16130	Nucleoside diphosphate kinase	10.7% ± 7.87% (n=2)	Delayed	-	-
Tb927.11.880	Cyclophilin type peptidyl-propyl cis-trans isomerase (Cyclophilin A)	8.66% ± 5.87 (n = 2)	Normal	Normal	Delayed
Tb927.10.12330	Zinc Finger protein	27.6% ± 17.1% (n=3)	Normal	Normal	Delayed

Table 3-1: Gene expression, growth, motility, and social motility phenotypes of candidate genes selected from the suspension versus surface-cultivated transcriptome analysis. Candidate gene expression level was knocked down by RNAi, and expression level in the knockdown cell lines was assessed by RT-qPCR. Knockdown cell lines were then assessed for growth in suspension. If growth was normal, cell lines were then assayed for motility in suspension culture, and if motility was normal, social motility was then tested. The phenotypes for the knockdown of each candidate gene are shown.

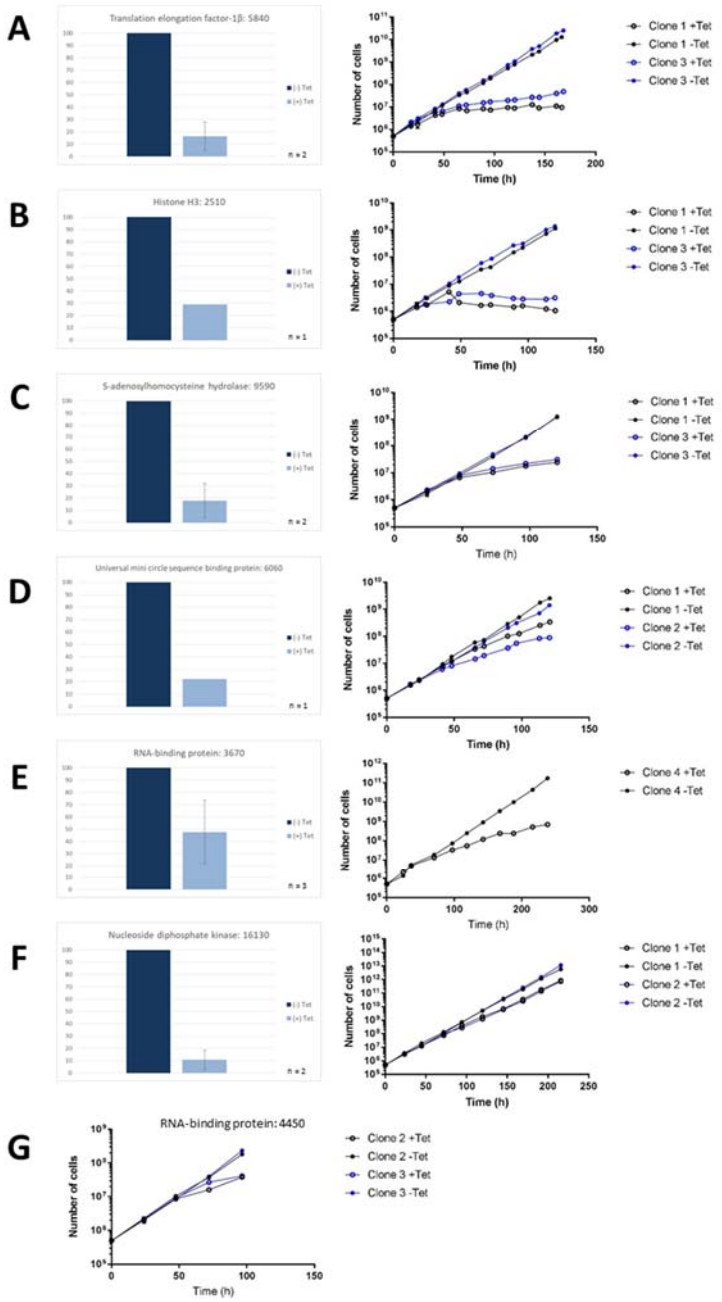

Figure 3-2: Many candidate genes are essential or exhibit slow growth.

A-F, left) The relative level of gene knockdown for each tetracycline-inducible RNAi cell line was measured by RT-qPCR. –Tet indicates non-induced cells, while +Tet indicates knockdown cells. In some cases, as indicated, multiple clones were assessed for knockdown, and the average

level of knockdown is shown. Error bars represent standard deviation. Note that the RT-qPCR results for RNA-binding protein: 4450 are in progress, and thus not included here.

A-F right, G) Growth rate of tetracycline-inducible RNAi cell lines was monitored in suspension culture. Growth of –Tet cell lines are shown as closed circles, while +Tet cell lines are shown by open circles. In most cases two clones were assessed, except for RNA-binding protein: 3670, in which just one clone was monitored. Black and blue colors indicate independent clonal knockdown cell lines.

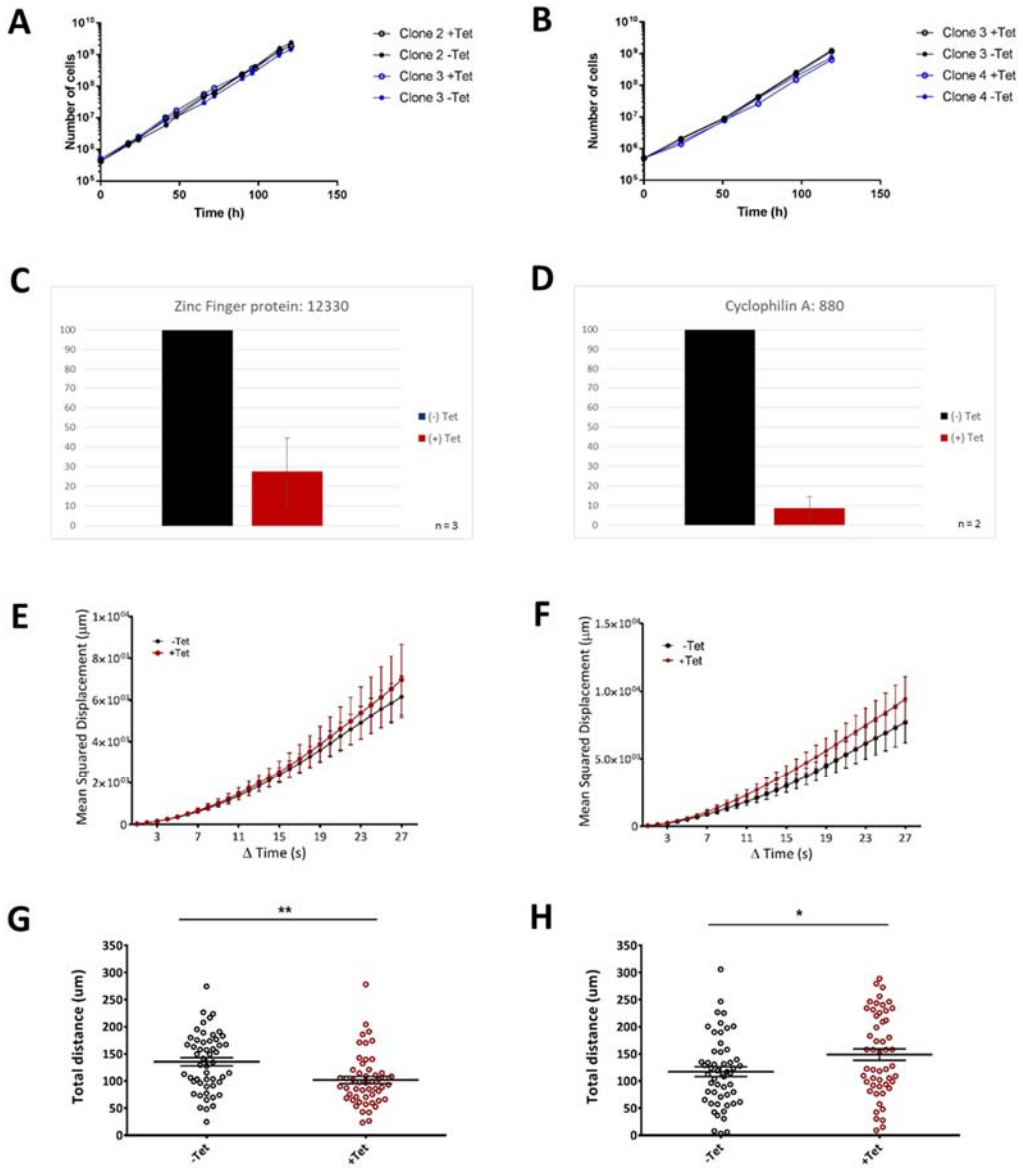

Figure 3-3: Zinc-finger protein and Cyclophilin A are non-essential and knockdown cells have normal growth and motility in culture.

A & B) Growth of two clones (blue and black lines) each of Zinc finger protein and Cyclophilin A in suspension culture was monitored for five days. –Tet is shown by closed circles, and +Tet is shown by open circles.

C & D) The average relative knockdown of the Tet-inducible RNAi lines of Zinc Finger protein and Cyclophilin A are shown. –Tet is black, and +Tet is red. Error bars represent standard deviation.

E & F) Motility of knockdown cells in suspension culture was assessed. Mean-squared displacement is shown for both Zinc finger protein (E) and Cyclophilin A (F). Motility was monitored for 30 seconds. Statistical test: unpaired two-tailed t-test.

G & H) The total distance each cell moved in 30 seconds is shown. Error bars represent standard deviation. * $p \leq 0.05$, ** $p \leq 0.01$, unpaired two-tailed t-test.

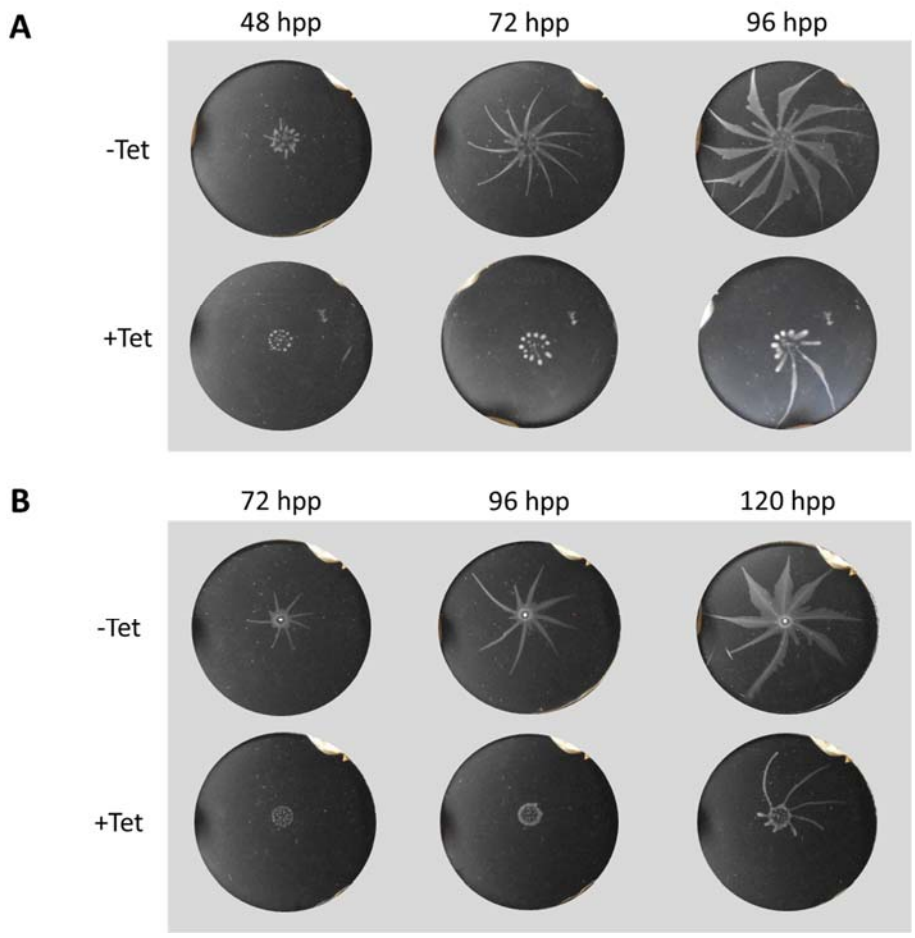

Figure 3-4: Zinc-finger protein and Cyclophilin-A knockdown cells exhibit a delayed SoMo phenotype.

A time course of social motility of Tet-inducible knockdown cell lines for Zinc finger protein (A) and Cyclophilin A (B) are shown with or without tetracycline induction. The same plate was photographed either 2, 3, and 4 days post-plating (A) or 3, 4, and 5 days post-plating (B).

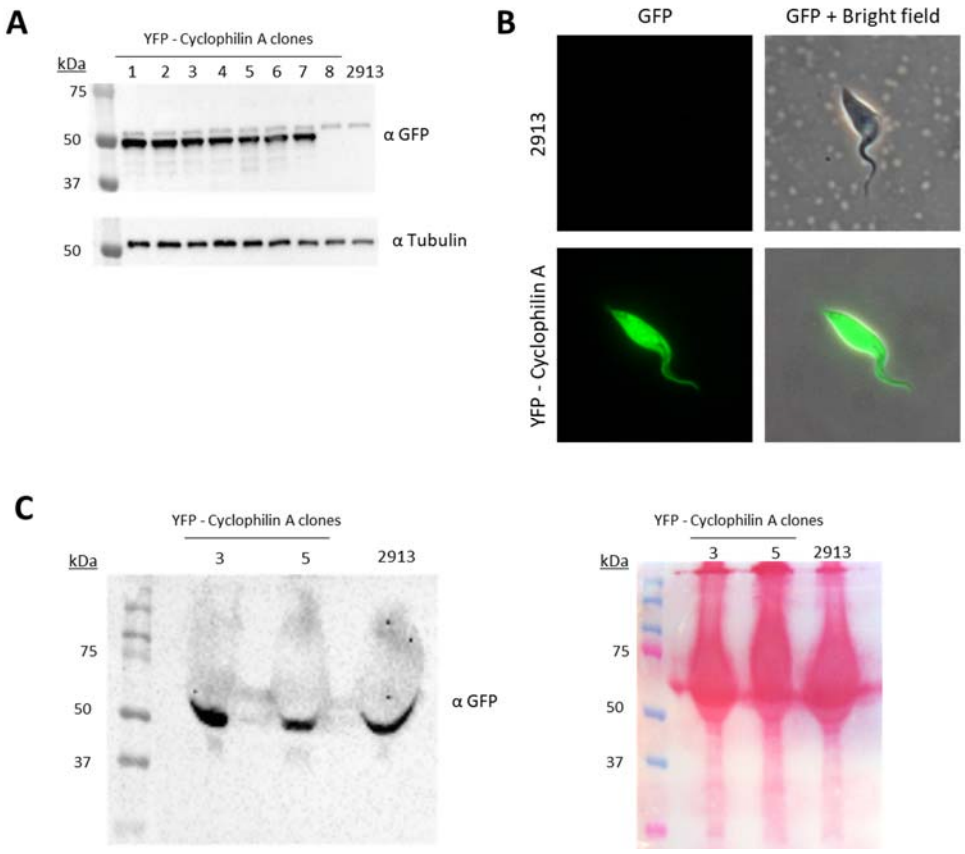

Figure 3-5: Cyclophilin-A localizes to the cytoplasm and the flagellum of *T. brucei,* and it may be secreted.

A) Western blot analysis of N-terminal YFP-tagged Cyclophilin A. A GFP-antibody was used to blot for the YFP tag. Tubulin served as a loading control.

B) Immunofluorescence of a representative wildtype cell (2913) and a YFP-Cyclophilin A cell under GFP and GFP + Bright field illumination.

C) Western blot analysis of concentrated supernatant from YFP-Cyclophilin A and 2913 cells (negative control) using a GFP antibody (left). The same gel used for the Western blot was stained with Ponceau S to serve as a loading control for the amount of protein present in each sample.

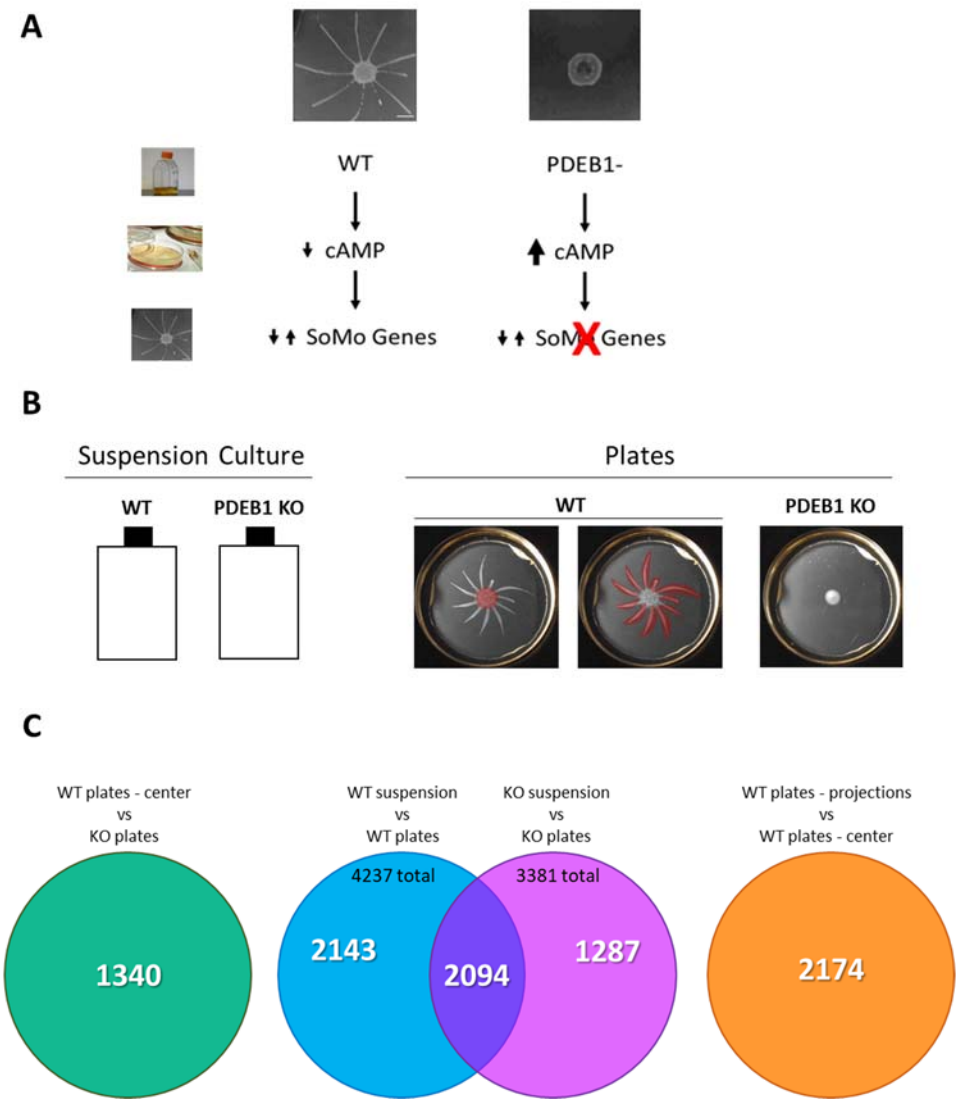

Figure 3-6: RNAseq of WT versus PDEB1 mutant cells allows for the identification of candidate genes that are downstream of cAMP in regulating SoMo.

A) Schematic of strategy to identify genes downstream of cAMP that regulate social motility. B) Growth conditions of *T. brucei* cells to be analyzed by RNAseq: WT and PDEB1 KO cells grown in suspension culture; WT cells only from the center of the SoMo group (pseudo-colored red), WT cells only from the SoMo projections (pseudo-colored red), and PDEB1 KO cells on a SoMo plate. RNA was isolated from cells on plates 3 days post-plating.

C) The number of differentially expressed genes in specific conditions are shown. The WT suspension vs WT plates condition (blue circle) includes genes that are differentially expressed in WT suspension vs WT plates-center and WT suspension vs WT plates-projections. The intersection of the WT suspension vs WT plates circle (blue) with the KO suspension vs KO plates circle (pink) includes 2094 genes that are common to both.

		Biological Process	Molecular Function	Cellular Component
WT plates – center Vs PDEB1 KO plates 1340 genes	Up on WT center (Down on PDEB1 KO plates): 689 genes	• cellular nitrogen compound biosynthetic process • organic substance biosynthetic process • biosynthetic process	• structural constituent of ribosome • structural molecule activity • lyase activity	• ribosome • ribonucleoprotein complex • intrinsic component of membrane
	Down on WT center (Up on PDEB1 KO plates): 651 genes	• directional locomotion • forward locomotion • movement of cell or subcellular component	• calmodulin binding • protein binding • oxidoreductase activity, acting on the aldehyde or oxo group of donors, disulfide as acceptor	• cytoskeleton • cytoskeletal part • axoneme
WT plates - projections Vs WT plates - center 2174 genes	Up on WT projections (Down on WT center): 1059 genes	• cellular process • cellular component organization or biogenesis • ncRNA metabolic process	• protein heterodimerization activity • protein dimerization activity • heterocyclic compound binding	• nucleus • intracellular membrane-bounded organelle • membrane-bounded organelle
	Down on WT projections (Up on WT center): 1115 genes	• cyclic nucleotide biosynthetic process • cyclic nucleotide metabolic process • signal transduction	• phosphorus-oxygen lyase activity • adenylate cyclase activity • cyclase activity	• cytoskeletal part • cytoskeleton • axoneme

Table 3-2: GO-term analysis reveals many differences in WT vs PDEB1 KO cells, cells grown in suspension vs plates, and WT cells in the projections vs the center.

The top three GO-terms in Biological Process, Molecular Function, and Cellular Component are shown for both the up- and down- regulated genes in each comparison listed.

Gene ID #	Gene Name	Identification in WT vs PDEB1 KO transcriptome
Tb927.3.1060	cAMP response protein 4 (CARP4)	Down-regulated on PDEB1 KO plates compared to WT plates.
Tb927.11.8260	Carbonic anhydrase-like protein	Down-regulated on plates compared to suspension culture for both WT and PDEB1 KO cells.

Table 3-3: Candidate genes from WT vs PDEB1 KO transcriptome analysis.

Two candidate genes were chosen from the intersection of WT suspension vs WT plates and KO suspension vs KO plates.

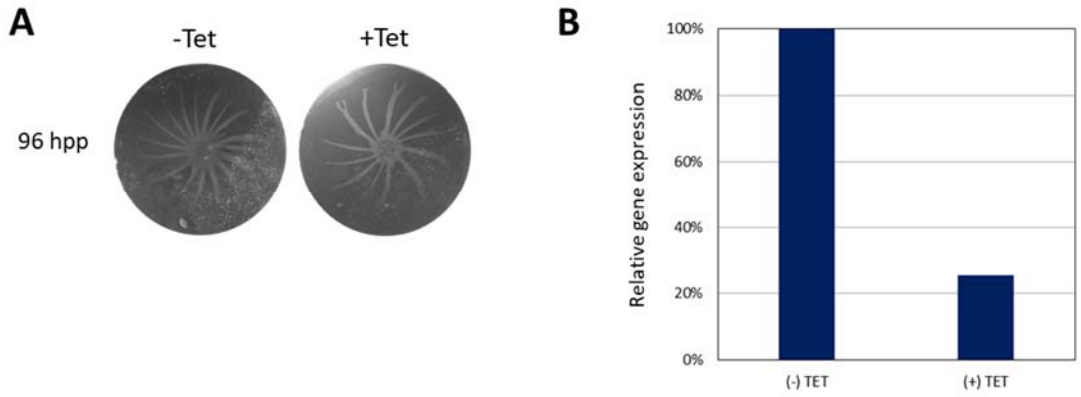

Figure 3-7: Reduction of CARP4 expression has no effect on social motility.

A) Representative SoMo plates of CARP4 RNAi cells are shown 96 hours post-plating (hpp) with and without knockdown induction by tetracycline.

B) RT-qPCR of CARP4 RNAi cells in suspension culture reveals that 25.4% of CARP4 expression remains in knockdown cells.

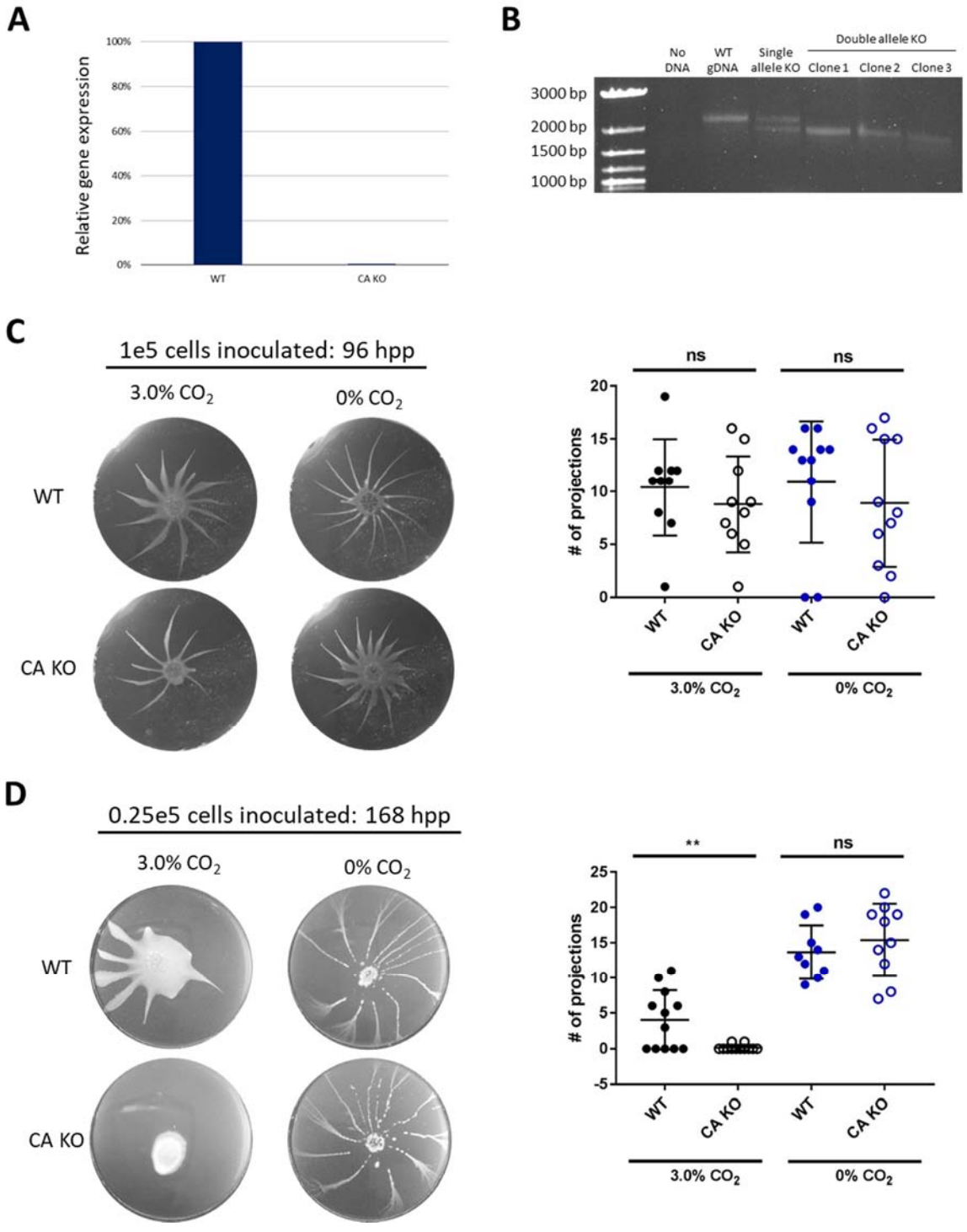

Figure 3-8: Loss of Carbonic Anhydrase expression affects SoMo in a cell density and CO_2 dependent manner.

A) RT-qPCR of WT and CA KO cells shows a loss of Carbonic Anhydrase gene expression in the knockout cell line.

B) CA KO is also confirmed by PCR. Primers sit outside of the region of homologous recombination.

C) Representative SoMo plates of WT or Carbonic Anhydrase KO cells (CA KO) 96 hpp either at 3.0% or 0% CO_2 (left). 1e5 cells were initially inoculated. The number of projections made by WT and CA KO cells during SoMo are quantified (right).

D) Representative SoMo plates of WT or Carbonic Anhydrase KO cells (CA KO) 96 hpp either at 3.0% or 0% CO_2 (left). 0.25e5 cells were initially inoculated. The number of projections made by WT and CA KO cells during SoMo are quantified (right).

Bibliography

1. Crespi, B.J., *The evolution of social behavior in microorganisms.* Trends Ecol Evol, 2001. **16**(4): p. 178-183.
2. Shapiro, J.A., *Thinking about bacterial populations as multicellular organisms.* Annu Rev Microbiol, 1998. **52**: p. 81-104.
3. Bassler, B.L. and R. Losick, *Bacterially speaking.* Cell, 2006. **125**(2): p. 237-46.
4. Harshey, R.M., *Bacterial motility on a surface: many ways to a common goal.* Annu Rev Microbiol, 2003. **57**: p. 249-73.
5. Harshey, R.M. and J.D. Partridge, *Shelter in a Swarm.* J Mol Biol, 2015.
6. Li, S.I. and M.D. Purugganan, *The cooperative amoeba: Dictyostelium as a model for social evolution.* Trends Genet, 2011. **27**(2): p. 48-54.
7. Oberholzer, M., et al., *Social motility in african trypanosomes.* PLoS Pathog, 2010. **6**(1): p. e1000739.
8. Van Den Abbeele, J., et al., *Trypanosoma brucei spp. development in the tsetse fly: characterization of the post-mesocyclic stages in the foregut and proboscis.* Parasitology, 1999. **118 (Pt 5)**: p. 469-78.
9. Vickerman, K., *Developmental cycles and biology of pathogenic trypanosomes.* Br Med Bull, 1985. **41**(2): p. 105-14.
10. Siegel, T.N., et al., *Genome-wide analysis of mRNA abundance in two life-cycle stages of Trypanosoma brucei and identification of splicing and polyadenylation sites.* Nucleic Acids Res, 2010. **38**(15): p. 4946-57.
11. Savage, A.F., et al., *Transcriptome Profiling of Trypanosoma brucei Development in the Tsetse Fly Vector Glossina morsitans.* PLoS One, 2016. **11**(12): p. e0168877.

12. Naguleswaran, A., N. Doiron, and I. Roditi, *RNA-Seq analysis validates the use of culture-derived Trypanosoma brucei and provides new markers for mammalian and insect life-cycle stages.* BMC Genomics, 2018. **19**(1): p. 227.

13. Imhof, S., et al., *Social motility of African trypanosomes is a property of a distinct life-cycle stage that occurs early in tsetse fly transmission.* PLoS Pathog, 2014. **10**(10): p. e1004493.

14. Oberholzer, M., E.A. Saada, and K.L. Hill, *Cyclic AMP Regulates Social Behavior in African Trypanosomes.* MBio, 2015. **6**(3): p. e01954-14.

15. Lopez, M.A., E.A. Saada, and K.L. Hill, *Insect stage-specific adenylate cyclases regulate social motility in African trypanosomes.* Eukaryot Cell, 2015. **14**(1): p. 104-12.

16. Imhof, S., et al., *A Glycosylation Mutant of Trypanosoma brucei Links Social Motility Defects In Vitro to Impaired Colonization of Tsetse Flies In Vivo.* Eukaryot Cell, 2015. **14**(6): p. 588-92.

17. Shaw, S., et al., *Flagellar cAMP signaling controls trypanosome progression through host tissues.* Nat Commun, 2019. **10**(1): p. 803.

18. Wirtz, E., et al., *A tightly regulated inducible expression system for conditional gene knock-outs and dominant-negative genetics in Trypanosoma brucei.* Mol Biochem Parasitol, 1999. **99**(1): p. 89-101.

19. Oberholzer, M., et al., *Approaches for functional analysis of flagellar proteins in African trypanosomes.* Methods Cell Biol, 2009. **93**: p. 21-57.

20. Redmond, S., J. Vadivelu, and M.C. Field, *RNAit: an automated web-based tool for the selection of RNAi targets in Trypanosoma brucei.* Mol Biochem Parasitol, 2003. **128**(1): p. 115-8.

21. Wickstead, B., K. Ersfeld, and K. Gull, *Targeting of a tetracycline-inducible expression system to the transcriptionally silent minichromosomes of Trypanosoma brucei.* Mol Biochem Parasitol, 2002. **125**(1-2): p. 211-6.

22. Baron, D.M., et al., *Functional genomics in Trypanosoma brucei identifies evolutionarily conserved components of motile flagella.* J Cell Sci, 2007. **120**(Pt 3): p. 478-91.

23. Langousis, G., et al., *Loss of the BBSome perturbs endocytic trafficking and disrupts virulence of Trypanosoma brucei.* Proc Natl Acad Sci U S A, 2016. **113**(3): p. 632-7.

24. Dean, S., et al., *A toolkit enabling efficient, scalable and reproducible gene tagging in trypanosomatids.* Open Biol, 2015. **5**(1): p. 140197.

25. Gadelha, C., et al., *Cryptic paraflagellar rod in endosymbiont-containing kinetoplastid protozoa.* Eukaryot Cell, 2005. **4**(3): p. 516-25.

26. Ralston, K.S., N.K. Kisalu, and K.L. Hill, *Structure-function analysis of dynein light chain 1 identifies viable motility mutants in bloodstream-form Trypanosoma brucei.* Eukaryot Cell, 2011. **10**(7): p. 884-94.

27. Shimogawa, M.M., et al., *Parasite motility is critical for virulence of African trypanosomes.* Sci Rep, 2018. **8**(1): p. 9122.

28. Kabututu, Z.P., et al., *CMF70 is a subunit of the dynein regulatory complex.* J Cell Sci, 2010. **123**(Pt 20): p. 3587-95.

29. Ye, J., et al., *Primer-BLAST: a tool to design target-specific primers for polymerase chain reaction.* BMC Bioinformatics, 2012. **13**: p. 134.

30. Brenndörfer, M. and M. Boshart, *Selection of reference genes for mRNA quantification in Trypanosoma brucei.* Mol Biochem Parasitol, 2010. **172**(1): p. 52-5.

31. Chu, D.T. and M.W. Klymkowsky, *The appearance of acetylated alpha-tubulin during early development and cellular differentiation in Xenopus.* Dev Biol, 1989. **136**(1): p. 104-17.

32. Nigro, P., G. Pompilio, and M.C. Capogrossi, *Cyclophilin A: a key player for human disease.* Cell Death Dis, 2013. **4**: p. e888.

33. Moro, A., et al., *Secretion by Trypanosoma cruzi of a peptidyl-prolyl cis-trans isomerase involved in cell infection.* EMBO J, 1995. **14**(11): p. 2483-90.

34. Saada, E.A., et al., *"With a Little Help from My Friends"-Social Motility in Trypanosoma brucei.* PLoS Pathog, 2015. **11**(12): p. e1005272.

35. Gould, M.K., et al., *Cyclic AMP effectors in African trypanosomes revealed by genome-scale RNA interference library screening for resistance to the phosphodiesterase inhibitor CpdA.* Antimicrob Agents Chemother, 2013. **57**(10): p. 4882-93.

36. Kramer, S., N.C. Kimblin, and M. Carrington, *Genome-wide in silico screen for CCCH-type zinc finger proteins of Trypanosoma brucei, Trypanosoma cruzi and Leishmania major.* BMC Genomics, 2010. **11**: p. 283.

37. Clayton, C. and M. Shapira, *Post-transcriptional regulation of gene expression in trypanosomes and leishmanias.* Mol Biochem Parasitol, 2007. **156**(2): p. 93-101.

38. Erben, E.D., et al., *A genome-wide tethering screen reveals novel potential post-transcriptional regulators in Trypanosoma brucei.* PLoS Pathog, 2014. **10**(6): p. e1004178.

39. Dean, S., J.D. Sunter, and R.J. Wheeler, *TrypTag.org: A Trypanosome Genome-wide Protein Localisation Resource.* Trends Parasitol, 2017. **33**(2): p. 80-82.

40. Pellé, R., et al., *The African trypanosome cyclophilin A homologue contains unusual conserved central and N-terminal domains and is developmentally regulated.* Gene, 2002. **290**(1-2): p. 181-91.

41. Kulkarni, M.M., et al., *Secreted trypanosome cyclophilin inactivates lytic insect defense peptides and induces parasite calcineurin activation and infectivity.* J Biol Chem, 2013. **288**(12): p. 8772-84.

42. Xu, Q., et al., *Leukocyte chemotactic activity of cyclophilin.* J Biol Chem, 1992. **267**(17): p. 11968-71.

43. Berriman, M., et al., *The genome of the African trypanosome Trypanosoma brucei.* Science, 2005. **309**(5733): p. 416-22.

44. Oberholzer, M., et al., *Independent analysis of the flagellum surface and matrix proteomes provides insight into flagellum signaling in mammalian-infectious Trypanosoma brucei.* Mol Cell Proteomics, 2011. **10**(10): p. M111.010538.

45. Chen, Y., et al., *Soluble adenylyl cyclase as an evolutionarily conserved bicarbonate sensor.* Science, 2000. **289**(5479): p. 625-8.

46. Klengel, T., et al., *Fungal adenylyl cyclase integrates CO2 sensing with cAMP signaling and virulence.* Curr Biol, 2005. **15**(22): p. 2021-6.

47. Bahn, Y.S., et al., *Carbonic anhydrase and CO2 sensing during Cryptococcus neoformans growth, differentiation, and virulence.* Curr Biol, 2005. **15**(22): p. 2013-20.

48. Zippin, J.H., et al., *Bicarbonate-responsive "soluble" adenylyl cyclase defines a nuclear cAMP microdomain.* J Cell Biol, 2004. **164**(4): p. 527-34.

49. Tresguerres, M., et al., *Established and potential physiological roles of bicarbonate-sensing soluble adenylyl cyclase (sAC) in aquatic animals.* J Exp Biol, 2014. **217**(Pt 5): p. 663-72.

50. Visconti, P.E., et al., *Bicarbonate dependence of cAMP accumulation induced by phorbol esters in hamster spermatozoa.* Biochim Biophys Acta, 1990. **1054**(2): p. 231-6.

51. Choi, H.B., et al., *Metabolic communication between astrocytes and neurons via bicarbonate-responsive soluble adenylyl cyclase.* Neuron, 2012. **75**(6): p. 1094-104.

52. Paunescu, T.G., et al., *Association of soluble adenylyl cyclase with the V-ATPase in renal epithelial cells.* Am J Physiol Renal Physiol, 2008. **294**(1): p. F130-8.

53. Vermelho, A.B., et al., *Carbonic anhydrases from Trypanosoma and Leishmania as anti-protozoan drug targets.* Bioorg Med Chem, 2017. **25**(5): p. 1543-1555.

54. Liniger, M., et al., *Cleavage of trypanosome surface glycoproteins by alkaline trypsin-like enzyme(s) in the midgut of Glossina morsitans.* Int J Parasitol, 2003. **33**(12): p. 1319-28.

Chapter 4 – Identification of positive chemotaxis in the protozoan pathogen *Trypanosoma brucei*

Abstract

To complete its infectious cycle, the protozoan parasite, *Trypanosoma brucei*, must navigate through diverse tissue environments in both its tsetse fly and mammalian hosts. This is hypothesized to be driven by yet unidentified chemotactic cues. Prior work has shown that parasites engaging in social motility *in vitro* alter their trajectory to avoid other groups of parasites, an example of negative chemotaxis. However, movement of *T. brucei* toward a stimulus, positive chemotaxis, has so far not been reported. Here we show that upon encountering *E. coli,* socially behaving *T. brucei* parasites redirect group movement toward the neighboring bacterial colony. This response occurs at a distance from the bacteria, and involves active changes in parasite motility. By developing a quantitative chemotaxis assay, we show that the attractant is a soluble, diffusible signal dependent on actively growing *E. coli*. Time-lapse and live video microscopy revealed that *T. brucei* chemotaxis involves changes in both group and single cell motility. Groups of parasites change direction and accelerate their movement as they approach the source of attractant, and this correlates with increasingly constrained movement of individual cells within the group. Identification of positive chemotaxis in *T. brucei* opens new opportunities to study mechanisms of chemotaxis in these medically and economically important pathogens. This will lead to deeper insights into how these parasites interact with and navigate through their host environments.

Importance

Almost all living things need to be able to move, whether it is toward desirable environments or away from danger. For vector-borne parasites, successful transmission and infection require that these organisms be able to sense where they are and use signals from their environment to direct where they go next, a process known as chemotaxis. Here we show that *Trypanosoma brucei*, the deadly protozoan parasite that causes African sleeping sickness, can sense and move toward an attractive cue. To our knowledge, this is the first report of positive chemotaxis in these organisms. In addition to describing a new behavior in *T. brucei*, our findings enable future studies of how chemotaxis works in these pathogens, which will lead to deeper understanding of how they move through their hosts and may lead to new therapeutic or transmission-blocking strategies.

Introduction

A fundamental aspect of virtually all motile organisms is the ability to move in response to a change in the environment. One strategy to do this is through chemotaxis, the movement of an organism toward or away from a chemical cue. In microbial systems, chemotaxis has been best characterized in bacteria and social amoeba, which both employ chemotaxis to locate nutrients and avoid unfavorable environments [1-3]. Many bacterial pathogens in particular rely on chemotaxis to move toward their desired site of infection [4-7]. For protozoan pathogens, which typically must navigate through multiple hosts and a variety of different tissues in each host, chemotaxis has also been hypothesized to be necessary for pathogenesis and transmission [8-13].

Trypanosoma brucei is a protozoan pathogen that causes African sleeping sickness in humans and Nagana in cattle. *T. brucei* is transmitted to a mammalian host through the bite of an

infected tsetse fly. In the mammalian host, the parasite first mounts a bloodstream infection before penetrating the blood vessel endothelium to enter the central nervous system, resulting in lethality if not treated [14]. *T. brucei* also infiltrates adipose and dermal tissue and these extravascular sites represent biologically significant parasite reservoirs that may influence pathogenesis and transmission [15-17]. Within the tsetse fly vector, *T. brucei* must complete an ordered series of directional migrations through specific host tissues in order to be transmitted to a new mammalian host [18]. Mechanisms underlying tissue tropisms observed in the mammalian host and insect vector are unknown.

Evidence demonstrating that *T. brucei* can adjust its motility in response to external cues comes from *in vitro* studies of social motility (SoMo), which occurs in procyclic-form *T. brucei* (tsetse fly midgut stage) when cultivated on semi-solid agarose [19]. During SoMo, *T. brucei* cells assemble into groups that engage in collective motility, moving outward from the point of inoculation to form radial projections. Movement outward is cell density-dependent, suggesting a quorum sensing component to control of motility [20]. Furthermore, when parasites in projections sense other *T. brucei* cells, they actively avoid one another, either by stopping their forward movement or changing their direction of movement, thus exhibiting capacity for negative chemotaxis [19]. Additional work revealed that SoMo depends on cAMP signaling in the flagellum [21-23], and recent *in vivo* work has demonstrated that flagellar cAMP signaling is required for *T. brucei* progression through fly tissues [8]. Thus, simply being able to move is not sufficient to complete the transmission cycle and the combined findings support the idea that *T. brucei* depends on chemotaxis in response to extracellular signals to direct movement through host tissues. To our knowledge however, positive chemotaxis has not been reported for *T. brucei*.

Here we report that *T. brucei* engaging in SoMo exhibit positive chemotaxis toward *E. coli*, a behavior we term "BacSoMo." While *T. brucei* does not typically interact with *E. coli* in its natural hosts, it does encounter other bacteria, and *E. coli* serves as an easy-to-control bacterial sample for use in dissecting chemotaxis *in vitro*. We find that the response is mediated by an active change in parasite motility that occurs at a large distance from the bacteria, indicating response to a chemical cue. Supporting this idea, we show that attraction is mediated by a signal that diffuses through the culture medium and requires actively growing *E. coli*. Our findings allowed us to begin dissecting cellular behavior that underlies chemotaxis in *T. brucei*, revealing changes in motility at both the group and individual cell level. We expect these studies to lead to a deeper understanding of how trypanosomes navigate through diverse environments encountered during their transmission and infection cycle.

Materials and Methods

Trypanosomes

T. brucei brucei 29-13 procyclic culture forms were used in this study [24]. Parasites were cultured in SM media with 10% heat-inactivated fetal bovine serum (FBS) at 28°C and 5% CO_2. GFP-tagged 29-13 cells were generated by transfection with Spe1-linearized pG-eGFP-Blast (gift of Isabel Roditi, University of Bern) as described previously [23]. PDEB1 knockout cells were generated in the 29-13 background by two sequential rounds of homologous recombination using pTub plasmids conferring resistance to blasticidin and phleomycin [25]. 452 bp upstream and 635 bp downstream of the PDEB1 coding sequence were used as regions of homology, the same regions used to independently create a PDEB1 KO cell line as in [8]. Transfection of the

knockout plasmids was performed as described previously [26]. Primers used to amplify the PDEB1 regions of homology were described previously in [8], and are also listed here:

Upstream FWD: atatGCGGCCGCTGCATTATGTTACTTGGGGGCA

Upstream REV: atatCTCGAGGACGTAGTGTCCAACTGTGC

Downstream FWD: atatGGATCCAGTCAGTTGACCGGTGGTAG

Downstream REV: atatTCTAGACCGCCACAACTCCCTCTTAC

Bacteria

E. coli strain DH5α with an ampicillin resistance plasmid were used for all experiments. *E. coli* from a glycerol stock were grown overnight in SM. 0.3µl of log-phase *E. coli* were inoculated on SoMo plates. Bacterial growth on SoMo plates was monitored over 4 days by washing colonies off independent SoMo plates twice per day and measuring the OD600 for 3 biological replicates.

Social Motility assay

Plates for social motility assays were prepared based on [19]. Briefly, a solution of 4% (wt/vol) SeaPlaque GTG agarose (Lonza) in MilliQ water was sterilized for 30 minutes at 250°C. Water that evaporated was replaced with sterile MilliQ water after heating, and the solution was then cooled to 70°C. SM made without antibiotics was pre-warmed to 42°C. The stock agarose solution was then diluted to 0.4% in the pre-warmed SM. The SM and agarose mixture was then mixed with ethanol (0.05% final solution) and methanol (0.05% final solution). 11.5 ml of the final mixture was poured in 100 mm by 15 mm petri dishes (Fisherbrand), which were allowed to dry with the lids off in a laminar flow hood for 1 hour.

Parasites in mid-log phase growth ($1x10^6$ – $7x10^6$ cells/ml) were counted, harvested, and concentrated to 2 x 10^7 cells/ml, and 5 µl of concentrated parasites were placed on the SoMo plate. Plates were allowed to incubate at room temperature for 10 minutes and were then wrapped in parafilm and placed at 28°C and 3% CO_2. 24 hours post-plating, SoMo plates were moved to 28°C and 0% CO_2.

Chemotaxis assays

Chemotaxis assays were developed based on [27]. SoMo plates, *T. brucei*, and *E. coli* were prepared as stated above. *T. brucei* was inoculated 1.5 cm from the center of the SoMo plate, and *E. coli* or the sample being tested was inoculated 2.0 cm from the center, opposite the *T. brucei*. At 120 hours post-plating, the number of projections that had entered a 2-cm diameter circle centered on the test sample location were counted. A chemotaxis index was calculated for each sample by comparing the average number of projections entering the circle for the sample condition to the average number of projections in control plates with *T. brucei* alone. Error bars represent standard error of the mean, and unpaired two-tailed t-tests were used to determine significance compared to the *T. brucei* alone control condition.

Sterilized 1-cm diameter Whatman filter discs were used for the Filter Paper condition. For the *E. coli* on lid condition, 9 ml of a 1.0% SM and agarose solution was plated on the lid of the SoMo plate and allowed to dry in the same manner as the SoMo plate. *E. coli* were then plated 2 cm from the center on the lid on the plate. The lid was placed on the plate such that the *E. coli* on the lid and *T. brucei* on the plate aligned on the same horizontal axis. For the 0.2 µm filter experiment, 0.2 µm GNWP Nylon membranes from Millipore were used. Because the 0.2 µm filters had a slightly larger diameter than the standard 2 cm diameter used in the other

chemotaxis experiments, the number of projections that contacted the 0.2 μm filter were counted and compared in each condition.

For conditions in which *E. coli* cell lysate or formaldehyde-treated *E. coli* were tested, the number of bacterial cell equivalents that would have been present four days post-plating, as determined in our bacterial growth curve, were used. To generate hypotonically lysed *E. coli*, $1x10^{11}$ cells/ml from a log-phase overnight culture in LB were centrifuged at 8000 rpm for 10 minutes at 4°C. The supernatant was replaced with sterile MilliQ water. The sample was centrifuged again under the same conditions as above, and the supernatant was again replaced with water and lysozyme. The sample was then sonicated on ice 6 times for 10 seconds and then spun at 4000 rpm for 10 minutes to pellet the cell debris. The supernatant was filter-sterilized through a 0.2μm filter. For boiled *E. coli* lysate, $1x10^{11}$ cells/ml from a log-phase overnight culture in LB were centrifuged at 8000 rpm for 10 minutes at 4°C, and the supernatant was replaced with sterile MilliQ water. The sample was then boiled for 10 minutes. Finally, for formaldehyde-treated *E. coli*, $1x10^{11}$ cells/ml from a log-phase overnight culture in LB were centrifuged at 8000 rpm for 10 minutes at 4°C, washed in 1x phosphate buffered saline (PBS), and the PBS was replaced with 4% paraformaldehyde. Tubes with formaldehyde-treated *E. coli* were rotated at 4°C for 10 minutes, washed 3 times in 1x PBS, and spun down and re-suspended in the appropriate volume of 1x PBS.

Time-lapse video analysis

SoMo assays were performed as described above. At 24 hours post-plating, SoMo plates were inverted and placed on a ring stand over a light box. Still photographs were taken every 30 minutes for 162 – 185 hours by a Brinno TLC200 Pro camera, positioned above the inverted

plate. Camera settings were configured to compile still images into an .avi file with a play back speed of 10 frames/second. The .avi movies were converted into stacks using Fiji (Version 1.0) [28], and the segmented-line tool was used to measure the distance each projection moved over time.

Non-linear regression analysis:

A non-linear regression program was written in MATLAB to model the speed versus time data for the projections in the time-lapse videos. The "fit non-linear regression model" feature in MATLAB was used to create models for a piece-wise function that changed from a line with zero slope to a linear slope, an exponential function, and a linear function to find the best fit for the data.

Individual Cell Motility analysis

For Figure 4-7, SoMo assays were performed as described above using a population of trypanosomes in which 10% GFP-tagged 29-13 cells were mixed with untagged cells and inoculated on the SoMo plate. Projections that had come near enough to *E. coli* to being moving toward it were placed in the "Attraction" category, and those that were not were placed in the "No Attraction" category. Tips of these projections were then imaged on a Zeiss Axiovert 200 M inverted microscope at 20x magnification under bright-field microscopy. Movies (30 seconds each) of fluorescent cells in these same projections were then captured at 30 frames per second with Adobe Premiere Elements 9 using 20x magnification under fluorescence microscopy. Fluorescent cells were tracked using a *T. brucei*-specific cell-tracking algorithm developed in MATLAB [29], and the resulting mean-squared displacement and curvilinear and straight-line

velocities were calculated as described [30]. Linearity is calculated as the ratio of straight-line velocity to curvilinear velocity. We only considered cells that were in focus for a minimum of 300 consecutive frames out of 900.

Time-course analysis assessing projection movement simultaneously with individual cell motility

For time-course analyses in Figure 4-8, SoMo assays using 1% GFP-tagged cells mixed with untagged cells were performed as described above. At each time point indicated, SoMo plates were photographed using a Fujifilm FinePix JZ250 digital camera, tips of projections were imaged on a Zeiss Axiovert 200 M inverted microscope as described above, and a 30-second video of GFP-expressing cells was captured as described above for each projection. This analysis was done for 11 projections each for *T. brucei* alone and *T. brucei* + *E. coli*.

Projection Curvature calculation

Bright-field images at 20x magnification were acquired for the tips of projections. A straight line of 3-inch standard length was used to measure the angle of curvature of the tip of projections. One end of the standard was placed tangent to the peak of the projection tip, and a straight line was drawn at the other end, perpendicular to the standard until it intersected with the projection. The interior angle was then calculated and assigned as the angle of curvature (Figure 4-4C).

Results

1. Socially behaving *T. brucei* exhibit chemotaxis toward *E. coli*.

During social motility (SoMo), *T. brucei* cells engage in collective motility to form radial projections that have a clockwise curvature (when viewed from above, Figure 4-1A, left) [19]. When parasites in these projections sense other *T. brucei* cells, they actively avoid one another, either by stopping their forward movement, or by changing their direction of movement (Figure 4-1A, center) [19]. We found, however, that when encountering *E. coli* on the SoMo plate, the parasite projections continue moving to make contact with the bacteria, and even appear to alter their movement to move directly toward the bacteria (Figure 4-1A, right).

We hypothesized that the movement toward bacteria is chemotactic in nature, but we also considered whether it might instead reflect preferential growth in the direction of bacteria. To distinguish between these possibilities, we used time-lapse imaging to examine dynamics of *T. brucei* movement. SoMo assays were performed with or without bacteria. Images were taken every 30 minutes over the course of 162 hours (Figure 4-1B, Movie 4-1) or 185 hours (Figure 4-1C, Movie 4-2) and compiled into movies. Plates were turned upside-down to prevent condensation on the lid from interfering with the analysis, and then imaged from the bottom side of the plate. Therefore, the curvature of the projections observed in videos and time-lapse images is counter-clockwise.

In the absence of bacteria, parasites moved continually outward, forming arced projections that radiated away from the inoculation site and rarely altered their general direction of movement (Figure 4-1B and Movie 4-1). At early stages, projections maintained relatively even spacing and uniform width, having a single leading edge without branching. As projections neared the periphery, the space between projections increased and parasites advanced from the lateral edge to form branches (arrows Figure 4-1B; Movies 4-1 and 4-3). The observation that branching only occurred when spacing between neighboring projections increased supports the

idea [19] that inhibitory signals from parasites in adjacent projections prevent parasite movement from the side of projections. In some cases, thickening of a projection was observed prior to branching (Figure 4-2, Movie 4-3), suggesting that cell density-dependent signals driving parasite movement outward [20] may overcome inhibitory signals between projections. Parasites in branches continued to adjust their movements so that they did not make contact with adjacent parasites (Figure 4-1B, Figure 4-2, Movies 4-1 and 4-3), demonstrating that parasite-dependent inhibitory signals were still active.

Time-lapse imaging of SoMo assays carried out in the presence of a neighboring bacterial colony allowed us to define the point at which parasites sense and respond to bacteria, both spatially and temporally, and this revealed several important findings. First, these analyses clearly demonstrate that parasite movement toward bacteria is an active response and not simply an absence of avoidance. Notice for example, that rather than continuing to the periphery of the plate, as occurs in the absence of bacteria, parasite projections curve sharply to move directly toward bacteria (Figure 4-1C: Numbers 1-3, 88.5 – 116.5 hpp). Moreover, in the presence of bacteria, projections change curvature from counterclockwise to clockwise (Figure 4-1C: triangle, 74.5 and 88.5 hpp) and exhibit extensive branching (Figure 4-1C, 130.5 hpp – 158.5 hpp), with branches moving directly toward the bacteria. Second, these changes in movement occur at a large distance from the edge of the bacterial colony, indicating that parasites are responding to a chemical cue derived from the bacteria, rather than detecting the bacteria by direct contact (Figure 4-1C, Movie 4-2).

A third important result to come from time-lapse studies is that the timescale of the response rules out the possibility that movement toward bacteria simply represents preferential growth in this direction. For example, between 88.5 and 116.5 hpp (Figure 4-1C: Numbers 1-3),

parasites have turned sharply toward bacteria and advanced to contact the bacterial colony. This projection impacted the bacteria at 109 hpp (Movie 4-2). Growing on plates, *T. brucei* has a doubling time of approximately 24 hours [19], thus the 20.5-hour time interval between 88.5 hpp and 109 hpp, thus represents slightly less than one cell doubling time, yet the parasites moved 22.61 mm (Movie 4-2), which corresponds to approximately 1046 cell lengths [31]. Clearly this distance cannot be accounted for by cell doubling. Therefore, parasites alter their movement in response to a signal that acts at a distance to move directly toward bacteria.

In the moments before parasite projections impact the bacterial colony, we see individual parasites move directly from parasite projections into the bacterial colony (Movie 4-5). After contact, parasites spread out as they infiltrate the bacterial colony (Movie 4-6). Meanwhile, bacteria from the colony advance outward along parasite projections (Figure 4-1C: arrowheads). As bacteria advance along one projection, parasites from adjacent projections become attracted to the position now occupied by bacteria (Figure 4-1C, 144.5 and 158.5 hpp). Therefore, repositioning of the bacterial population directly correlates with a change in position of the attractant source. As parasites move to this attractant, they now even cross other projections of parasites to reach the bacteria (Figure 4-1C: asterisks, 158.5 hpp), a phenomenon never observed in the absence of attractant. This indicates that the attractive cue from the bacteria is stronger than the repulsive cue that otherwise prevents contact and crossing of projections [19]. Altogether, time-lapse video analysis demonstrated that parasites in projections are not exhibiting preferential growth towards *E. coli*, but are actively directing their movement toward it through positive chemotaxis in response to an attractant that acts at a large distance from the source.

2. The attractant is diffusible and requires actively growing *E. coli*.

To define characteristics of the attractant, we employed a quantitative chemotaxis assay (Figure 4-3A) developed based on similar assays used to study chemotaxis in parasitic worms [27]. In this assay a chemotactic index is calculated for each sample by determining the number of projections that enter a 2-cm diameter centered around the sample, compared to how many projections enter a circle centered at the same position when no sample is present. A positive chemotaxis index indicates attraction, while a negative index indicates repulsion, and "perfect" attraction or repulsion is defined as + 1 or – 1, respectively. In this assay, a colony of live bacteria has a positive chemotactic index, + 0.37, indicating *T. brucei* is strongly attracted to *E. coli*. We previously showed that *T. brucei* is repelled by other groups of *T. brucei* [19]. Therefore, as a negative control, we used a *T. brucei* PDEB1 knockout mutant that does not form projections [8] and produces a colony approximately equal in size to bacterial colonies grown on SoMo plates (Figure 4-3A). We found that *T. brucei* was "perfectly" repelled by PDEB1 KO *T. brucei*, with a chemotaxis index of – 1, supporting the capacity of the assay to distinguish attractive versus repulsive chemotaxis.

We next considered whether attraction to bacterial colonies might simply reflect a response to a physical perturbation in the agarose surface created by the physical presence of the bacterial colony. To assess this, the chemotactic index of a piece of filter paper was tested, and *T. brucei* showed no significant chemotactic response (Figure 4-3A), reinforcing the hypothesis that the response to bacteria is a chemotactic response.

Bacteria can produce both volatile – released into the air – and soluble compounds, which can serve as chemotactic cues [32, 33]. To differentiate between these, we first asked whether *T. brucei* would respond positively to aerosolized volatile compounds. To do this, we employed a

variation in the chemotaxis assay in which *E. coli* was plated on the lid of the petri dish while *T. brucei* was inoculated on the bottom. *T. brucei* showed no response to *E. coli* on the lid, indicating that the attractive cue is non-volatile and suggesting it is a soluble factor that diffuses through the culture medium.

To test if the attractant was diffusible through the culture medium, we assessed chemotaxis to *E. coli* plated on 0.2µm filter discs placed on the SoMo plate. The filter disc prevents bacteria from directly contacting the culture medium, but allows small molecules to diffuse through it. In this case, the chemotactic index was determined relative to a 0.2µm filter disc with no bacteria (Figure 4-3B). *T. brucei* were attracted to *E. coli* grown on the 0.2µm filter, with a positive chemotactic index of + 0.42, indicating that attraction occurs in response to a factor smaller than 0.2µm that diffuses through the culture medium. It is important to note that the attractant may be a signal produced directly from the bacteria, or it may be a product of a chemical reaction between a factor produced by the bacteria and a substance present in the culture medium.

Because *T. brucei* are attracted to a diffusible cue emanating from *E. coli*, we next asked if this required dead or dying bacteria. When bacteria die, they often lyse, releasing intracellular metabolites into the environment, which can serve as nutrient sources for other microbes [34, 35], so we asked if *T. brucei* were attracted to products released from lysed *E. coli*. To determine the number of lysed bacterial cell equivalents to test, we determined the number of *E. coli* cells present 96 hpp (Figure 4-4) because parasites show an attractive response to bacteria within 96 hpp (Figure 4-1C). First, hypotonically lysed bacteria were tested to ask if the attractant might be a protein released from lysed bacteria, but no chemotactic effect was seen (Figure 4-3A). Second, boiled *E. coli* cell lysates were tested. Boiling *E. coli* would denature proteins and

inactivate heat labile compounds, but other potential metabolites would still be present; however, boiled lysates were repulsive to *T. brucei*. We also assessed the chemotactic index of dead but non-lysed *E. coli*, using formaldehyde-killed bacteria and found that *T. brucei* were repelled by formaldehyde-killed bacteria. Taken together, these results indicate that the attractant is diffusible through the culture medium, and actively growing bacteria are required for its production. Efforts to isolate the attractant have so far been unsuccessful.

3. Projections of parasites accelerate upon sensation of an attractant.

The attraction of social *T. brucei* to *E. coli* presents an opportunity to investigate changes in *T. brucei* cell behavior underlying chemotaxis. In time-lapsed video analysis we noticed that projections appeared to speed up just before they made contact with the bacterial colony (Figure 4-5A; Movies 4-1 and 4-2). To quantify this, we measured the distance each projection travelled between each frame of the time-lapsed video, either in the presence or absence of bacteria. A plot of distance traveled over time was then generated for each projection (Figure 4-5B).

In the absence of bacteria, projections moved with mostly constant speed, as indicated by the constant slope of the line generated by the distance vs time analysis (Figure 4-5B, left). Distance vs time measurements were fit to a linear or quadratic regression model (Table 4-1). All three projections fit the linear model very well ($R^2 = 0.99$). Although the quadratic model also fit ($R^2 = 0.99$), the constant in front of x^2 value in each of the three equations was always very small, indicating that in the absence of bacteria, the projections do in fact move with a constant speed (~0.1 cm/hr) (Table 4-1, Table 4-2). For projections moving in the presence of bacteria, the distance traveled versus time analysis indicated that the projections moved at a constant speed at first, as indicated by the constant slope at early time points. In the hours before impact

with the bacteria however, the slope of the line continually increased, indicating that the projections of parasites were accelerating toward the bacteria (Figure 4-5B, right).

Because it is difficult to fit an equation to a line that changes from a constant slope to an increasing slope, we plotted the change in distance between each time point (i.e. the derivative), which represents the speed versus time (Figure 4-5C). While there was noise in the speed versus time analysis for each projection measured, all projections in the presence of bacteria clearly increased their speed above the baseline speed of projections in the absence of bacteria (Figure 4-5C, Figure 4-6). For example, in the final 30 minutes before they impacted bacteria, projections reached speeds from 0.24 to 0.59 cm/hr (Figure 4-5C).

To model the speed change of projections in the presence of bacteria, we used different non-linear regression models designed in MATLAB to analyze the speed versus time data (Figure 4-5D, Table 4-3). Because projections appeared to move with a constant speed early and then accelerate before colliding with the bacteria, we first asked how well the data could be modeled by a piecewise function that began with a line with zero slope (i.e. constant speed), and then at an unknown time point (denoted by the term "k") changed to a line with a constant and positive slope (i.e. increasing speed) (Table 4-3). We also asked how well the speed data fit an exponential equation, which would give an equation with an almost zero slope at early time points and then continuously change to an increasing slope. Finally, we also asked how well the data fit a linear equation, which would give an equation of a line with an unchanging slope. We found that while the piecewise function that modeled a zero slope to constant slope fit the speed data well ($R^2 = 0.522 – 0.929$), the exponential regression provided a slightly better model for the data ($R^2 = 0.544 – 0.973$) (Table 4-3). Linear regression did not fit the data as well as the other two models (Table 4-3, Table 4-2). These same models were applied to the speed of

projections in the absence of bacteria, and most models gave equations of lines with close to zero slope, confirming that these projections move with a constant speed. These analyses indicate that in the presence of bacteria, projections move with a mostly constant speed, but in the hours before they reach the bacteria the group increases its speed dramatically. Analysis of additional time-lapse videos in the presence or absence of bacteria are consistent with these findings (Figure 4-6, Table 4-2).

4. Individual cell motility within the group is constrained when sensing an attractant.

To assess changes in individual cell behavior occurring in response to attractant, untagged wild type cells were mixed with 10% GFP-expressing cells. Through the use of a cell-tracking algorithm [29], the movements of individual GFP-tagged cells were assessed within the group. Individual cells at the tips of projections that were either not attracted to *E. coli* (n = 1368 cell tracks) or attracted to *E. coli* (n = 1403 cell tracks) were traced in 30-second videos (Figure 4-7A). We assessed mean-squared displacement (MSD), which takes into account both the speed of cells and how far they move from their initial locations. We found that cells undergoing chemotaxis to *E. coli* had a lower MSD than cells in projections that were not undergoing chemotaxis (Figure 4-7B). The lower MSD could mean that individual cells move more slowly in response to the attractant or that they alter how they move. To examine this further, we plotted the distribution of each cell's curvilinear velocity versus straight-line velocity. We found that cells sensing an attractant had reduced straight-line velocity compared to cells not engaged in chemotaxis, suggesting that when an attractant is detected, parasites restrict their motion to smaller and more curving paths to remain near to the attractant (Figure 4-7C). To quantify this change, we determined linearity for each cell, calculated as the ratio of straight-line velocity to

curvilinear velocity. The mean linearity for cells not undergoing chemotaxis was 0.174, while the mean linearity for those undergoing chemotaxis was significantly decreased at 0.110 (two-tailed t-test, $p < 0.0001$). A similar paradigm, i.e. cells constraining their movements as they move closer to an attractant source, has been described for bacterial chemotaxis to K^+ ions within a biofilm [36].

5. Group movement and single-cell movement are correlated.

To ask if acceleration of projections toward *E. coli* correlates directly with constrained motility of individual cells, we monitored projection movement and individual cell motility in parallel as a function of time. SoMo assays were done with a mixture of 1% GFP-tagged cells mixed with untagged cells. 30-second movies of individual fluorescent cells at the tips of the projections were taken at the same time-points as photographs of projections over a two day time course. In a representative SoMo plate of *T. brucei* co-inoculated with *E. coli*, the distance projections moved was measured every 2 hours from 68.5 to 74 hours post-plating and from 90 to 96 hours post-plating, moments before the projection collided with the bacteria (Figure 4-8A). As expected, projections increased their speed as they moved toward bacteria, accelerating from 0.0231 cm/hr to 0.1563 cm/hr (Figure 4-8C, Table 4-4). In contrast, in the absence of bacteria, the speed of the projection did not change substantially: 0.0315 cm/hr to 0.0502 cm/hr (Figure 4-8D, Table 4-4). It should be noted that these speeds as slower overall than those seen in the time-lapse videos in Figure 4-5, which may be due to slight technical differences between the two assays. Over the time-course analysis of the projection tips became more curved (Figure 4-8A and B, center), but this was observed regardless of whether bacteria were present (Figure 4-4B), indicating it is likely a characteristic of advancing projections.

To ask how the movement of individual cells within the projections changed over time, we monitored the movement of individual cells in the same projections used for the speed analysis above. In the presence of *E. coli* parasite cells showed a decrease in MSD and exhibited increasingly constrained motility over time (Figure 4-8A right and E), consistent with the results from Figure 4-7B and C. While there was variation in the MSD of individual cells over time, a significant decrease in MSD was clear by 94 and 96 hpp (One-way ANOVA, $p < 0.0001$). Interestingly, the decrease in MSD seen in the presence of bacteria was not observed until the last two time-points before the projection impacted the bacteria (Figure 4-8E, 94 and 96 hpp), even though the projection as a whole had already begun increasing its speed in the prior two time-points (Figure 4-8C, 90 and 92 hpp). This finding suggests that, while changes in group and individual movement in the presence of bacteria are correlated, projection speed increases first, and individual cells constrain their motility later. We suspect there is some aspect of individual cell behavior that leads to the increased speed of the group as a whole, but so far, this has not been revealed in our current assays. In the absence of bacteria, *T. brucei* cells showed variation in MSD over time (Figure 4-8F), which was reflected in variation of how constrained the movement of cells was over time (Figure 4-8B right). However, no single time-point exhibited a significant decrease in MSD from all of the others (One-way ANOVA) (Figure 4-8F), indicating that cells in the absence of bacteria were not changing how they moved within the projection, in contrast to how individual cells behave in the presence of bacteria.

When individual cells in multiple projections were monitored over time, this same trend held true (Figure 4-8F and G). In the presence of bacteria, the mean linearity of cells in projections decreased over time (Figure 4-8G), indicating that their movements were becoming more constrained as they moved toward the bacteria. However, in the absence of bacteria the

mean linearity stayed relatively constant over time (Figure 4-8H). Taken together, these time-course experiments indicate that in response to bacteria, the speed of projections increases, and subsequently, individual cells within projections constrain their motion.

Discussion

We have shown that socially behaving *T. brucei* engage in positive chemotaxis towards a diffusible cue produced by actively growing *E. coli*, and we have begun to elucidate the changes in group and individual cell behaviors that characterize this response. While chemotaxis has been well-studied in bacteria and other protozoans [1-3], to our knowledge, our results provide the first demonstration of positive chemotaxis in *T. brucei* and illustrate the capacity for interkingdom interactions between bacteria and protozoa.

In its tsetse fly host, *T. brucei* must undergo a series of specific migrations and differentiations as it moves from the fly midgut to the proventriculus, and finally to the salivary glands. It is therefore reasonable to anticipate that *T. brucei* may employ chemotaxis to direct movement in response to signals in specific fly tissues. Supporting this idea, prior work connected cAMP as a second messenger to control of parasite group movements *in vitro* [22, 23], and recent work demonstrated that *T. brucei* requires an intact cAMP signaling pathway in order to progress through tsetse fly tissues *in vivo* [8]. The idea that chemotactic cues direct parasite progression through their insect vectors has been proposed for other kinetoplastid parasites, including *Leishmania* spp and *Trypanosoma cruzi,* which have been shown to engage in chemotaxis *in vitro* [9, 11, 12]. Our discovery of positive chemotaxis in *T. brucei* demonstrates that, in addition to moving away from external signals [19], these organisms can detect and move toward specific signals in their extracellular environment.

The ability to sense and respond to signals is also expected to be important for *T. brucei* within its mammalian hosts. Prior work has shown that in addition to the bloodstream and central nervous system, skin and adipose tissues represent important reservoirs contributing to pathogenesis and transmission [15-17]. Mechanisms underlying *T. brucei* tropism to extravascular tissues remain to be determined, but positive chemotaxis could be involved. Study of the malaria parasite, *Plasmodium berghei*, in a mammalian host found that as parasites moved closer to blood vessels, their trajectories became more constrained [37], which mirrors the more constrained individual cell motility exhibited by *T. brucei* in response to attractant (Figure 4-7C, 4-8A, 4-8G). Chemotaxis may also help *T. brucei* evade the immune system, analogous to what has been proposed for evasion of host neutrophils by *Leishmania* parasites [10]. Motility is essential for *T. brucei* virulence in the mammalian host, perhaps allowing for quick changes in direction to avoid immune cells [29]. Thus, the change in individual cell motility observed as parasites move toward an attractant (Figure 4-7C, 4-8A, 4-8G) may be an important mechanism to infiltrate tissues and/or evade immune cells within the host.

The question arises as to why *T. brucei* exhibits chemotaxis toward bacteria. Notably, although *E. coli* is not typically present within the tsetse fly, the fly is home to three species of endosymbiotic Gram-negative bacteria: *Sodalis glossinidius*, *Wigglesworthia glossinidia*, and *Wolbachia* spp [38]. While *Wolbachia* is restricted to the reproductive tract, *Wigglesworthia*, an obligate endosymbiont, is found intracellularly in bacteriocytes within a specialized structure called the bacteriome near the anterior midgut, and extracellularly in the milk glands [39, 40]. *Sodalis* is found throughout the fly midgut and in a variety of other tissues [38]. Evidence for functional interactions between *T. brucei* and bacterial endosymbionts of the tsetse comes from work demonstrating *T. brucei* reliance on bacterial products during fly transmission [38]. For

example, *Wigglesworthia* produces folate and phenylalanine, but *T. brucei* cannot. *T. brucei* does, however, encode transporters for these metabolites [41]. Similarly, *T. brucei* encodes an incomplete threonine biosynthesis pathway [42]. While the tsetse cannot provide homoserine that is necessary for *T. brucei* threonine biosynthesis [43], *Sodalis* can [44]. A long-standing interaction between *T. brucei* and *Sodalis* is also evidenced by an example of horizontal gene transfer of the gene phospholipase A1 from *Sodalis* to *T. brucei* [45, 46]. Of note, numerous studies of lab-reared and field-caught tsetse flies have demonstrated that the presence of *Sodalis* in the tsetse increases the likelihood of infection by *T. brucei* [47-50]. Therefore, *T. brucei* likely interacts closely with *Sodalis* during the transmission cycle, and chemotaxis toward *Sodalis* would be advantageous. While *Sodalis* can be cultured *in vitro*, we were unable to culture them on *T. brucei* media, or vice versa, and thus the chemotactic index of *T. brucei* toward *Sodalis* could not be determined.

In addition to containing three endosymbiotic bacteria, the midgut of field-caught tsetse flies harbor a wide variety of bacterial species, with variation among different species of tsetse flies and geographic distribution [50]. The most common genera of bacteria found in tsetse fly midguts included *Enterobacter*, *Enterococcus*, and *Acinetobacter* [50]. While the three endosymbionts discussed above are all Gram-negative bacteria, other common genera found in the fly midgut encompass both Gram-negative and Gram-positive bacterial species. We did not detect attraction or repulsion toward the Gram-positive bacterium *B. subtilis* (data not shown). Future work will be needed to assess whether *T. brucei* shows chemotaxis to other examples of Gram-positive and Gram-negative bacteria.

The exact *in vivo* correlates of group movements observed in SoMo remain unclear. However, our findings, together with recent work [8, 20, 22, 23, 51, 52], clearly illustrate the

value of SoMo for uncovering novel aspects of trypanosome biology that are relevant *in vivo*. The discovery here of BacSoMo, positive chemotaxis in *T. brucei*, and development of quantitative chemotaxis assays enabled us to begin investigating cellular mechanisms underlying directed movement in these pathogens. These systems enable studies at the scale of groups of cells and at the level of individual cells within groups. In bacteria, both scales of analysis have provided important insights. In *Pseudomonas* and *Myxococcus* for example, analyses of group chemotaxis led to the discovery of signaling molecules and systems that regulate bacterial social behavior and motility on a surface [53, 54]. In cyanobacteria, studies of individual cell movements within a group revealed how movement of individuals can dictate the trajectory of the group during the phototactic response [55]. Thus, our analyses of changes in both group and individual cell behavior in response to attractant set the stage for further study of the cellular and molecular mechanisms underlying these responses.

Looking forward, the quantitative chemotaxis assays reported here will serve as an important tool to enable dissection of cellular and molecular mechanisms used by trypanosomes to detect and respond to environmental signals. As a straightforward *in vitro* assay, screens for small molecules that inhibit or alter trypanosome sensory behavior without affecting parasite fitness could identify novel transmission blocking targets. Additionally, RNAi library screens for genes involved in sensation signaling, or other chemotactic functions could be identified, further elucidating signaling systems required for parasite transmission and pathogenesis. Overall, the identification of positive chemotaxis in *T. brucei* will lead to deeper insights into how parasites sense and respond to cues in their changing host environments, facilitating the development of novel therapeutic and transmission blocking strategies.

Acknowledgements

We thank Hunter Bennet for technical assistance with initial studies, and Michael Albanese for help developing non-linear regression models utilizing MATLAB. For their numerous helpful suggestions and discussions, we thank Drs. Wenyuan Shi and Marvin Whiteley as well as Dr. Beth Lazazzera, whom additionally provided the *B. subtilis* flagellar mutant. Members of the Hill laboratory are thanked for discussions and comments on the manuscript. K.H.: NIH grant AI052348. S.D. Ruth L. Kirschstein National Research Service Award GM007185 and Ruth L. Kirschstein National Research Service Award AI007323.

Author Contributions

E.S. and M.L. discovered BacSoMo. S.D. and K.H. designed the experiments, analyzed the data, and wrote initial drafts of the paper. S.D. conducted the experiments and performed the statistical analysis and mathematical modeling. S.D., E.S., M.L., and K.H. edited and gave feedback on the manuscript.

Figures and Tables

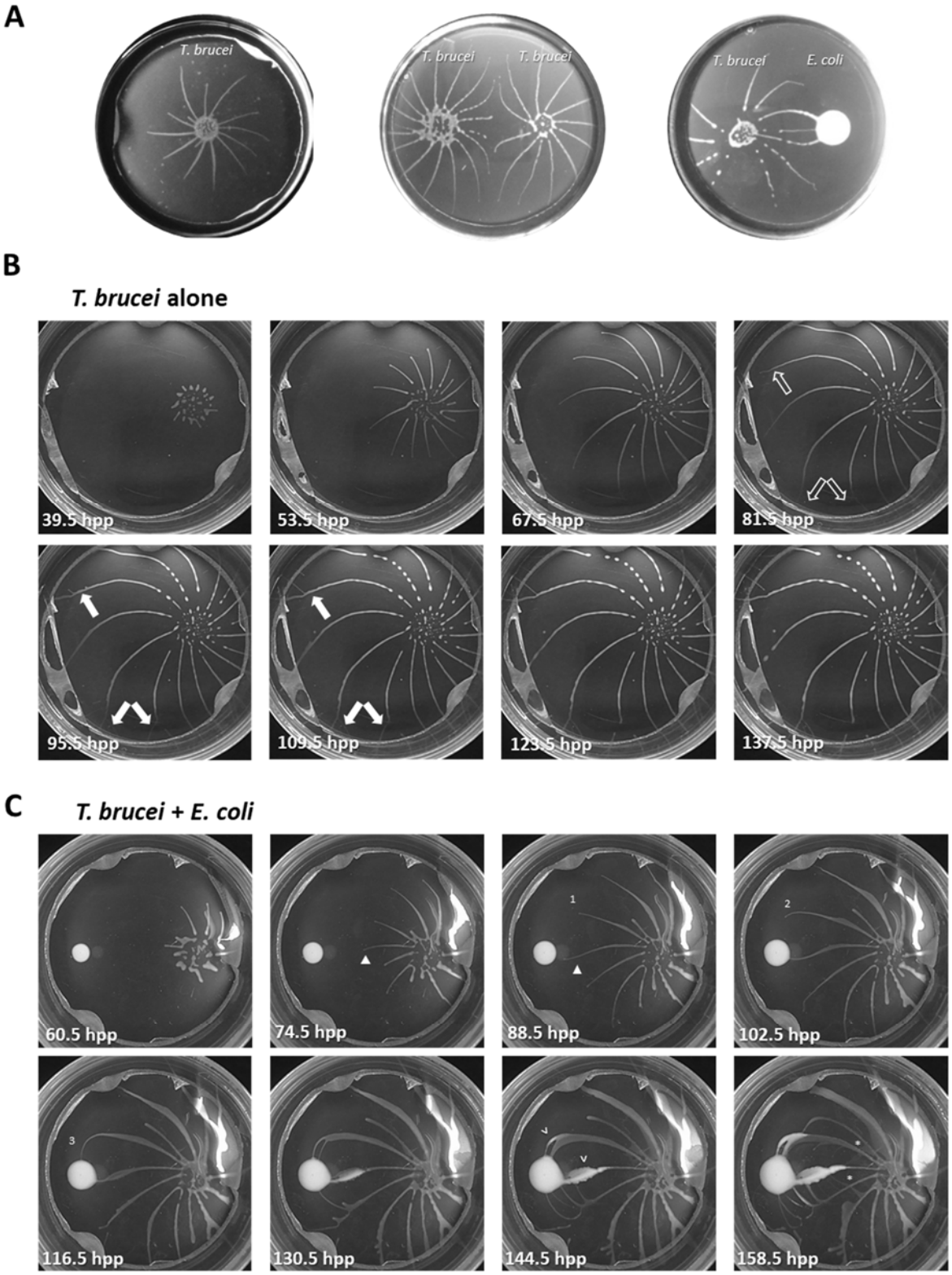

Figure 4-1: Socially behaving *T. brucei* is attracted to *E. coli*.

A) *T. brucei* on a semi-solid surface engages in social motility (SoMo) (left). Projections of two groups of *T. brucei* originating from the same suspension culture are repelled by one another (center). *T. brucei* is attracted to *E. coli* (right).

B) Stills from a time-lapse video of *T. brucei* engaging in SoMo (Movie 4-1). Unfilled arrows point to projections before branching. Filled arrows point to projections that have formed branches.

C) Stills from a time-lapse video of *T. brucei* exhibiting positive chemotaxis toward *E. coli* (Movie 4-2). Time-stamps are indicated in hours post-plating (hpp). Numbers 1-3 indicate a projection that alters its path in response to *E. coli*. Closed arrowhead points to a change in curvature of the projection as it changes its path. Open arrowheads point to locations where *E. coli* has entered the projections. Asterisks indicate regions where a projection has crossed a different projection.

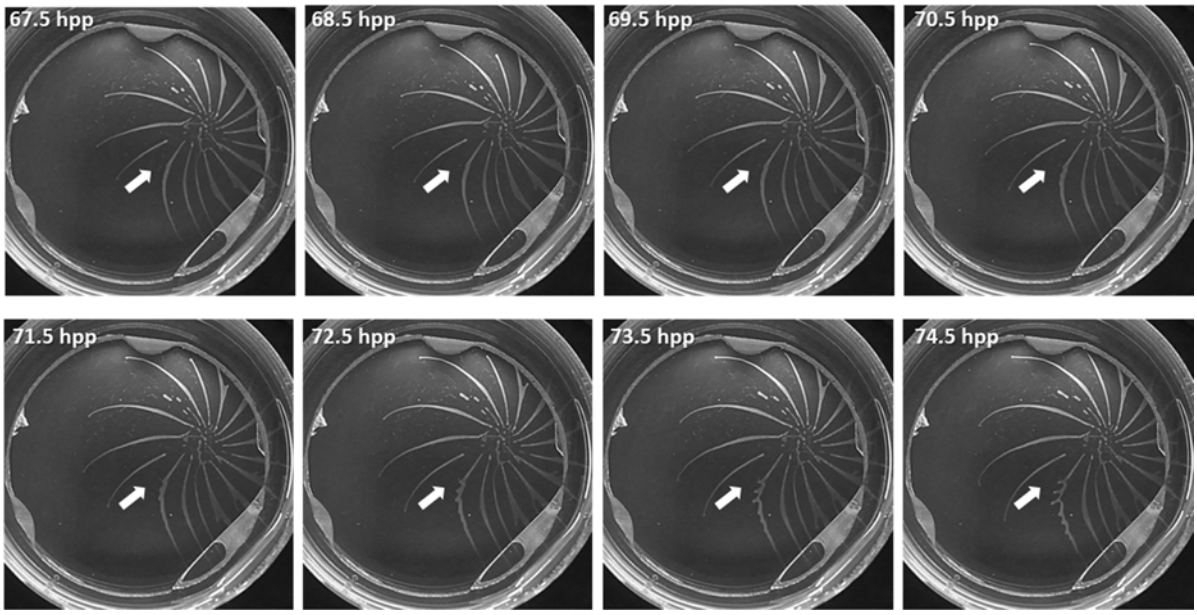

Figure 4-2: *T. brucei* projections thicken prior to branching.

Stills from a time-lapse video of *T. brucei* engaging in SoMo (Movie 3). Arrow points to the projection that thickens before branching. Time-stamps are indicated in hours post-plating (hpp).

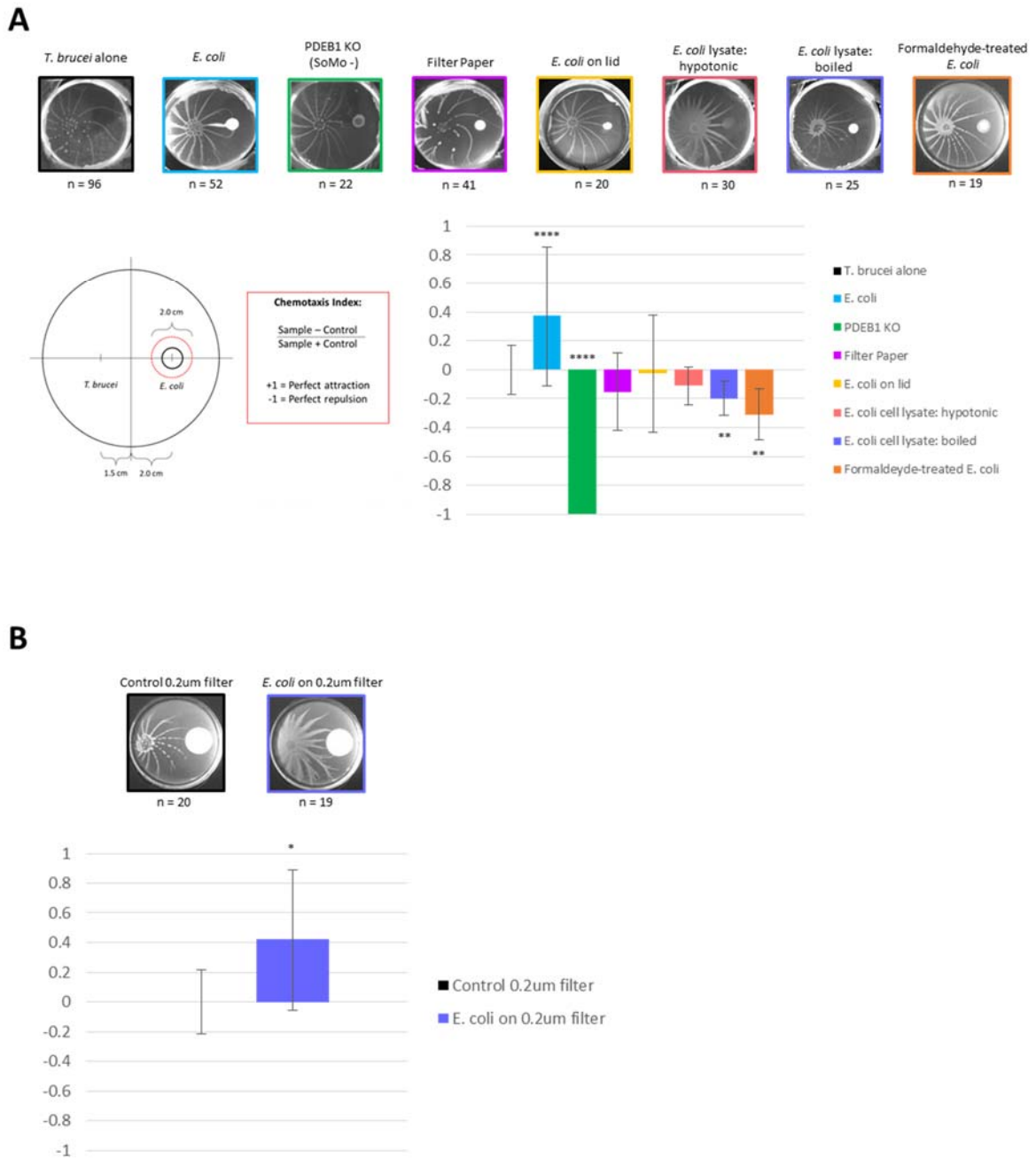

Figure 4-3: The attractant is diffusible and requires actively growing *E. coli*.

A) Requirements for attraction were quantified by a chemotaxis index (diagram at lower-left), defined as the number of projections entering the 2-cm diameter red circle in the experimental sample subtracted by the number of projections entering the same circle on control plates (*T.*

brucei alone), divided by the total number of projections in both samples. Representative pictures of each condition tested are shown (upper row) with their chemotaxis indices (lower-right). Error bars represent SEM. Unpaired two-tailed t-test with Welch's correction was used to measure significance compared to the *T. brucei* alone control: **** $p < 0.0001$, ** $p < 0.01$.
B) A chemotaxis index was calculated for *T. brucei* in response to *E. coli* growing on a 0.2µm filter compared to a 0.2µm filter alone. Error bars represent SEM. Unpaired two-tailed t-test with Welch's correction was used to measure significance compared to the *T. brucei* in response to 0.2µm filter alone control: * $p < 0.05$.

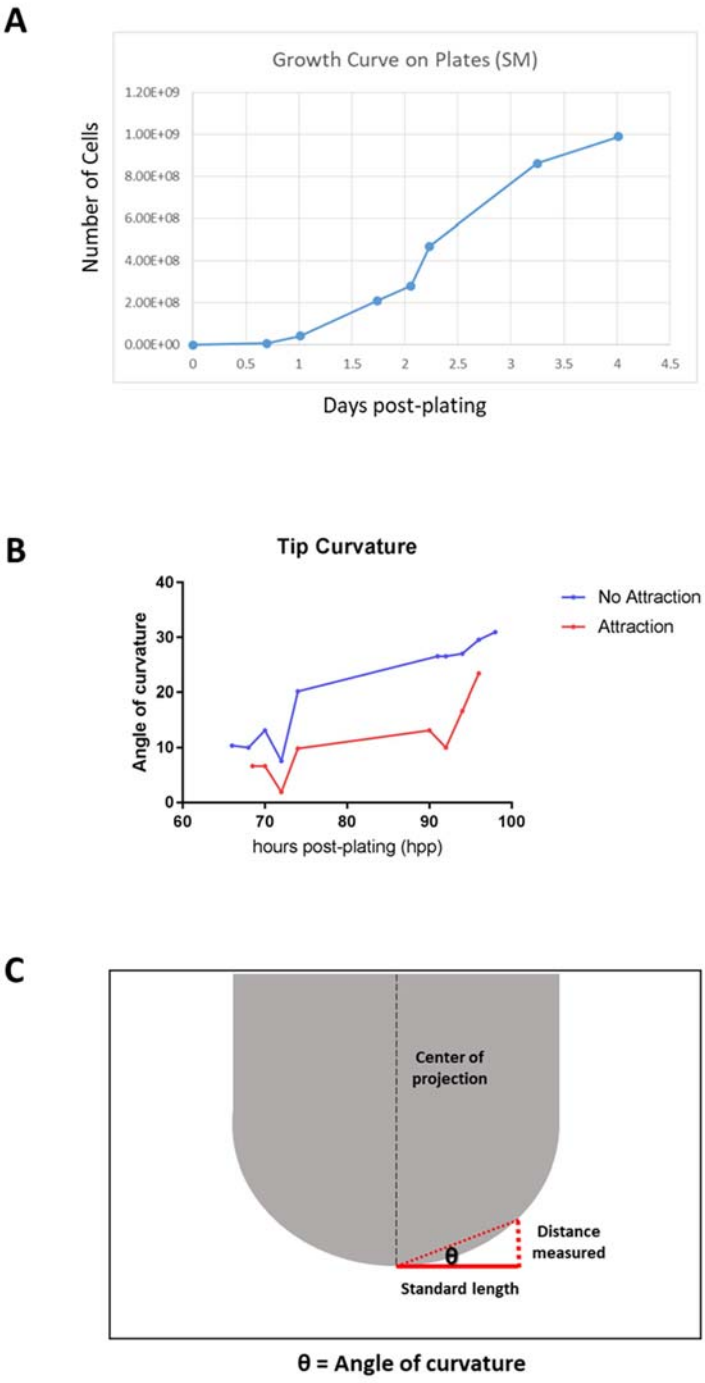

Figure 4-4: Growth analysis of *E. coli* colonies on SoMo plates, and the curvature of the tip of *T. brucei* projections increases in the presence and absence of *E. coli*

A) Growth of *E. coli* colonies was measured on SM supplemented agarose plates over the course of five days.

B) The angle of curvature of the tip of the projections in panels A and B of Figure 4-8 are plotted over time (hours post-plating).

C) A schematic of how the angle of curvature was determined in panel B is shown.

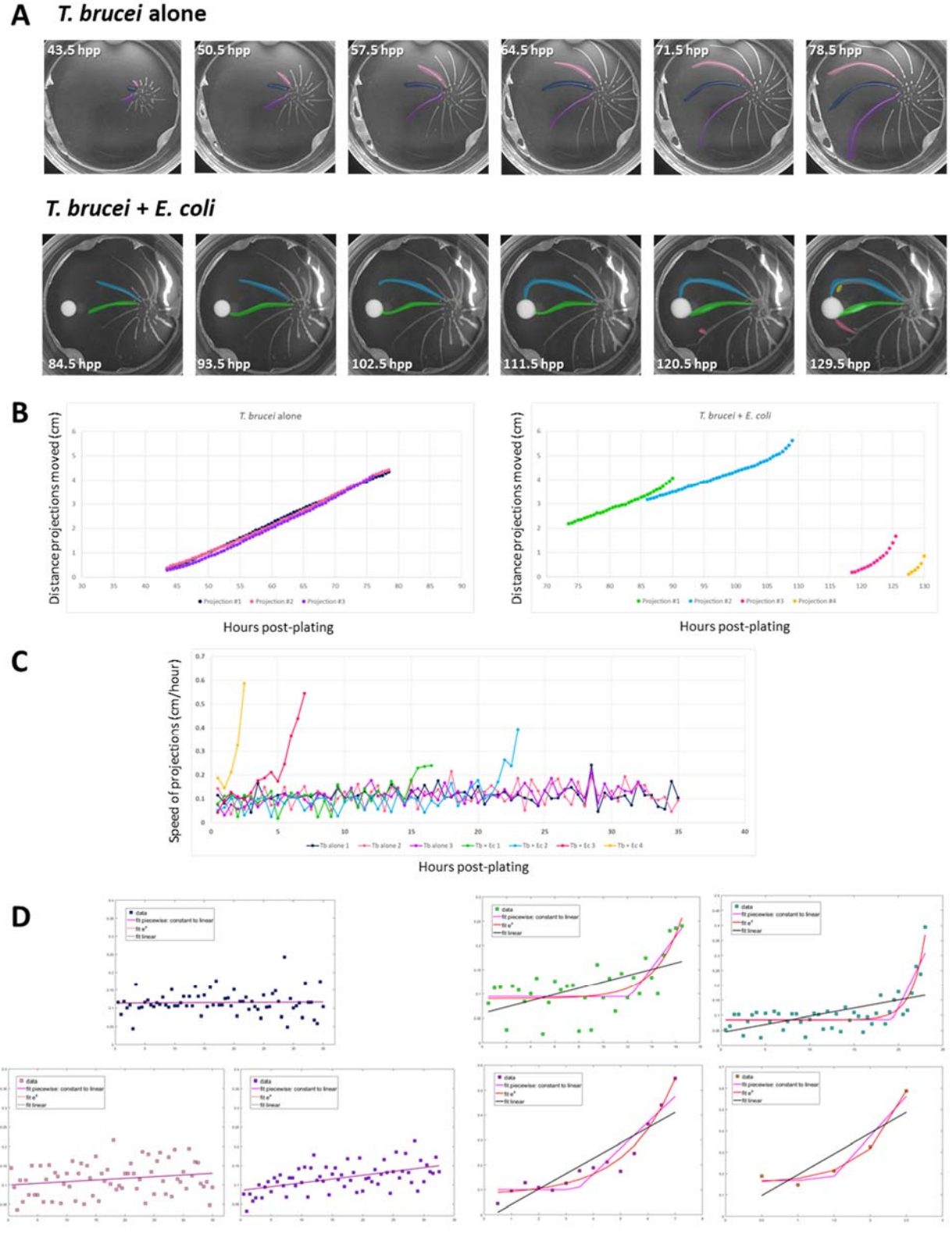

Figure 4-5: Projections of parasites accelerate upon sensation of attractant.

A) Representative images of *T. brucei* engaging in SoMo alone (upper) (Movie 4-1) or with *E. coli* present (lower) (Movie 4-2). Projections are pseudo-colored and match the plot colors shown in panel B. Time-stamps are indicated in hours post-plating (hpp).

B) The distance each projection moved was measured over time from the time-lapse videos shown in panel A.

C) The speed of each projection is plotted over time with the colors of each projection corresponding to their respective colors shown in panels A and B.

D) Non-linear regression models designed in MATLAB were used to model the best fit of the speed vs time data for projections in the presence of *E. coli*. The pink line represents the piece-wise function, the red line is for an exponential function, and the black line represents a linear function. The colors of the data points correspond to the respective pseudo-colors for each projection.

Distance vs. Time graphs		
Projection	Linear regression: $y = ax + b$	Quadratic regression $y = ax^2 + bx + c$
T. brucei alone 1	$y = 0.1172x - 4.8248$ $R^2 = 0.9996$	$y = -2e\text{-}05x^2 + 0.1191x - 4.8819$ $R^2 = 0.9996$
T. brucei alone 2	$y = 0.1184x - 4.9054$ $R^2 = 0.9975$	$y = 0.0006x^2 + 0.0441x - 2.7047$ $R^2 = 0.9997$
T. brucei alone 3	$y = 0.1209x - 5.1828$ $R^2 = 0.9965$	$y = 0.0008x^2 + 0.027x - 2.4479$ $R^2 = 0.9995$

Table 4-1: Equations of the regression models for *T. brucei* projections in the absence of bacteria: Distance vs Time.

Equations for the best fit for both a linear regression and quadratic regression model were calculated for the indicated *T. brucei* projection in the absence of bacteria shown in Figure 4-5B. R^2 values were calculated in Microsoft Excel for each regression analysis.

Distance vs. Time graphs		
Projection	Linear regression: $y = ax + b$	Quadratic regression $y = ax^2 + bx + c$
T. brucei alone 1	$y = 0.0868x - 3.782$ $R^2 = 0.9898$	$y = 0.0009x^2 - 0.0277x - 0.387$ $R^2 = 0.9995$
T. brucei alone 2	$y = 0.0906x - 3.9619$ $R^2 = 0.9939$	$y = 0.0007x^2 - 0.0008x - 1.2546$ $R^2 = 0.9996$
T. brucei alone 3	$y = 0.96x - 4.2688$ $R^2 = 0.9941$	$y = 0.0007x^2 + 0.0049x - 1.5682$ $R^2 = 0.9992$

Speed vs. Time graphs			
Projection	Piece-wise function: Constant to a line For $x \le k$, $y = a$ For $x > k$, $y = bx + c$	Exponential regression $y = a\,e^{bx} + c$	Linear regression $y = ax + b$
T. brucei alone 1	For $x \le 0$, $y = 0.044$ For $x > 0$, $y = 1.87e^{-3}x + 0.0527$ $R^2 = 0.378$	$y = 5.83\,e^{3.19e-4x} - 5.77$ $R^2 = 0.368$	$y = 1.87e^{-3}x + 0.0527$ $R^2 = 0.378$
T. brucei alone 2	For $x \le 0$, $y = 0.044$ For $x > 0$, $y = 1.87e^{-3}x + 0.0561$ $R^2 = 0.491$	$y = 6.80\,e^{2.73e-4x} - 6.75$ $R^2 = 0.491$	$y = 1.87e^{-3}x + 0.0561$ $R^2 = 0.491$
T. brucei alone 3	For $x \le 0$, $y = 0.0437$ For $x > 0$, $y = 1.87e^{-3}x + 0.0594$ $R^2 = 0.402$	$y = 10.61\,e^{1.75e-4x} - 10.55$ $R^2 = 0.402$	$y = 1.87e^{-3}x + 0.0594$ $R^2 = 0.402$
T. brucei + *E. coli* 1	For $x \le 25.92$, $y = 0.0698$ For $x > 25.92$, $y = 0.0248x - 0.574$ $R^2 = 0.417$	$y = 9.58e^{-9}\,e^{0.541x} + 0.0695$ $R^2 = 0.439$	$y = 1.30e^{-3}x + 0.0592$ $R^2 = 0.0701$
T. brucei + *E. coli* 2	For $x \le 35.27$, $y = 0.0659$ For $x > 35.27$, $y = 0.0377x - 1.265$ $R^2 = 0.568$	$y = -21.47\,e^{-5.88e-5x} + 21.52$ $R^2 = 0.11$	$y = 1.26e^{-3}x + 0.0503$ $R^2 = 0.11$
T. brucei + *E. coli* 3	For $x \le 68.35$, $y = 0.0525$ For $x > 68.35$, $y = 0.0805x - 5.449$ $R^2 = 0.684$	$y = -36.44\,e^{-9.79e-6x} + 36.49$ $R^2 = 0.00495$	$y = 3.57e^{-4}x + 0.0526$ $R^2 = 0.00496$

Table 4-2: Equations of the regression models for *T. brucei* projections from Movie 4-3: Distance vs Time, and for Movies 4-3 and 4-4: Speed vs Time.

Equations for the best fit for both a linear regression and quadratic regression model were calculated for the indicated *T. brucei* projection in the absence of bacteria shown in Figure 4-6B. R^2 values were calculated in Microsoft Excel for each regression analysis. Additionally, equations for the best fit for a non-linear fitting algorithm for a piece-wise, exponential, and linear function were calculated for the Speed vs Time data of *T. brucei* projections in the presence and absence of *E. coli*. R^2 values were calculated by the non-linear fit model in MATLAB for each regression analysis.

Speed vs. Time graphs			
Projection	Piece-wise function: Constant to a line For $x \leq k$, $y = a$ For $x > k$, $y = bx + c$	Exponential regression $y = a\, e^{bx} + c$	Linear regression $y = ax + b$
T. brucei alone 1	For $x \leq 0$, $y = 0.1$ For $x > 0$, $y = 8.95e^{-5}x + 0.11$ $R^2 = -0.0138$	$y = 2.47\, e^{3.6e-5\,x} - 2.35$ $R^2 = -0.0138$	$y = 8.95e^{-5}x + 0.11$ $R^2 = -0.0138$
T. brucei alone 2	For $x \leq 0$, $y = 0.09$ For $x > 0$, $y = 8.7e^{-4}x + 0.099$ $R^2 = 0.0308$	$y = 11.2\, e^{7.74e-5\,x} - 11.1$ $R^2 = 0.0308$	$y = 8.70e^{-4}x + 0.01$ $R^2 = 0.0308$
T. brucei alone 3	For $x \leq 0$, $y = 0.076$ For $x > 0$, $y = 0.00199x + 0.085$ $R^2 = 0.278$	$y = 9.224\, e^{2.15e-4}\, x - 9.14$ $R^2 = 0.278$	$y = 0.00199x + 0.085$ $R^2 = 0.278$
T. brucei + *E. coli* 1	For $x \leq 12.21$, $y = 0.094$ For $x > 12.21$, $y = 0.033x - 0.309$ $R^2 = 0.522$	$y = 8.67e^{-5}\, e^{0.458\,x} + 0.090$ $R^2 = 0.544$	$y = 0.0065x + 0.0596$ $R^2 = 0.304$
T. brucei + *E. coli* 2	For $x \leq 19.34$, $y = 0.086$ For $x > 19.34$, $y = 0.061x - 1.088$ $R^2 = 0.674$	$y = 3.87e^{-8}\, e^{0.687\,x} + 0.085$ $R^2 = 0.754$	$y = 0.0054x + 0.0428$ $R^2 = 0.3$
T. brucei + *E. coli* 3	For $x \leq 3.40$, $y = 0.1$ For $x > 3.40$, $y = 0.104x - 0.254$ $R^2 = 0.874$	$y = 8.66e^{-3}\, e^{0.571\,x} + 0.078$ $R^2 = 0.957$	$y = 0.0618x - 0.0212$ $R^2 = 0.784$
T. brucei + *E. coli* 4	For $x \leq 1.45$, $y = 0.167$ For $x > 1.45$, $y = 0.376x - 0.377$ $R^2 = 0.929$	$y = 3.17e^{-3}\, e^{1.97\,x} + 0.154$ $R^2 = 0.973$	$y = 0.196x - 0.002$ $R^2 = 0.673$

Table 4-3: Equations of the regression models for *T. brucei* projections in the absence or presence of bacteria: Speed vs Time.

Equations for the best fit for a non-linear fitting algorithm for a piece-wise, exponential, and linear function were calculated for the Speed vs Time data of *T. brucei* projections in the absence

or presence of *E. coli*. R^2 values were calculated by the non-linear fit model in MATLAB for each regression analysis.

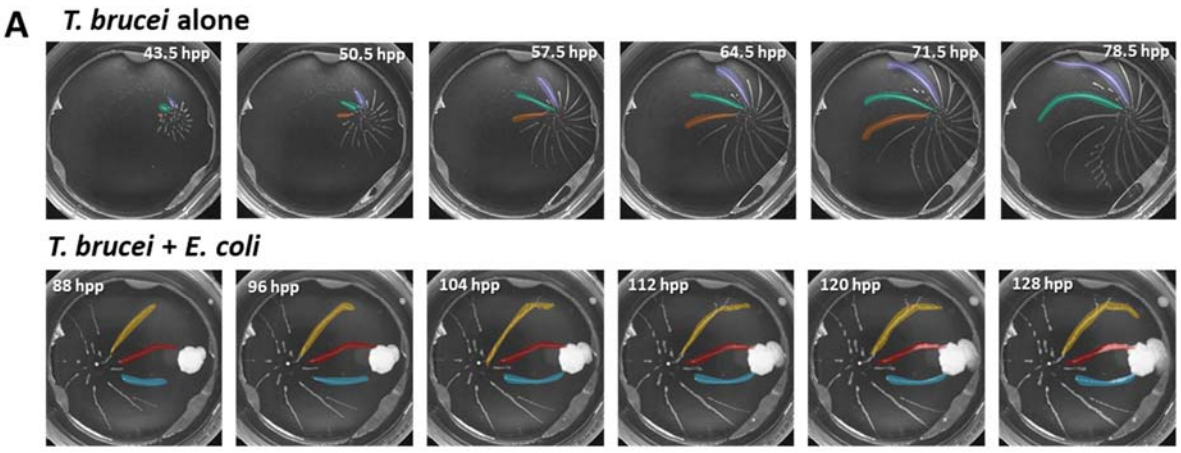
A
T. brucei alone
43.5 hpp
50.5 hpp
57.5 hpp
64.5 hpp
71.5 hpp
78.5 hpp
T. brucei + E. coli
88 hpp
96 hpp
104 hpp
112 hpp
120 hpp
128 hpp

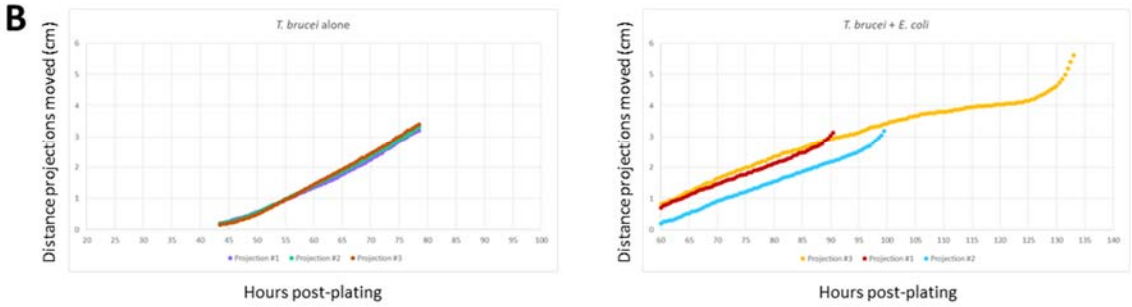
B
T. brucei alone
T. brucei + E. coli
Distance projections moved (cm)
Hours post-plating

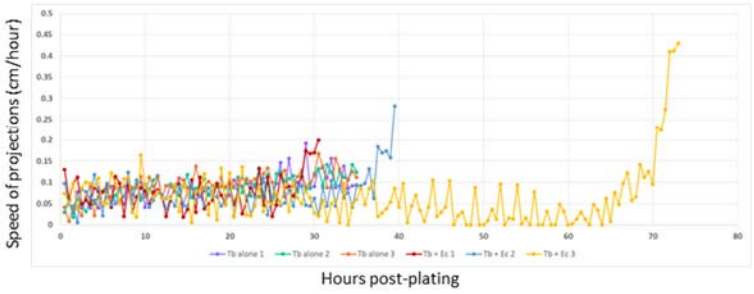
C
Speed of projections (cm/hour)
Hours post-plating

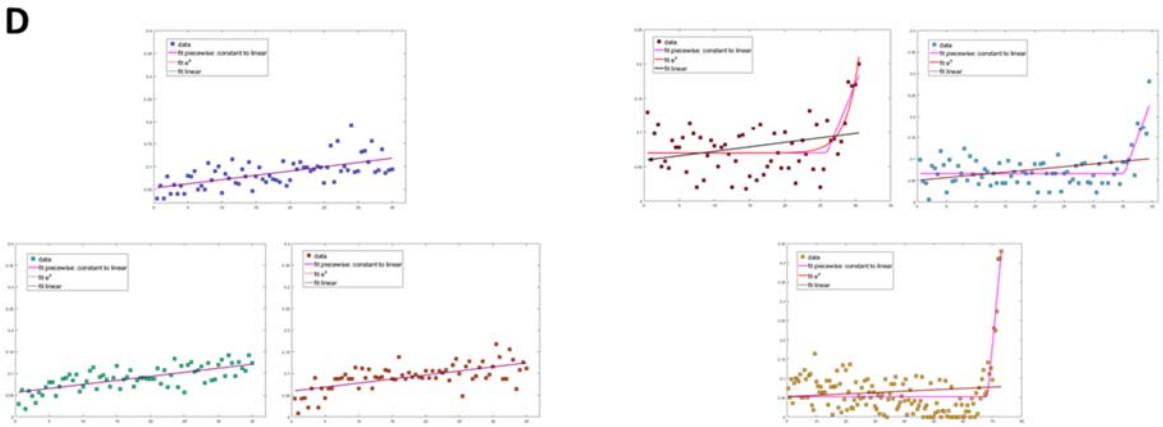
D

Figure 4-6: Velocity analysis of projections from additional time-lapse videos (Movies 4-3 and 4-4) in both the presence and absence of bacteria.

A) Representative images of *T. brucei* engaging in SoMo alone (upper) (Movie 4-3) or *T. brucei* engaging in SoMo with *E. coli* present (lower) (Movie 4-4). Projections are pseudo-colored and match the colors shown in panel B. Time-stamps are indicated in hours post-plating (hpp).

B) The distance each projection moved was measured over time from the time-lapse videos shown in panel A.

C) The speed of each projection is plotted over time with the colors of each projection corresponding to their respective colors shown in panels A and B.

D) Non-linear regression models designed in MATLAB were used to model the best fit of the speed vs time data for projections in both the presence and absence of *E. coli*. The pink line represents the piece-wise function, the red line is for an exponential function, and the black line represents a linear function. The colors of the data points correspond to the respective pseudo-colors for each projection.

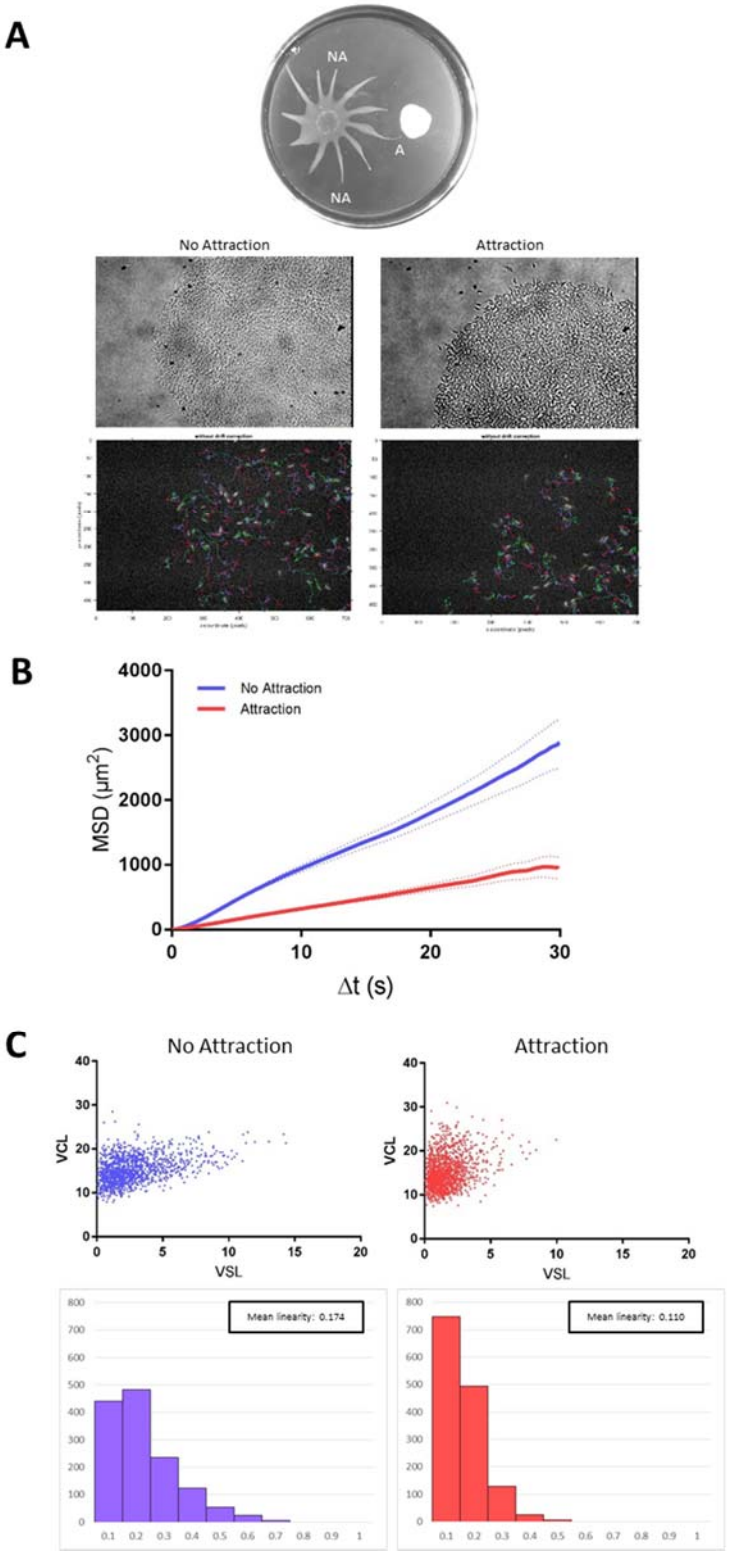

Figure 4-7: Individual cell motility within the group becomes more constrained in the presence of attractant.

A) A representative SoMo plate is shown with a projection undergoing chemotaxis to *E. coli* (Attraction, "A") and two projections not engaged in chemotaxis (No Attraction, "NA"). Representative phase contrast images of the tips of projections at 20x magnification are shown. Fluorescent images of the same tips of projections show GFP-tagged cells superimposed with their cell traces over a 30 second timeframe.
B) Mean-squared displacement of individual cells at the tips of projections undergoing chemotaxis (Attraction) or not (No Attraction). Data acquired from 37 videos with 1368 total tracks (No Attraction), or 22 videos with 1403 total tracks (Attraction).
C) Curvilinear versus straight line velocity plots with corresponding linearity plots are shown for Attraction and No Attraction conditions.

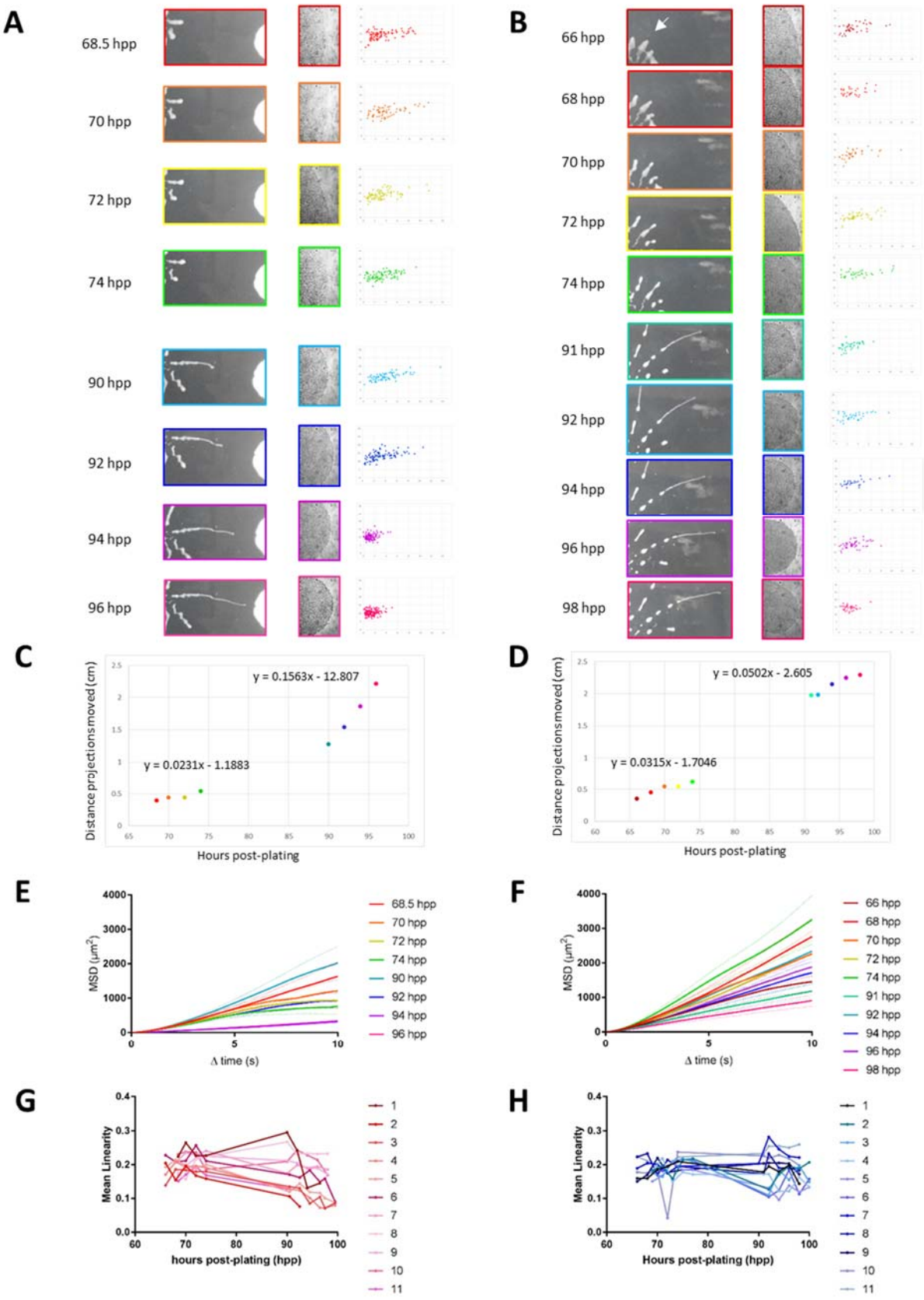
A
68.5 hpp
70 hpp
72 hpp
74 hpp
90 hpp
92 hpp
94 hpp
96 hpp
B
66 hpp
68 hpp
70 hpp
72 hpp
74 hpp
91 hpp
92 hpp
94 hpp
96 hpp
98 hpp
C
y = 0.1563x - 12.807
y = 0.0231x - 1.1883
Distance projections moved (cm)
Hours post-plating
D
y = 0.0502x - 2.605
y = 0.0315x - 1.7046
Distance projections moved (cm)
Hours post-plating
E
MSD (μm²)
Δ time (s)
68.5 hpp
70 hpp
72 hpp
74 hpp
90 hpp
92 hpp
94 hpp
96 hpp
F
MSD (μm²)
Δ time (s)
66 hpp
68 hpp
70 hpp
72 hpp
74 hpp
91 hpp
92 hpp
94 hpp
96 hpp
98 hpp
G
Mean Linearity
hours post-plating (hpp)
1
2
3
4
5
6
7
8
9
10
11
H
Mean Linearity
Hours post-plating (hpp)
1
2
3
4
5
6
7
8
9
10
11

Figure 4-8: Changes in group movement correlate with changes in single-cell movement during positive chemotaxis. Speed of projections and MSD of individual cells within tips of these projections were examined over time in samples with or without *E. coli*.

A) Sequential images of a projection moving toward *E. coli* (left column). At each time point, the tip of the projection is shown at 20x magnification (center column), and the curvilinear velocity vs straight-line velocity is shown for individual cells in the projection (right column).

B) Projection of *T. brucei* alone analyzed as described in A.

C and D) Distance from point of origin to the projection tip is plotted as a function of time for *T. brucei* projections moving in the presence (C) or absence (D) of *E. coli*. Equations for line-of-best fit using a linear regression are shown above the corresponding portions of each graph.

E and F) Mean-squared displacement was determined for individual cells in the tip of each projection shown in A (C) and B (D). Line colors correspond to the colors used for time-points in A and B.

G and H) Mean linearity of individual cells at the tips of projections was plotted over time for 11 projections each of *T. brucei* in the presence and absence of *E. coli.*

E. coli* + *T. brucei	
68.5 – 74 hpp	90 – 96 hpp
Linear regression	Linear regression
y = 0.0231x - 1.1883 R^2 = 0.8609	y = 0.1563x - 12.807 R^2 = 0.9959
***T. brucei* alone**	
66 – 74 hpp	91 – 98 hpp
Linear regression	Linear regression
y = 0.0315x - 1.7046 R^2 = 0.9245	y = 0.0502x - 2.605 R^2 = 0.9572

Table 4-4: Equations for the lines of best fit for *T. brucei* projections in the time-course analyses: Distance vs Time.

Equations for the line of best fit for each section of the graphs in Figure 4-8C and D were determined using a linear regression analysis. R^2 values were calculated in Microsoft Excel for each regression analysis.

Supplemental Material Legends:

Movie 4-1: Time-lapse video of *T. brucei* engaging in SoMo.

Still images were taken every 30 minutes for 162 hours beginning 24 hours post-plating. Still images playback at 10 frames per second.

Movie 4-2: Time-lapse video of *T. brucei* engaging in positive chemotaxis toward *E. coli*.

Still images were taken every 30 minutes for 185 hours beginning 24 hours post-plating using a Brinno TLC200 Pro time-lapse camera. Still images playback at 10 frames per second.

Movie 4-3: Time-lapse video of *T. brucei* engaging in SoMo.

Still images were taken every 30 minutes for 161.5 hours beginning 24 hours post-plating using a Brinno TLC200 Pro time-lapse camera. Still images playback at 10 frames per second.

Movie 4-4: Time-lapse video of *T. brucei* engaging in positive chemotaxis toward *E. coli*.

Still images were taken every 30 minutes for 183.5 hours beginning 24 hours post-plating using a Brinno TLC200 Pro time-lapse camera. Still images playback at 10 frames per second.

Movie 4-5: Live video of *T. brucei* cells at the tip of a projection upon initial impact with an *E. coli* colony.

Cells were imaged at 20x magnification, and video was recorded and played back at 30 fps.

Movie 4-6: Time-lapse video of a projection impacting an *E. coli* colony

Still images were taken every 1 second at 5x magnification using AxioVision 4.7.2 (12-2008) and played back at 5 frames per second.

Bibliography

1. Wadhams, G.H. and J.P. Armitage, *Making sense of it all: bacterial chemotaxis.* Nat Rev Mol Cell Biol, 2004. **5**(12): p. 1024-37.
2. Swaney, K.F., C.H. Huang, and P.N. Devreotes, *Eukaryotic chemotaxis: a network of signaling pathways controls motility, directional sensing, and polarity.* Annu Rev Biophys, 2010. **39**: p. 265-89.
3. Willard, S.S. and P.N. Devreotes, *Signaling pathways mediating chemotaxis in the social amoeba, Dictyostelium discoideum.* Eur J Cell Biol, 2006. **85**(9-10): p. 897-904.
4. Matilla, M.A. and T. Krell, *The effect of bacterial chemotaxis on host infection and pathogenicity.* FEMS Microbiol Rev, 2018. **42**(1).
5. Huang, J.Y., et al., *Chemodetection and Destruction of Host Urea Allows Helicobacter pylori to Locate the Epithelium.* Cell Host Microbe, 2015. **18**(2): p. 147-56.
6. O'Toole, R., et al., *The chemotactic response of Vibrio anguillarum to fish intestinal mucus is mediated by a combination of multiple mucus components.* J Bacteriol, 1999. **181**(14): p. 4308-17.
7. Yao, J. and C. Allen, *Chemotaxis is required for virulence and competitive fitness of the bacterial wilt pathogen Ralstonia solanacearum.* J Bacteriol, 2006. **188**(10): p. 3697-708.
8. Shaw, S., et al., *Flagellar cAMP signaling controls trypanosome progression through host tissues.* Nat Commun, 2019. **10**(1): p. 803.
9. Barros, V.C., et al., *Leishmania amazonensis: chemotaxic and osmotaxic responses in promastigotes and their probable role in development in the phlebotomine gut.* Exp Parasitol, 2006. **112**(3): p. 152-7.

10. Detke, S. and R. Elsabrouty, *Leishmania mexicana amazonensis: plasma membrane adenine nucleotide translocator and chemotaxis.* Exp Parasitol, 2008. **118**(3): p. 408-19.

11. Diaz, E., et al., *Effect of aliphatic, monocarboxylic, dicarboxylic, heterocyclic and sulphur-containing amino acids on Leishmania spp. chemotaxis.* Parasitology, 2015. **142**(13): p. 1621-30.

12. de Thomaz, A., et al., *Optical tweezers for studying taxis in parasites.* Journal of Optics, 2011. **13**(4).

13. Zaki, M., N. Andrew, and R.H. Insall, *Entamoeba histolytica cell movement: a central role for self-generated chemokines and chemorepellents.* Proc Natl Acad Sci U S A, 2006. **103**(49): p. 18751-6.

14. Büscher, P., et al., *Human African trypanosomiasis.* Lancet, 2017. **390**(10110): p. 2397-2409.

15. Capewell, P., et al., *The skin is a significant but overlooked anatomical reservoir for vector-borne African trypanosomes.* Elife, 2016. **5**.

16. Trindade, S., et al., *Trypanosoma brucei Parasites Occupy and Functionally Adapt to the Adipose Tissue in Mice.* Cell Host Microbe, 2016. **19**(6): p. 837-48.

17. Caljon, G., et al., *The Dermis as a Delivery Site of Trypanosoma brucei for Tsetse Flies.* PLoS Pathog, 2016. **12**(7): p. e1005744.

18. Vickerman, K., *Developmental cycles and biology of pathogenic trypanosomes.* Br Med Bull, 1985. **41**(2): p. 105-14.

19. Oberholzer, M., et al., *Social motility in african trypanosomes.* PLoS Pathog, 2010. **6**(1): p. e1000739.

20. Imhof, S., et al., *Social motility of African trypanosomes is a property of a distinct life-cycle stage that occurs early in tsetse fly transmission.* PLoS Pathog, 2014. **10**(10): p. e1004493.

21. Saada, E.A., et al., *Insect stage-specific receptor adenylate cyclases are localized to distinct subdomains of the Trypanosoma brucei Flagellar membrane.* Eukaryot Cell, 2014. **13**(8): p. 1064-76.

22. Lopez, M.A., E.A. Saada, and K.L. Hill, *Insect stage-specific adenylate cyclases regulate social motility in African trypanosomes.* Eukaryot Cell, 2015. **14**(1): p. 104-12.

23. Oberholzer, M., E.A. Saada, and K.L. Hill, *Cyclic AMP Regulates Social Behavior in African Trypanosomes.* MBio, 2015. **6**(3): p. e01954-14.

24. Wirtz, E., et al., *A tightly regulated inducible expression system for conditional gene knock-outs and dominant-negative genetics in Trypanosoma brucei.* Mol Biochem Parasitol, 1999. **99**(1): p. 89-101.

25. Langousis, G., et al., *Loss of the BBSome perturbs endocytic trafficking and disrupts virulence of Trypanosoma brucei.* Proc Natl Acad Sci U S A, 2016. **113**(3): p. 632-7.

26. Oberholzer, M., et al., *Approaches for functional analysis of flagellar proteins in African trypanosomes.* Methods Cell Biol, 2009. **93**: p. 21-57.

27. Hallem, E.A., et al., *A sensory code for host seeking in parasitic nematodes.* Curr Biol, 2011. **21**(5): p. 377-83.

28. Schindelin, J., et al., *Fiji: an open-source platform for biological-image analysis.* Nat Methods, 2012. **9**(7): p. 676-82.

29. Shimogawa, M.M., et al., *Parasite motility is critical for virulence of African trypanosomes.* Sci Rep, 2018. **8**(1): p. 9122.

30. Jaqaman, K., et al., *Robust single-particle tracking in live-cell time-lapse sequences.* Nat Methods, 2008. **5**(8): p. 695-702.

31. Sharma, R., et al., *Asymmetric cell division as a route to reduction in cell length and change in cell morphology in trypanosomes.* Protist, 2008. **159**(1): p. 137-51.

32. Tyc, O., et al., *The Ecological Role of Volatile and Soluble Secondary Metabolites Produced by Soil Bacteria.* Trends Microbiol, 2017. **25**(4): p. 280-292.

33. Audrain, B., et al., *Role of bacterial volatile compounds in bacterial biology.* FEMS Microbiol Rev, 2015. **39**(2): p. 222-33.

34. Barron, G.L., *Microcolonies of bacteria as a nutrient source for lignicolous and other fungi.* Canadian Journal of Botany, 1988. **66**(12): p. 2505-2510.

35. Middelboe, M. and N. Jorgensen, *Viral lysis of bacteria: an important source of dissolved amino acids and cell wall compounds.* Journal of the Marine Biological Association of the United Kingdom, 2006. **86**(3): p. 605-612.

36. Humphries, J., et al., *Species-Independent Attraction to Biofilms through Electrical Signaling.* Cell, 2017. **168**(1-2): p. 200-209.e12.

37. Hopp, C.S., et al., *Longitudinal analysis of Plasmodium sporozoite motility in the dermis reveals component of blood vessel recognition.* Elife, 2015. **4**.

38. Wang, J., B.L. Weiss, and S. Aksoy, *Tsetse fly microbiota: form and function.* Front Cell Infect Microbiol, 2013. **3**: p. 69.

39. Aksoy, S., *Tsetse--A haven for microorganisms.* Parasitol Today, 2000. **16**(3): p. 114-8.

40. Attardo, G.M., et al., *Analysis of milk gland structure and function in Glossina morsitans: milk protein production, symbiont populations and fecundity.* J Insect Physiol, 2008. **54**(8): p. 1236-42.

41. Berriman, M., et al., *The genome of the African trypanosome Trypanosoma brucei.* Science, 2005. **309**(5733): p. 416-22.

42. Ong, H.B., et al., *Homoserine and quorum-sensing acyl homoserine lactones as alternative sources of threonine: a potential role for homoserine kinase in insect-stage Trypanosoma brucei.* Mol Microbiol, 2015. **95**(1): p. 143-56.

43. Initiative, I.G.G., *Genome sequence of the tsetse fly (Glossina morsitans): vector of African trypanosomiasis.* Science, 2014. **344**(6182): p. 380-6.

44. Pontes, M.H., et al., *Quorum sensing primes the oxidative stress response in the insect endosymbiont, Sodalis glossinidius.* PLoS One, 2008. **3**(10): p. e3541.

45. Richmond, G.S. and T.K. Smith, *A novel phospholipase from Trypanosoma brucei.* Mol Microbiol, 2007. **63**(4): p. 1078-95.

46. Jackson, A.P., *Genome evolution in trypanosomatid parasites.* Parasitology, 2015. **142 Suppl 1**: p. S40-56.

47. Welburn, S.C., et al., *Rickettsia-like organisms and chitinase production in relation to transmission of trypanosomes by tsetse flies.* Parasitology, 1993. **107 (Pt 2)**: p. 141-5.

48. Farikou, O., et al., *Tripartite interactions between tsetse flies, Sodalis glossinidius and trypanosomes--an epidemiological approach in two historical human African trypanosomiasis foci in Cameroon.* Infect Genet Evol, 2010. **10**(1): p. 115-21.

49. Dale, C. and S.C. Welburn, *The endosymbionts of tsetse flies: manipulating host-parasite interactions.* Int J Parasitol, 2001. **31**(5-6): p. 628-31.

50. Soumana, I.H., et al., *The bacterial flora of tsetse fly midgut and its effect on trypanosome transmission.* J Invertebr Pathol, 2013. **112 Suppl**: p. S89-93.

51. Imhof, S., et al., *A Glycosylation Mutant of Trypanosoma brucei Links Social Motility Defects In Vitro to Impaired Colonization of Tsetse Flies In Vivo.* Eukaryot Cell, 2015. **14**(6): p. 588-92.

52. Eliaz, D., et al., *Exosome secretion affects social motility in Trypanosoma brucei.* PLoS Pathog, 2017. **13**(3): p. e1006245.

53. Tremblay, J., et al., *Self-produced extracellular stimuli modulate the Pseudomonas aeruginosa swarming motility behaviour.* Environ Microbiol, 2007. **9**(10): p. 2622-30.

54. Kearns, D.B. and L.J. Shimkets, *Chemotaxis in a gliding bacterium.* Proc Natl Acad Sci U S A, 1998. **95**(20): p. 11957-62.

55. Chau, R.M.W., et al., *Maintenance of motility bias during cyanobacterial phototaxis.* Biophys J, 2015. **108**(7): p. 1623-1632.

Chapter 5 – Conclusion and Perspectives

As *T. brucei* moves through its mammalian and insect hosts, it must sense and respond to a diverse array of extracellular cues to control when to enact a series of precise developmental changes and migrations. While the components of signaling systems involved in the differentiation from long slender to short stumpy bloodstream form parasites are now being elucidated from recent work [1, 2], signaling systems required for other aspects of the *T. brucei* transmission cycle, are mostly unknown. A useful strategy to investigate how this parasite senses and transduces extracellular signals is through the study of social motility. Because social motility is a surface-induced behavior, it allows for the dissection of signaling pathways that the parasite may enact when encountering surfaces within its hosts. Our studies here and in published work show that, as a behavior observed *in vitro*, social motility serves as a valuable assay to easily study signaling systems that are relevant in *T. brucei* transmission [3, 4].

Due to the importance of cAMP signaling on the regulation of social motility *in vitro* [5, 6], its potential role in *T. brucei* transmission *in vivo* was investigated [3] (Chapter 2). Through infection of tsetse flies with both wild type (WT) and phosphodiesterase B1 knockout (PDEB1 KO) parasites, we showed that cAMP signaling is required for *T. brucei* to migrate from the midgut lumen to the ectoperitrophic space. Prior studies had not considered this transition to be a bottleneck for *T. brucei* transmission, but this work demonstrated that an intact cAMP signaling system is required for *T. brucei* to make this migration, and that simply being able to move was not sufficient.

It is not yet clear how *T. brucei* crosses the peritrophic matrix to move into the ectoperitrophic space, but results from Chapter 2 offer some possibilities. Due to the inability of PDEB1 KO cells to engage in social motility, it is possible *T. brucei* must move across the

peritrophic matrix as a group. Future experiments such as time-course fly dissections, possibly in conjunction with electron microscopy of the peritrophic matrix, will be necessary to determine whether *T. brucei* cells cross as a group or as individuals. An alternative and not necessarily mutually exclusive possibility is that *T. brucei* uses chemotaxis to move across the peritrophic matrix and that cAMP signaling is required for this. Individual PDEB1 KO cells in suspension culture turn less than WT cells, which is a phenotype also seen in bacterial chemotaxis mutants [7]. It is possible that loss of PDEB1 expression disrupts the perception or transduction of a signal that is responsible for initiating chemotaxis either toward a particular cue in the peritrophic matrix/ectoperitrophic space or away from a cue in the midgut lumen. Prior study of social motility [8] and work presented in this dissertation (Chapter 4), demonstrate that *T. brucei* can engage in both negative [8] and positive (Chapter 4) chemotaxis, thus lending support to this possibility.

Through the PDEB1 fly infection studies, we developed a new dissection and imaging technique to study the midgut lumen to ectoperitrophic space transition. Prior study of parasites in these tissue environments relied on fluorescent parasites and electron microscopy [9-11]. Through the dual labelling of tsetse fly tissues and infection with fluorescently labelled trypanosomes, we could determine precisely where trypanosomes, WT and mutant, are located in relation to the tsetse fly tissues. This new technique can be used to investigate other *T. brucei* mutants for the role of their mutant gene in the ability of *T. brucei* to cross the peritrophic matrix.

Because the PDEB1 fly infection studies and prior work [12] demonstrated the value of SoMo in identifying candidate genes important for fly infection, two different systems-level analyses were done to identify additional candidate genes involved in social motility (Chapter 3). These analyses revealed large-scale changes in gene expression when *T. brucei* transitioned from

planktonic growth in suspension to surface growth on plates, and when WT or PDEB1 KO cells were cultivated and compared under these conditions. Through filtering these datasets, a number of candidate genes were identified, three of which seem to play a role in social motility: Zinc Finger protein, Cyclophilin A, and Carbonic Anhydrase. Additional work investigating each of these genes is necessary, as discussed in Chapter 3. Of the three candidate genes identified, Carbonic anhydrase is especially intriguing due to its connection to cAMP signaling [13-18]. Future experiments to test the ability of double knockout cells of Carbonic Anhydrase plus PDEB1 or one of the adenylate cyclases involved in SoMo (AC1 or AC6) to engage in social motility under high CO_2 and low cell density conditions could assess whether they act in the same pathway. Future investigation of these candidates should also include fly infection experiments to assess their role in *T. brucei's* fly transmission cycle.

An additional finding from the discovery of social motility was the ability of groups of *T. brucei* to sense and respond to an extracellular cue [8]. Projections of *T. brucei* are repelled by other projections of *T. brucei*, leading to the halting of their forward motion or diverting from their natural path. In Chapter 4, we describe the identification of positive chemotaxis in *T. brucei* in response to *E. coli*. This discovery was somewhat surprising because *T. brucei* does not typically interact with *E. coli* in the tsetse fly, but it does interact with other species of commensal bacteria [19]. Importantly, these findings led to the development of a quantitative chemotaxis assay for *T. brucei*. By establishing clear definitions for attraction, no response, and repulsion different candidates can be tested for their chemotactic characteristics with respect to *T. brucei*. Although we found that the attractive cue from *E. coli* is soluble, diffusible, and requires actively growing *E. coli* for its production, we were not successful in isolating the attractive activity from *E. coli*. Nonetheless, future investigations of chemotaxis in *T. brucei* can

use this assay to test candidate chemoattractants. One way to do this would be to use an *E. coli* mutant library to screen for an *E. coli* mutant that is non-attractive to *T. brucei*. Additionally, this assay can be used to identify *T. brucei* genes required for chemotaxis, which could later be tested for their ability to infect a tsetse fly.

In addition, by investigating how *T. brucei* behavior changes during chemotaxis, we have defined the phenotype of *T. brucei* during attraction. Projections of *T. brucei* accelerate toward *E. coli* while individual cells in those projections constrain their motion. Future work investigating the molecular and cellular mechanisms of chemotaxis in *T. brucei* can look to these behavioral changes as a readout for positive chemotaxis. Additionally, it is possible that these changes in both group and individual cell motility facilitate *T. brucei* progression through their hosts. Changes in motility could help *T. brucei* cells evade the immune system and/or even help them move through or across tissues.

Overall, this dissertation work has demonstrated that cAMP signaling is required for *T. brucei* tsetse fly transmission, identified three novel candidate regulators of social motility through systems-level analyses, and has identified and defined the requirements for positive chemotaxis in *T. brucei*. Using well-defined molecular and systems-level approaches in addition to newly developed techniques, this work has investigated *T. brucei's* sensory and signaling systems and led to a deeper understand of *T. brucei* biology. Understanding how *T. brucei* senses its diverse host environments and how it transduces and responds to signals in these environments could also lead to the development of novel transmission blocking agents and life-saving therapeutics for a devastating pathogen endemic to some of the world's poorest regions.

Bibliography

1. Mony, B.M., et al., *Genome-wide dissection of the quorum sensing signalling pathway in Trypanosoma brucei.* Nature, 2014. **505**(7485): p. 681-5.
2. Rojas, F., et al., *Oligopeptide Signaling through TbGPR89 Drives Trypanosome Quorum Sensing.* Cell, 2019. **176**(1-2): p. 306-317.e16.
3. Shaw, S., et al., *Flagellar cAMP signaling controls trypanosome progression through host tissues.* Nat Commun, 2019. **10**(1): p. 803.
4. Saada, E.A., et al., *"With a Little Help from My Friends"-Social Motility in Trypanosoma brucei.* PLoS Pathog, 2015. **11**(12): p. e1005272.
5. Lopez, M.A., E.A. Saada, and K.L. Hill, *Insect stage-specific adenylate cyclases regulate social motility in African trypanosomes.* Eukaryot Cell, 2015. **14**(1): p. 104-12.
6. Oberholzer, M., E.A. Saada, and K.L. Hill, *Cyclic AMP Regulates Social Behavior in African Trypanosomes.* MBio, 2015. **6**(3): p. e01954-14.
7. Parkinson, J.S. and S.E. Houts, *Isolation and behavior of Escherichia coli deletion mutants lacking chemotaxis functions.* J Bacteriol, 1982. **151**(1): p. 106-13.
8. Oberholzer, M., et al., *Social motility in african trypanosomes.* PLoS Pathog, 2010. **6**(1): p. e1000739.
9. Gibson, W. and M. Bailey, *The development of Trypanosoma brucei within the tsetse fly midgut observed using green fluorescent trypanosomes.* Kinetoplastid Biol Dis, 2003. **2**(1): p. 1.
10. Ellis, D.S. and D.A. Evans, *Passage of Trypanosoma brucei rhodesiense through the peritrophic membrane of Glossina morsitans morsitans.* Nature, 1977. **267**(5614): p. 834-5.

11. Vigneron, A., et al., *A fine-tuned vector-parasite dialogue in tsetse's cardia determines peritrophic matrix integrity and trypanosome transmission success.* PLoS Pathog, 2018. **14**(4): p. e1006972.

12. Imhof, S., et al., *A Glycosylation Mutant of Trypanosoma brucei Links Social Motility Defects In Vitro to Impaired Colonization of Tsetse Flies In Vivo.* Eukaryot Cell, 2015. **14**(6): p. 588-92.

13. Chen, Y., et al., *Soluble adenylyl cyclase as an evolutionarily conserved bicarbonate sensor.* Science, 2000. **289**(5479): p. 625-8.

14. Zippin, J.H., et al., *Bicarbonate-responsive "soluble" adenylyl cyclase defines a nuclear cAMP microdomain.* J Cell Biol, 2004. **164**(4): p. 527-34.

15. Tresguerres, M., et al., *Established and potential physiological roles of bicarbonate-sensing soluble adenylyl cyclase (sAC) in aquatic animals.* J Exp Biol, 2014. **217**(Pt 5): p. 663-72.

16. Visconti, P.E., et al., *Bicarbonate dependence of cAMP accumulation induced by phorbol esters in hamster spermatozoa.* Biochim Biophys Acta, 1990. **1054**(2): p. 231-6.

17. Choi, H.B., et al., *Metabolic communication between astrocytes and neurons via bicarbonate-responsive soluble adenylyl cyclase.* Neuron, 2012. **75**(6): p. 1094-104.

18. Paunescu, T.G., et al., *Association of soluble adenylyl cyclase with the V-ATPase in renal epithelial cells.* Am J Physiol Renal Physiol, 2008. **294**(1): p. F130-8.

19. Wang, J., B.L. Weiss, and S. Aksoy, *Tsetse fly microbiota: form and function.* Front Cell Infect Microbiol, 2013. **3**: p. 69.

Appendix 1 – "With a Little Help from My Friends" – Social Motility in *Trypanosoma brucei*

Microbial Social Behavior: "The Whole Is Greater Than the Sum of Its Parts"

In their natural environments, microbes are not found in isolation, but live in groups where the ability to communicate and cooperate with friends, while thwarting activities of enemies, is of paramount importance [1, 2]. The capacity for interaction among cells in a group allows for social behaviors, which present as emergent properties of the group as a whole that are not predicted from the sum of activities of individual cells. One example includes quorum sensing (QS), which enables cells in a population to coordinate gene expression and limit premature expenditure of resources. Other social behaviors include those occurring in the context of surfaces, such as biofilm formation and various forms of swarming motility across surfaces, as seen in bacteria and slime molds [3-5].

Recognizing cell–cell communication and social behaviors as ubiquitous among bacteria transformed our views of microbiology and microbial pathogenesis [1, 2]. Parasitic protozoa cause tremendous human suffering worldwide and, although they engage in cell–cell interactions, the paradigm of social behavior is not commonly applied in studies of these organisms. One long-known social activity in protozoan parasites is QS-driven differentiation of the African trypanosome, *Trypanosoma brucei*, in the bloodstream of a mammalian host. During infection, proliferating *T. brucei* cells undergo cell-density dependent differentiation into quiescent forms that are then competent to be transmitted by a tsetse fly vector (Figure A-1) [6, 7]. More recently, the discovery of social motility (SoMo) in insect-stage *T. brucei* (Figure A-1) [8] has highlighted the capacity of these organisms for group-level behavior, and several recent

studies of SoMo emphasize the potential for concepts underlying social behavior to provide insight into parasite biology.

Discovery of Social Motility in Trypanosoma brucei

African trypanosomes cause sleeping sickness in humans and nagana in livestock. They impose a substantial medical and economic burden across nearly 30 countries of sub-Saharan Africa, where approximately 70 million people live at risk of infection [9-11]. The parasites are transmitted between mammalian hosts by blood-feeding tsetse flies. Most studies and animal infection models consider *T. brucei* as individual cells in suspension, yet in their natural environments these parasites frequently live in contact with tissue surfaces. This is most evident in the tsetse fly, where trypanosomes undergo extensive movements across fly tissues, culminating in colonization of the salivary gland epithelium and subsequent differentiation into human-infectious forms [12].

To investigate the influence of surface interactions on trypanosome biology, Oberholzer and Lopez et al. cultivated procyclic form (insect midgut stage) *T. brucei* on semisolid agarose [8]. They discovered that parasites assemble into groups of cells that undergo collective movements, forming multicellular projections that radiate outward from the site of inoculation. Although individual parasites can move freely within a group, movement of the group is polarized such that it advances at a single, leading edge. Moreover, groups alter their movements when they sense other parasites nearby. The combined data reveal that procyclic trypanosomes can sense extracellular signals and coordinate their activities in response to these signals. This behavior was termed “social motility” based on analogies to social motility and other surface-associated motilities in bacteria.

Why Be Social?

In bacteria, social behaviors provide numerous advantages, including enhanced ability to colonize, transit, and penetrate surfaces; enhanced protection from host defenses; improved accessibility to nutrients; and opportunities for genetic exchange [1, 2, 5, 13, 14]. Although *in vivo* manifestations and ramifications of *T. brucei* social motility are not yet known, the parasites can foreseeably benefit from the same advantages afforded to bacteria.

To complete their transmission through the tsetse fly, trypanosomes must undertake an epic journey fraught with hazards [15-17]. Under optimized laboratory conditions, less than 20% of fly infections yield mammalian-infectious parasites, and rates in the field are even lower [17, 18]. The journey begins when ingested bloodstream parasites differentiate into procyclic-stage parasites that colonize the midgut lumen and must then get through or around the peritrophic matrix (PM) to establish infection on the midgut epithelium. The PM is a chitinous lining that protects the gut epithelium from digestive enzymes and presents a formidable barrier to *T. brucei* infection [19, 20]. Once beyond the PM, parasites must penetrate the proventriculus and move along the alimentary tract to the mouth parts. From there, they move up the salivary duct to the salivary gland, where they colonize the gland epithelium and complete differentiation into human-infectious forms. Along the way, *T. brucei* must compete for resources while overcoming harsh conditions and fly defenses, including antimicrobial peptides and lectins [16, 21].

Extensive surface colonization and the arduous nature of parasite movement through the fly present bottlenecks to infection [16, 22] and led Oberholzer and Lopez et al. to propose that SoMo supports one or more of these in vivo activities [8]. Recent work from the Roditi group has strengthened this hypothesis [23, 24]. Prior work defined parasites appearing within the first few days of tsetse infection as “early” procyclics, while “late” procyclics are those that appear at

later time points [25], after parasites have persistently colonized the ectoperitrophic space. Early and late procyclics can be distinguished by differences in surface protein expression [23]. Imhof and colleagues discovered that SoMo initiation is cell density-dependent and that early procyclics cultured *in vitro* undergo social motility, while late procyclics do not. Importantly, they showed that SoMo competence is linked to the early developmental stage, rather than to the presence of specific surface proteins that distinguish between early and late developmental stages. The precise point at which the switch from early to late procyclics occurs is not yet clear but is hypothesized to correlate with infiltration of the ectoperitrophic space, suggesting that SoMo may be a property of cells that colonize and penetrate the peritrophic matrix. Further evidence linking SoMo to successful midgut infection comes from studies of a null mutant of the Requires Fifty Three (RFT1) gene, which is required for N-glycosylation of parasite proteins [26]. RFT1 null mutants show defective SoMo in vitro and exhibit reduced and delayed establishment of midgut infections in the fly [24]. Thus, these combined studies establish SoMo as a property of a specific parasite developmental stage and correlate the *in vitro* behavior to a critical step of the *in vivo* transmission cycle.

More Than an Oar: The Trypanosome Flagellum Contains cAMP Signaling Systems That Control Social Motility

A universal requirement of microbial social behavior is the ability of cells to sense and respond to extracellular signals, and SoMo therefore provides a novel opportunity for dissecting trypanosome signal transduction. This presents an important advance because perception and transduction of extracellular signals are important features of parasite biology [27], but underlying mechanisms are poorly understood. In addition to a well-known role in motility, the

conserved role of the eukaryotic flagellum (also known as cilium) as a signaling center has emerged as a unifying theme in vertebrate development and pathophysiology of human genetic diseases [28]. This concept, together with the prominent role of cyclic nucleotides in cilium-dependent signaling and in control of microbial social behaviors [29-32], made flagellar cyclic-AMP (cAMP) a focal point for interrogation of SoMo signaling mechanisms.

Cellular cAMP levels are controlled through opposing activities of adenylate cyclases (ACs) and cAMP-specific phosphodiesterases (PDEs). Through proteomic analysis of flagellar membranes, Saada et al. identified *T. brucei* ACs that are localized to specific flagellum subdomains and upregulated in the procyclic life cycle stage [33], making them good candidates to test for a role in SoMo. Utilizing gene-specific RNAi, Lopez et al. found that knockdown of certain procyclic-specific ACs enhanced social motility, while knockdown of others had no effect [34]. The findings reveal that individual AC isoforms have specialized functions and indicate that a subset of ACs coordinates the response to signals governing SoMo. Importantly, AC point mutants that disrupt catalytic activity phenocopy RNAi knockdown, supporting the idea that attenuating cAMP production, as opposed to total loss of the protein, activates SoMo.

In complementary studies, Oberholzer and colleagues found that pharmacological or genetic inhibition of cAMP-specific phosphodiesterase B1 (PDEB1) blocks SoMo, indicating that elevated cAMP levels are inhibitory [35]. Supporting this, cAMP levels in live trypanosomes were monitored using a FRET sensor, demonstrating that SoMo inhibition directly correlates with a rise in intracellular cAMP. Additionally, membrane-permeant cAMP or non-hydrolyzable cAMP analogues were found to inhibit SoMo. Surprisingly, the authors also found that the SoMo defect of PDEB1 knockdown cells is rescued when these mutants are co-cultured with wild type (WT) cells. To do this, they employed WT and PDEB1 knockdown cell lines,

each expressing a different fluorescent protein, making it possible to independently monitor movement of WT and PDEB1 knockdown cells in a mixed culture. Despite being incapable of forming projections on their own, PDEB1 knockdown cells formed projections when mixed with WT cells. The result is the first demonstration of trans-complementation in trypanosomes and suggests that PDEB1 knockdown cells are competent for SoMo, but fail to engage in SoMo because they lack a factor that can be provided by WT cells.

Notably, PDEB1 localizes exclusively to the flagellum [36], as do all ACs analyzed thus far, with at least one AC involved in SoMo that is further restricted to the flagellum tip [33, 34, 37]. The combined data thus reveal that the *T. brucei* flagellum is specialized for cAMP signaling and suggest a model in which localized changes in cAMP levels within specific flagellum subdomains control SoMo [33-35, 38]. In this model, PDEB1 acts as a diffusion barrier along the length of the flagellum to confine cAMP signaling output to the site of its production by specific ACs. In the absence of PDEB1, cAMP becomes elevated and diffuses throughout the flagellum, inhibiting activities that would otherwise drive SoMo [35]. Interestingly, regulation of SoMo by cAMP in *T. brucei* has parallels to cyclic-nucleotide regulation of swarming motility in bacterial pathogens. In *Pseudomonas spp*., for example, loss of a diguanylate cyclase that produces cyclic-di-GMP results in hyper-swarming behavior, whereas loss of the cyclic-di-GMP phosphodiesterase results in the inability to swarm at all [39, 40].

Trypanosomal ACs have attracted interest because their domain structure suggests they may act as receptors for extracellular ligands [41]. However, the unusually large size of the AC gene family in *T. brucei* (>65 genes) and lack of assays for cAMP responses have hindered studies of these intriguing proteins. Likewise, although PDEs have been a focus of attention as a

drug target in bloodstream-stage *T. brucei*, their function in fly life cycle stages has received little attention. Indeed, although important advances have been made recently [34, 35, 42-44], cAMP signaling in general remains poorly understood in trypanosomes. In this context, SoMo signaling studies have broad impact because, in addition to identifying genes governing social behavior, they advance understanding of cAMP signaling systems in trypanosomes and demonstrate that the concept of the flagellum as a signaling organelle extends to a group of important human and animal pathogens.

Summary and Outlook

Studies of social motility in African trypanosomes have revealed new conceptual frameworks and produced novel approaches for considering these pathogens. For example, it was not previously possible to discern phenotypic differences between early and late procyclic developmental stages beyond the presence of a single surface protein. SoMo has been instrumental in establishing these as specific life cycle stages and defining a distinct developmental transition [23]. Likewise, although functional analyses of receptor-type adenylate cyclases previously provided insight into host-parasite interaction [44], such studies have been limited to a few members of this large and enigmatic protein family. SoMo now provides ready avenues for structure-function analyses of these understudied proteins [34, 45]. More broadly, the ease of visualizing individual trypanosomes in a mixed community and the genetic tractability of *T. brucei* mean that SoMo can be exploited for elucidating principles of self-assembly and cell–cell interactions in microbial systems.

With foundations established, the stage is now set to tackle several key questions. An obvious area of interest will be to evaluate the role of SoMo and underlying signaling events

during fly infection. With mutants now available, it will be possible to address this directly, and these efforts would be aided by development of methodologies for visualizing parasites in live tsetse flies. With regard to signaling mechanisms, it will be informative to elucidate the relationship between elevated cAMP and the late procyclic developmental stage, both of which inhibit SoMo. At least three models can be envisioned to explain these results (Figure A-2A). For example, cAMP and the late procyclic developmental stage might act independently. Alternatively, elevated cAMP at the flagellum tip might promote the early to late developmental transition, which then inhibits SoMo. However, the presence of GPEET procyclin, a marker of early procyclics, in PDEB1 knockdowns [35] argues against this model. Finally, development into late procyclics might promote elevation of cAMP at the flagellum tip, which would be the inhibitory trigger. Further studies are needed to distinguish between these models. Additional important topics include investigation of cellular signaling within early versus late-stage procyclic cells, determining the role of AC extracellular domains and location, as well as identification of AC ligands.

Beyond cAMP, SoMo undoubtedly depends on additional cell-derived as well as non-cell-derived elements. Of particular interest are factors that drive assembly of parasites into groups, those that promote outward movement of these groups, and those that govern repulsion of groups from one another. Also important will be to define factors responsible for trans-complementation. In bacteria, trans-complementation can be achieved through transfer of outer membrane proteins from one cell to another, and multiple signaling systems have been implicated in coordinating swarming [46-49]. The trypanosome flagellum houses several signaling systems with the capacity for metabotropic and ionotropic responses to external

signals—including ion transporters, kinases, ACs, and other putative receptors (Figure A-2B) [50, 51]—whose functions await discovery.

In closing, studies of social motility and quorum sensing have provided insight into trypanosome developmental biology and signal transduction, illustrating the value of considering these parasites in the context of microbial social behavior concepts. It will be informative to apply this paradigm more broadly among protozoan pathogens.

Acknowledgements

We thank members of the Hill laboratory as well as Isabel Roditi for many stimulating discussions about social motility.

Figures:

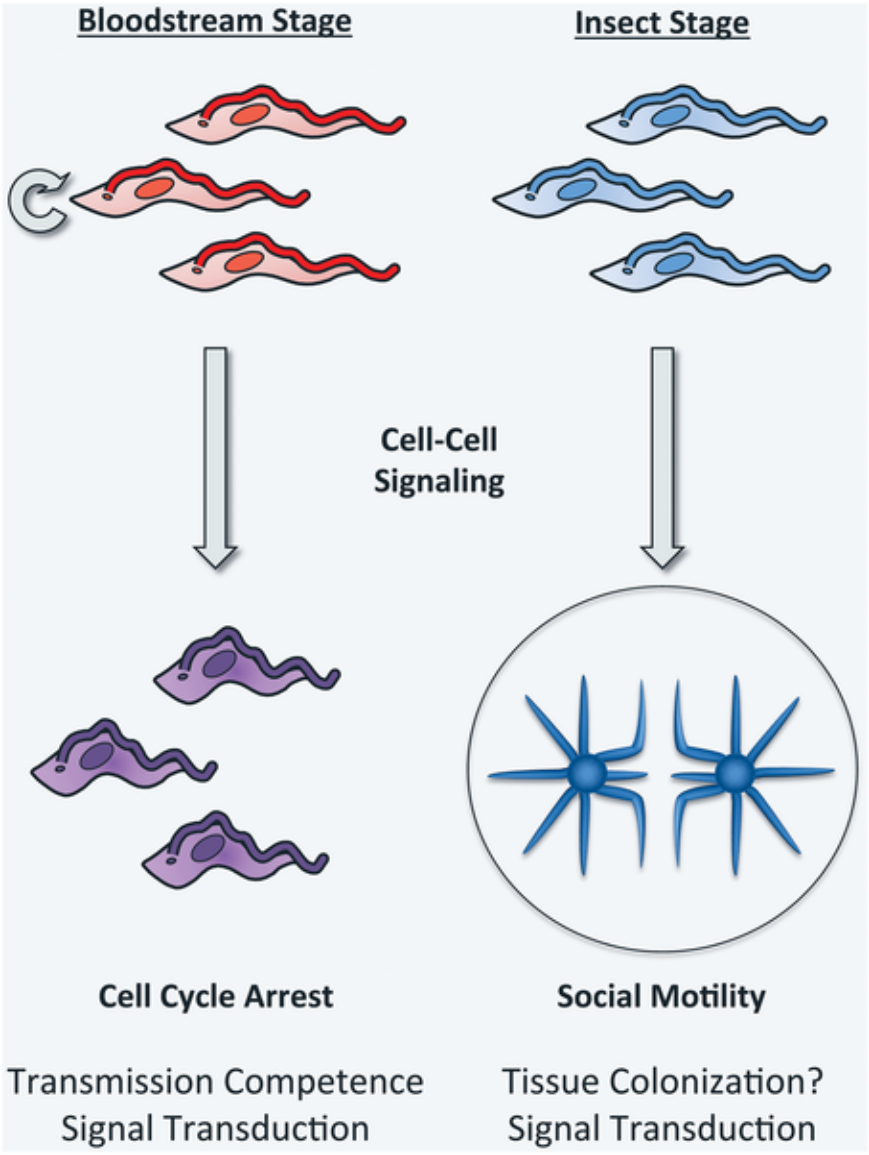

Figure A-1: Trypanosomes are social.

Trypanosome cell–cell interactions operate in bloodstream and insect stage parasites. In the bloodstream, "long slender form" parasites (red) differentiate into growth-arrested "short stumpy forms" (purple) through a quorum sensing-mediated mechanism. Stumpy parasites are pre-adapted for the tsetse fly environment and the transition thus establishes transmission competence, while also limiting bloodstream parasitemia [52, 53]. Procyclic *T. brucei* (insect

midgut stage, blue) undergo social motility when cultivated on semi-solid surfaces, using cell–cell signaling to promote collective motility across the surface and coordinating their movements in response to extracellular signals from nearby parasites. This leads to formation of radial projections that extend outward from the initial site of inoculation [8]. These activities are hypothesized to support colonization and/or transit of tissue surfaces in the fly. Beyond their direct impact on understanding parasite development, recent studies of stumpy formation and social motility have provided insight into parasite signal transduction. See text for details.

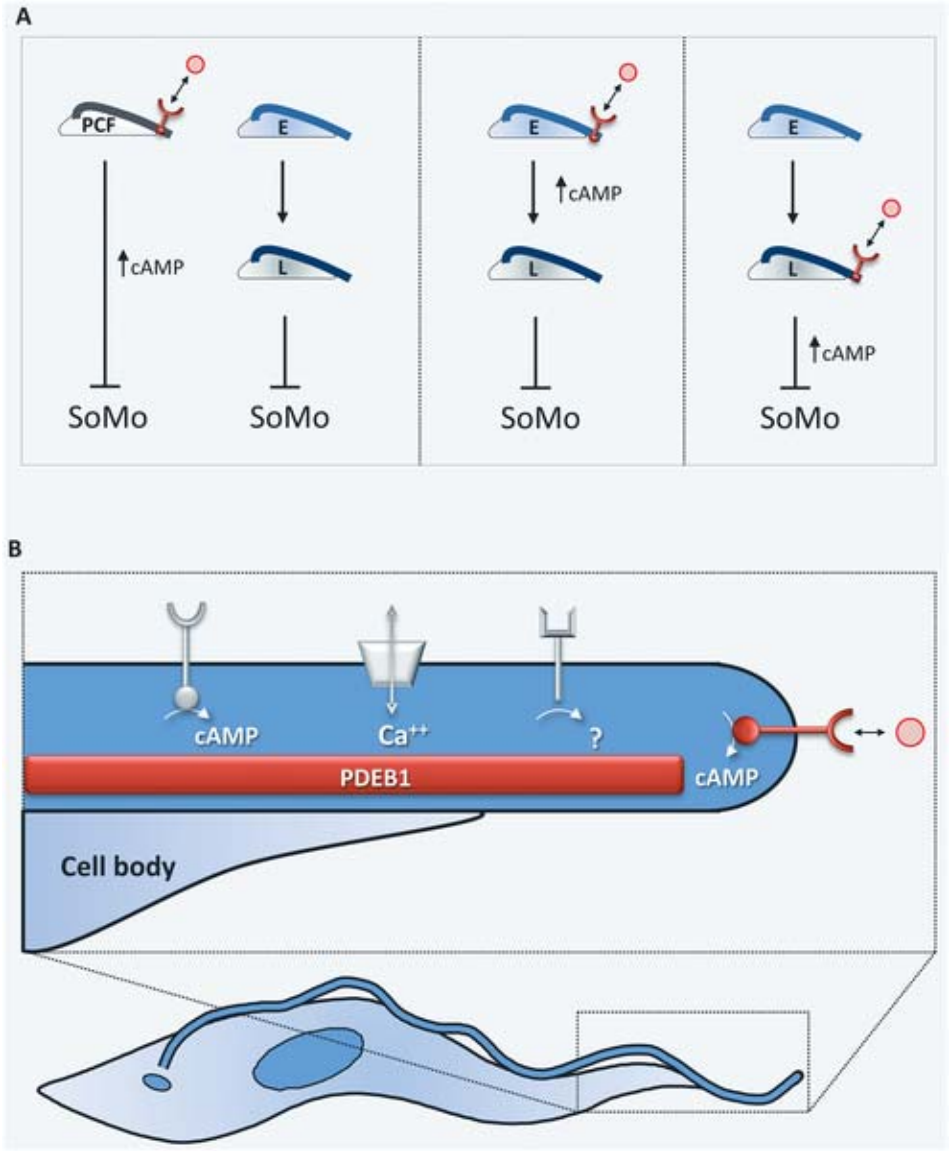

Figure A-2: Regulation of social motility.

(A) Three alternate models for regulation of social motility. (Left) Elevated cAMP at the flagellum tip (red) in response to regulation of tip-localized adenylate cyclase and the transition from early to late procyclics independently inhibit SoMo. (Middle) Elevated cAMP at the flagellum tip triggers the transition from early to late procyclics, which then inhibits SoMo. (Right) Development into late procyclics triggers elevated cAMP at the flagellum tip, which is then the inhibitory signal. (B) In addition to the known cAMP signaling systems that control

SoMo (red), the trypanosome flagellum harbors several predicted signaling systems, e.g., ion transporters, kinases, additional ACs, and other receptor-like proteins [50, 51] whose functions await discovery.

Bibliography

1. Shapiro, J.A., *Thinking about bacterial populations as multicellular organisms.* Annu Rev Microbiol, 1998. **52**: p. 81-104.
2. Bassler, B.L. and R. Losick, *Bacterially speaking.* Cell, 2006. **125**(2): p. 237-46.
3. Kaiser, D., *Coupling cell movement to multicellular development in myxobacteria.* Nat Rev Microbiol, 2003. **1**(1): p. 45-54.
4. Shaulsky, G. and R.H. Kessin, *The cold war of the social amoebae.* Curr Biol, 2007. **17**(16): p. R684-92.
5. Harshey, R.M., *Bacterial motility on a surface: many ways to a common goal.* Annu Rev Microbiol, 2003. **57**: p. 249-73.
6. Reuner, B., et al., *Cell density triggers slender to stumpy differentiation of Trypanosoma brucei bloodstream forms in culture.* Mol Biochem Parasitol, 1997. **90**(1): p. 269-80.
7. Mony, B.M., et al., *Genome-wide dissection of the quorum sensing signalling pathway in Trypanosoma brucei.* Nature, 2014. **505**(7485): p. 681-5.
8. Oberholzer, M., et al., *Social motility in african trypanosomes.* PLoS Pathog, 2010. **6**(1): p. e1000739.
9. Cecchi, G., et al., *Land cover and tsetse fly distributions in sub-Saharan Africa.* Med Vet Entomol, 2008. **22**(4): p. 364-73.
10. Simarro, P.P., et al., *The Atlas of human African trypanosomiasis: a contribution to global mapping of neglected tropical diseases.* Int J Health Geogr, 2010. **9**: p. 57.
11. WHO, *Mapping the risk of Human African Trypanosomiasis.* 2012.
12. Vickerman, K., et al., *Biology of African trypanosomes in the tsetse fly.* Biol Cell, 1988. **64**(2): p. 109-19.

13. Fraser, G.M. and C. Hughes, *Swarming motility.* Curr Opin Microbiol, 1999. **2**(6): p. 630-5.

14. Butler, M.T., Q. Wang, and R.M. Harshey, *Cell density and mobility protect swarming bacteria against antibiotics.* Proc Natl Acad Sci U S A, 2010. **107**(8): p. 3776-81.

15. Roditi, I. and M.J. Lehane, *Interactions between trypanosomes and tsetse flies.* Curr Opin Microbiol, 2008. **11**(4): p. 345-51.

16. Pan, J. and W.J. Snell, *Signal transduction during fertilization in the unicellular green alga, Chlamydomonas.* Curr Opin Microbiol, 2000. **3**(6): p. 596-602.

17. Peacock, L., et al., *The influence of sex and fly species on the development of trypanosomes in tsetse flies.* PLoS Negl Trop Dis, 2012. **6**(2): p. e1515.

18. Haines, L.R., *Examining the tsetse teneral phenomenon and permissiveness to trypanosome infection.* Front Cell Infect Microbiol, 2013. **3**: p. 84.

19. Gibson, W. and M. Bailey, *The development of Trypanosoma brucei within the tsetse fly midgut observed using green fluorescent trypanosomes.* Kinetoplastid Biol Dis, 2003. **2**(1): p. 1.

20. Lehane, M.J., *Peritrophic matrix structure and function.* Annu Rev Entomol, 1997. **42**: p. 525-50.

21. Dyer, N.A., et al., *Flying tryps: survival and maturation of trypanosomes in tsetse flies.* Trends Parasitol, 2013. **29**(4): p. 188-96.

22. Oberle, M., et al., *Bottlenecks and the maintenance of minor genotypes during the life cycle of Trypanosoma brucei.* PLoS Pathog, 2010. **6**(7): p. e1001023.

23. Imhof, S., et al., *Social motility of African trypanosomes is a property of a distinct life-cycle stage that occurs early in tsetse fly transmission.* PLoS Pathog, 2014. **10**(10): p. e1004493.

24. Imhof, S., et al., *A Glycosylation Mutant of Trypanosoma brucei Links Social Motility Defects In Vitro to Impaired Colonization of Tsetse Flies In Vivo.* Eukaryot Cell, 2015. **14**(6): p. 588-92.

25. Vassella, E., et al., *A major surface glycoprotein of trypanosoma brucei is expressed transiently during development and can be regulated post-transcriptionally by glycerol or hypoxia.* Genes Dev, 2000. **14**(5): p. 615-26.

26. Jelk, J., et al., *Glycoprotein biosynthesis in a eukaryote lacking the membrane protein Rft1.* J Biol Chem, 2013. **288**(28): p. 20616-23.

27. Matthews, K.R., *Controlling and coordinating development in vector-transmitted parasites.* Science, 2011. **331**(6021): p. 1149-53.

28. Singla, V. and J.F. Reiter, *The primary cilium as the cell's antenna: signaling at a sensory organelle.* Science, 2006. **313**(5787): p. 629-33.

29. Johnson, J.L. and M.R. Leroux, *cAMP and cGMP signaling: sensory systems with prokaryotic roots adopted by eukaryotic cilia.* Trends Cell Biol, 2010. **20**(8): p. 435-44.

30. Ferreira, R.B., et al., *Output targets and transcriptional regulation by a cyclic dimeric GMP-responsive circuit in the Vibrio parahaemolyticus Scr network.* J Bacteriol, 2012. **194**(5): p. 914-24.

31. Meili, R. and R.A. Firtel, *Follow the leader.* Dev Cell, 2003. **4**(3): p. 291-3.

32. Merritt, J.H., et al., *Specific control of Pseudomonas aeruginosa surface-associated behaviors by two c-di-GMP diguanylate cyclases.* MBio, 2010. **1**(4).

33. Bloodgood, R.A., *The future of ciliary and flagellar membrane research.* Mol Biol Cell, 2012. **23**(13): p. 2407-11.

34. Lopez, M.A., E.A. Saada, and K.L. Hill, *Insect stage-specific adenylate cyclases regulate social motility in African trypanosomes.* Eukaryot Cell, 2015. **14**(1): p. 104-12.

35. Oberholzer, M., E.A. Saada, and K.L. Hill, *Cyclic AMP Regulates Social Behavior in African Trypanosomes.* MBio, 2015. **6**(3): p. e01954-14.

36. Oberholzer, M., et al., *The Trypanosoma brucei cAMP phosphodiesterases TbrPDEB1 and TbrPDEB2: flagellar enzymes that are essential for parasite virulence.* FASEB J, 2007. **21**(3): p. 720-31.

37. Paindavoine, P., et al., *A gene from the variant surface glycoprotein expression site encodes one of several transmembrane adenylate cyclases located on the flagellum of Trypanosoma brucei.* Mol Cell Biol, 1992. **12**(3): p. 1218-25.

38. Oberholzer, M., et al., *Trypanosomes and mammalian sperm: one of a kind?* Trends Parasitol, 2007. **23**(2): p. 71-7.

39. Merritt, J.H., et al., *SadC reciprocally influences biofilm formation and swarming motility via modulation of exopolysaccharide production and flagellar function.* J Bacteriol, 2007. **189**(22): p. 8154-64.

40. Kuchma, S.L., et al., *BifA, a cyclic-Di-GMP phosphodiesterase, inversely regulates biofilm formation and swarming motility by Pseudomonas aeruginosa PA14.* J Bacteriol, 2007. **189**(22): p. 8165-78.

41. Pays, E. and D.P. Nolan, *Expression and function of surface proteins in Trypanosoma brucei.* Mol Biochem Parasitol, 1998. **91**(1): p. 3-36.

42. Gould, M.K., et al., *Cyclic AMP effectors in African trypanosomes revealed by genome-scale RNA interference library screening for resistance to the phosphodiesterase inhibitor CpdA.* Antimicrob Agents Chemother, 2013. **57**(10): p. 4882-93.

43. de Koning, H.P., et al., *Pharmacological validation of Trypanosoma brucei phosphodiesterases as novel drug targets.* J Infect Dis, 2012. **206**(2): p. 229-37.

44. Salmon, D., et al., *Adenylate cyclases of Trypanosoma brucei inhibit the innate immune response of the host.* Science, 2012. **337**(6093): p. 463-6.

45. Saada, E.A., et al., *Insect stage-specific receptor adenylate cyclases are localized to distinct subdomains of the Trypanosoma brucei Flagellar membrane.* Eukaryot Cell, 2014. **13**(8): p. 1064-76.

46. Nickzad, A., F. Lépine, and E. Déziel, *Quorum Sensing Controls Swarming Motility of Burkholderia glumae through Regulation of Rhamnolipids.* PLoS One, 2015. **10**(6): p. e0128509.

47. Shrout, J.D., et al., *The contribution of cell-cell signaling and motility to bacterial biofilm formation.* MRS Bull, 2011. **36**(5): p. 367-373.

48. Pathak, D.T., X. Wei, and D. Wall, *Myxobacterial tools for social interactions.* Res Microbiol, 2012. **163**(9-10): p. 579-91.

49. Pathak, D.T., et al., *Cell contact-dependent outer membrane exchange in myxobacteria: genetic determinants and mechanism.* PLoS Genet, 2012. **8**(4): p. e1002626.

50. Oberholzer, M., et al., *Independent analysis of the flagellum surface and matrix proteomes provides insight into flagellum signaling in mammalian-infectious Trypanosoma brucei.* Mol Cell Proteomics, 2011. **10**(10): p. M111.010538.

51. Subota, I., et al., *Proteomic analysis of intact flagella of procyclic Trypanosoma brucei cells identifies novel flagellar proteins with unique sub-localization and dynamics.* Mol Cell Proteomics, 2014. **13**(7): p. 1769-86.

52. Turner, C.M., J.D. Barry, and K. Vickerman, *Loss of variable antigen during transformation of Trypanosoma brucei rhodesiense from bloodstream to procyclic forms in the tsetse fly.* Parasitol Res, 1988. **74**(6): p. 507-11.

53. MacGregor, P., et al., *Trypanosomal immune evasion, chronicity and transmission: an elegant balancing act.* Nat Rev Microbiol, 2012. **10**(6): p. 431-8.